

**Systematic Oversteepening in Longitudinal Profiles of Mixed Bedrock-
Alluvial Channels at Tributary Junctions: Appalachians, Virginia**

by
Leah M. Windhorst

B.S. Earth, Atmospheric, and Planetary Sciences
Massachusetts Institute of Technology, 2003

SUBMITTED TO THE DEPARTMENT OF EARTH, ATMOSPHERIC, AND
PLANETARY SCIENCES IN PARTIAL FULFILLMENT OF THE
REQUIREMENTS FOR THE DEGREE OF

MASTER OF SCIENCE
AT THE
MASSACHUSETTS INSTITUTE OF TECHNOLOGY

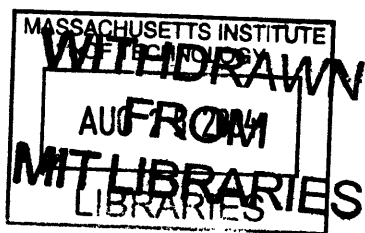
MAY 2004
[June 2004]

© 2004 Massachusetts Institute of Technology. All rights reserved.

Signature of Author: _____
Department of Earth, Atmospheric, and Planetary Sciences
May 18, 2004

Certified by: _____
Kelin X. Whipple
Associate Professor of Geology
Thesis Supervisor

Accepted by: _____
Maria Zuber
Department Head



Systematic Oversteepening in Longitudinal Profiles of Mixed Bedrock-Alluvial Channels
at Tributary Junctions: Appalachians, Virginia

by

Leah M. Windhorst

Submitted to the Department of Earth, Atmospheric, and Planetary Sciences in Partial
Fulfillment of the Requirements for the Degree of

Master of Science

ABSTRACT

Certain mixed bedrock/alluvial channels located in the Valley and Ridge province of the Appalachians in Virginia were identified as having a pattern of systematic oversteepening of channel gradients at tributary junctions. Where drainage area increased, channel slopes were either increasing or remaining constant. Subsequent investigation of 10m resolution digital elevation models found this pattern to be widespread throughout several large nearby drainage basins ($A \sim 10^8 \text{m}^2$). Several hypotheses for the causes and constraints of the pattern were tested in two ways: (1) digital profiles were compared to pre-existing data sets for grain-size, channel width, lithology, and drainage area; (2) a short field venture was conducted to test the accuracy of the DEMs and to provide additional data sets such as grain-size and channel width against which to compare the digital longitudinal profiles. Results show that there is some correlation between lithology, drainage area, and a pattern of downstream fining. However, the relationships are not strong and begs an analysis of the region at large to explain this channel gradient phenomenon. Periodically high levels of sediment flux moving through the drainage system, eg. debris flows, are a promising mechanism for the initiation of systematic oversteepening in the longitudinal profiles.

TABLE OF CONTENTS

Abstract	2
Table of Contents	3
1 Introduction	4
2 Background	6
2.1 Stream Profile Analysis Theory	6
2.2 Appalachian Mountains	7
2.3 Field Area	8
3 Digital Elevation Models: Methods and Analysis	11
3.1 DEMs and Stream Profile Techniques	11
3.2 Results	13
3.2.1 Longitudinal Profiles	13
3.2.2 Grain-size	14
3.2.3 Lithology	15
3.2.4 Channel Width	16
3.2.5 Drainage Area	17
4 Field Methods and Analysis	18
4.1 Objectives	18
4.2 Methods	18
4.3 Results	20
4.3.1 Longitudinal Profiles	20
4.3.2 Grain-size Data	20
4.3.3 Channel Width	21
5 Discussion	23
6 Acknowledgements	27
7 References	28
8 Figures	30
9 Appendix	50
9.1 Hack (1957) Principal measurements at selected localities	51
9.1.1 Data Tables	51
9.1.2 Data Locations	53
9.1.2.1 North River	54
9.1.2.2 Middle River	55
9.1.2.3 Tye River	56
9.2 Related Longitudinal Profiles	57
9.2.1 North Fork of the Shenandoah Basin	57
9.2.2 Dry River Basin	76
9.2.3 North River Basin	86
9.2.4 Middle River Basin	97

1 INTRODUCTION

The complex dynamics of the interplay among tectonics, climate, and surficial processes has been the focus of many interdisciplinary studies in recent years. Controls on the processes and rates of channel incision into bedrock are essential to understanding temporally and morphologically the evolution of mountainous regions. While many studies have focused on the longitudinal profile response to variations in tectonic uplift and orographic precipitation (eg. Snyder et al., 2000; Roe et al., 2002; Whipple, 2004) there is still not a complete understanding of channel response both in incision rate and morphology to local variations in sediment flux, eg. debris flows and tributaries, local grain-size, and lithology within the context of a declining orogenic system (Whipple and Tucker, 2002; Whipple, 2004). The Appalachian Mountains are an apt environment within which to conduct an investigation to further understand the influence of such controls. Within the Valley and Ridge province, the Appalachians have been in a state of tectonic quiescence since the Late Triassic (Hatcher, 1989) allowing channel longitudinal profiles to be free of any uplift influence.

This study began with a few observations of longitudinal profiles where channel slope increases with the addition of drainage area at tributary junctions. These profiles were extracted from 30 meter resolution digital elevation models (DEMs) of the North River in northwestern Virginia (Whipple and Tucker, 2002). These unexpected increases correspond to high local concavities of the main stem between major tributary junctions in contrast to the concavity of the entire stream. When channel slope and drainage area are plotted in log log space, an unusual “sawtooth” pattern emerges (Figure 1).

Quantifying the fluctuations of the concavity index is important because these changes can be indicative of geographic variations in substrate properties, orographic precipitation patterns, and/or uplift rates. Also, if this see-saw pattern could be linked to, for example, either systematic variations of grain-size or substrate properties, this would constitute important evidence that channel slopes are sensitive to these variables. Moreover, under some circumstances it would be possible to infer cause and effect.

The next question to be addressed was whether or not such a pattern is ubiquitous. DEMs and previously developed channel profile analysis techniques were adapted to this particular field area and used to extract longitudinal profiles throughout the Appalachians of northwestern Virginia in search of this systematic oversteepening in channel slope (Snyder et al., 2000; Kirby and Whipple, 2001; Wobus et al., in press). Initial assumptions for possible causes of this sawtooth pattern included the ratio of drainage of the tributary to trunk stream as well as differences in lithology, grain-size, and channel width between the tributary and main stem. These same properties which can all affect channel gradient (eg, Hack, 1957; Whipple, 2004) were also evaluated between streams where the pattern was observed and where it was not.

Hypotheses were tested through several means: (1) digital data sets such as digital orthoquads were used to gather information about channel width, vegetation coverage, etc.; (2) profiles were compared to data sets including grain-size distributions, substrate lithology, sediment source lithology, debris flow frequencies, and erosion rates collected from previous work in the region (Hack, 1957; Hack, 1965; Eaton et al., 2003; Matmon et al., 2003); (3) a short field investigation was planned after the majority of the digital data had been collected to test, clarify, and affirm certain observations.

2 BACKGROUND

2.1 Stream Profile Analysis Theory

The observed smooth concave-up profile characteristic of longitudinal profiles in bedrock rivers can be described for a wide range of tectonic, lithologic, and climatic settings by the well-known relationship between channel slope and drainage area: Flint's Law (Flint, 1974).

$$S = k_s A^{-\theta}$$

(1)

Where S is the slope, k_s is the steepness index, A is the drainage area, and θ is the concavity index. Whipple (2004) discusses the breakdown of this scaling relation at a critical drainage area (A_{cr}) where debris flows dominantly set the profile form. The value for A_{cr} could be as large as 10km². In this study I intend to focus solely on the fluvial regime, and the process by which the transition between the regimes is identified in the profiles is discussed herein.

A log-transform of equation (1) predicts a linear relationship between $\log S$ (slope) and $\log A$ (drainage area). The slope of a best fit line through the data on a plot of $\log S$ against $\log A$ results in the concavity (Figure 1). It is important to examine both the magnitudes of concavity between profiles, as well as variations in concavity along a single profile. Changes in both can be indicative of a wide range of forcings on the

profiles including tectonic uplift, climate, incision rate, and rock strength (eg. Whipple, 2004).

In the setting of this study, concavities along entire profiles throughout the region are consistently moderate ($0.4 \leq \theta \leq 0.7$) and average to about 0.55. Throughout many profiles, however, there is an unusual and systematic sawtooth pattern in the slope/area data of locally high concavities between tributary junctions (Figure 1). According to equation (1), channel slope should decrease with increasing drainage area; yet, the observation in the slope/area data is that at major tributary junctions channel gradients are oversteepened from the theoretical prediction. Thus, the controlling factors on such a phenomena warrant investigation.

2.2 Appalachian Mountains

Construction of the Appalachians occurred through a series of collision events throughout the Paleozoic. Several volcanic arcs amalgamated during the Taconic and Acadian orogenies along the eastern coast of the North American continent to form the beginnings of the mountain range. Later in the Alleghanian orogeny, Africa collided with North America creating the highest elevations in the evolution of the Appalachians. Extensional rifting followed in the early Late Triassic dividing the two continents and resulting in the topography observed today (Hatcher, 1989).

Since the end of the major tectonic events of the Paleozoic, the Appalachians have remained orogenically quiescent (Hack 1965, 1979; Hatcher, 1989). Although decline of topography through time is expected (Pinet and Souriau, 1988, Pazzaglia and Brandon, 1996; Baldwin et al., 2003), recently acquired denudation rates by Matmon

(2003) confirm that relief in the Appalachians has become statistically invariant over relevant timescales within the accuracy of their data. This has been the case for approximately the past 200×10^6 m.y. (Matmon, 2003). The longevity and stability of the range are impressive and also opportune for this study. Several studies have documented the effects of varying uplifts both along the longitudinal profile and between drainage basins on k_s and θ (eg. Snyder et al., 2000; Kirby and Whipple, 2001; Whipple and Tucker, 2002). Channel widths are also known to adjust to changes in uplift rates (eg. Montgomery, 2002). However, with uplift essentially constant both temporally and geographically, any observations of systematic changes in these properties will be due to some other, as yet, unknown cause to be discussed herein.

2.3 Field Area

I focused on five drainage basins throughout the course of this study: the North Fork of the Shenandoah River, the Dry River, the North River, the Middle River, and the Tye River basin (Figure 2). The North River was where the pattern of oversteepened channel gradients at tributary junctions was first identified. Investigation proceeded to the North Fork of the Shenandoah, the Dry River, and the Middle River for several reasons: their proximity to the North River, similar underlying lithologies, pre-existing data sets for grain-size, channel width, etc. (Hack, 1957), and 10 m DEM coverage. I also studied the Tye River for its drastically different underlying lithology, and Hack (1957) also had data sets of other local channel properties for this basin. All of the basins are located within the Valley and Ridge province in northwestern Virginia near the border with West Virginia. In this region the average maximum elevation is

approximately 1km. These mountains are also free from glaciation effects found in the Appalachian ranges further to the north (Denton, 1981). This is important for truly capturing the behavior of a fluvial network.

The lithology underlying the North Fork of the Shenandoah, Dry River, and North River basins is predominantly Devonian and Mississippian sandstones interbedded with occasional beds of shale (Figure 3). The Tye River primarily flows across a resistant granodiorite. The Middle River crosses many different lithologies as it flows across anticlines and synclines that exposed alternating beds of sandstone and shale of Silurian and Devonian age. The highest parts of the Middle River basin are rooted in Devonian sandstones and the lowest, but largest, reaches of the river lie in Ordovician limestones and dolomites (Figure 3) (map compiled by Hack, 1965).

Channels in this vicinity can be best characterized as mixed bedrock-alluvial, a combination of alternating exposed bedrock and sediment (gravels and cobbles) laden braided reaches. Using the classification scheme for bed morphology developed by Montgomery and Bluffington (1997), tributaries at the highest elevations have step-pool morphology. These quickly transition to a plane-bed morphology then gradually to pool-riffle conditions. The observed near-alluvial and gravel-bedded conditions in many locations along the channel fit with the sediment flux predictions associated with Montgomery and Bluffington's bed morphology categories (1997). Plane-bed and pool-riffle conditions are related to a high sediment flux (Q_s) to transport capacity (Q_c) ratio which approximates the beginning of transport-limited conditions ($Q_s/Q_c \sim 1$). Thus, channel incision in this region is most likely transport-limited (Whipple and Tucker, 2002).

Previous research in this locale provided a large data set against which I compared the results from the longitudinal profiles extracted from the DEMs. Hack (1957) collected a wide variety of data for large portions of the North River, Middle River, and Tye River basins: grain-size point counts, channel width, channel length, lithology of underlying bedrock, source lithology of sediment in channel, and other pertinent observations (Appendix 9.1). Hack also mapped out surficial deposits for the entire area (1965).

3 DIGITAL ELEVATION MODELS: METHODS AND ANALYSIS

3.1 DEMs and Stream Profile Techniques

Digital elevation models (DEMs) provided by the United States Geological Survey (USGS) were used as the primary data source for the stream profile analysis. A USGS DEM is produced from interpolating elevations from stereomodel digitized contours derived from 1:24,000 scale USGS topographic maps. The DEM consists of a square grid, cast on Universal Transverse Mercator (UTM) projection, with equally spaced resolution values at either 10 or 30 m intervals. Each DEM is provided in a 7.5 by 7.5-minute block that corresponds to a standard USGS 7.5-minute quadrangle.

For this study, I primarily used 10 m DEMs for their ability to resolve subtle features. Using profile extraction methods summarized in Wobus et al. (in press), the 10 m DEMs produce profiles with significantly reduced noise compared to the 30 m data. The higher quality of the 10 m DEMs allows the profile to be analyzed without any sort of smoothing that might eliminate the subtle pattern in the slope/area data. Because these DEMs were produced by the interpolation of digitized topographic contour maps, systematic artificial stair-steps were produced where the profile is crossed by a contour line. For the 10 m DEMs, a specific script discussed in Wobus et al., (in press) can locate these steps and recover the true profile form without smoothing or altering any data. In this way, subtle but true changes in the longitudinal profile and slope/area data could be identified. It is also important to have the 10 m DEM coverage for this area for its ability to accurately capture channel behavior for smaller drainage areas ($\sim 10^5 \text{ m}^2$).

One obstacle in the use of these DEMs is the consistency of coverage in one resolution. Throughout Virginia, both 10 m and 30 m DEMs are available. In order to utilize the stream profile methods accurately and efficiently, the river of interest must entirely be in one resolution or another. Coverage of 10 m resolution existed for most of the mountain range. Out into the large valleys, coverage became much less consistent. Many quadrangles had either 10 m or 30 m data available. Therefore, basins could only be delineated to extents dictated by the data, but always to lengths that allowed for meaningful analysis. To evaluate the largest areas possible, I created two mosaic DEMs for each drainage basin: one of 10 m resolution and one of 30m. In this way I was able to gain an understanding for the behavior of the profiles at lower elevations especially in relation to various data sets collected by Hack (1957). It should also be noted that where the 10 m resolution coverage ended, the rivers appeared to transition to a fully alluvial state as demarcated by increased channel sinuosity at large drainage areas ($A \sim 500 \text{ km}^2$). The alluvial case is not addressed in the course of this study.

As mentioned earlier, Whipple (2004) summarized Stock and Dietrich's (2003) discussion of the potential for debris flows to set channel slopes within smaller drainage areas ($A \leq 10\text{km}^2$): therefore, beyond the scope of fluvial process rules (Stock and Dietrich, 2003). Throughout the majority of the longitudinal profiles in this study, the scaling between channel slope and drainage area ended at approximately 1 km^2 . To stay focused on the fluvial system, I did not include these small drainage areas in the analysis. The interpretation of slope/area data for drainage areas between $1\text{-}10\text{km}^2$ was given special consideration. I classified singular occurrences of oversteepened channel slopes differently from patterns of systematic oversteepening that began at drainage areas

greater than 10km² and continued through to 1km². In this way I hoped to capture effects that truly occurred within the fluvially dominated regime.

3.2 Results

3.2.1 Longitudinal Profiles

Certain areas of several basins were determined to be useless for slope/area analysis. The Dry River is difficult to interpret from the slope/area data because there are two large dams in place on the two major branches within the basin. The dams not only disrupt the slope/area regression, but they also have an enormous influence on the behavior of a channel profile. A major branch of the North River is also dammed, preventing an accurate profile analysis. I still investigated areas upstream of the dams because the response of the main stem's longitudinal profile to incoming tributaries should still be the same upstream of the dam.

Approximately 13 of the 17 major rivers in these basins display a pattern of systematic oversteepening at tributary junctions (Figures 4, 5, 6, 7). In 84% of the steepened confluences both the tributary and main stem profiles experience an increase in channel slope, or the slope remains constant, not decreasing with increasing drainage area. Many times it is difficult to distinguish between the scenarios two at the resolution of the slope/area data. However, there are very few clear cases where both the tributary and main stem slopes make significant increases in slope. In the other 16% of confluences, only the main stem's gradient responds by steepening to the tributary. Locations and profiles where singular instances of an increase in channel slope occurred were not included in this tally. The interest here was to look for systematic large scale

patterns across several basins where the slope increase could not be attributed to some local influence.

Concavities through the channels containing the sawtooth pattern average around 0.57. Interestingly this is equivalent to the reference concavity for the region, meaning with or without the see-saw pattern the average concavity is the same. I also measured the concavity of oversteepened sections in the slope/area data. These sections range from 0.57 to 1.7 and averaged to be about 1. On each individual profile, the sections do not maintain the same concavity and usually vary by +/- 0.20 (Figure 8). There are, however, substantial uncertainties in the concavity values determined by regression for these sections. Despite the uncertainties, these values are still an interesting approximation for the concavity of the individual segments.

3.2.2 Grain-size

Hack (1957) claimed that the slope of a channel will not decrease with increasing drainage area if the increase in grain-size is sharp. To address this from a remote perspective, I extracted profiles specifically in areas where a large trunk stream joined with a short tributary with a small drainage area. It could roughly be assumed, within a singular lithology, that a short tributary would have less time to sort out larger clasts or abrade them into smaller ones. Thus, this could approximate a coarse sediment load into the larger channel. This method yielded no effective results, however.

Longitudinal profiles were also compared to Hack's grain-size data for the region (Appendix 9.1). Along the North River, Hack observed a pattern of downstream fining. Over the entire stretch of the Middle River, there is no pattern of downstream fining.

However, when the Middle River reaches the lowest elevations in the valley the sinuosity increases and the channel becomes fully alluvial. A large portion of Hack's data was taken in this depositional regime. If his grain-size measurements are limited to the higher elevations in the mixed bedrock-alluvial channels there is also a pattern of downstream fining. The downstream fining then positively correlates to streams that do appear to systematically oversteepen at tributary junctions.

3.2.3 Lithology

The Tye River basin contained no profiles exhibiting oversteepened tributary junctions. The river crosses a major lithologic boundary about half-way down its profile from a resistant granodiorite to sandstone. The fluctuations in the slope/area data around the knickpoint made it difficult to interpret any influence from incoming tributaries (Figure 9). The underlying lithology appears to be the dominant control in setting the channel slope here. DEM coverage for the basin also limits the size of the region for examination downstream of the lithologic contact.

Throughout the basins, tributaries that begin in a less resistant lithology, as in shale, steepen up predictably when they join to a main stem carrying a sediment load derived from a more resistant lithology, such as sandstone (Figure 10). Channels that originate in a resistant lithology do not display any distinct changes to their equilibrium profiles when they enter a less resistant lithology. I hypothesized that in this area a channel underlain by shale and carrying a sediment load primarily derived in shale would steepen up when it was joined by a tributary from a sandstone source. The channel would have to increase its gradient at the confluence in order to maintain efficient

transport of the incoming coarser, more resistant sediment load. However, there appears to be no consistent correlation.

The locations where the sawtooth pattern is observed appear to be restricted to sandstone or have major branches in the sandstone. However, not all streams in the sandstone appear to be systematically oversteepened. Much of the sandstone in this region is interbedded to varying degrees with shale. Lateral variations in facies may partially account for this absence. However, more detailed field observations would be needed to confirm or deny this possibility.

3.2.4 Channel Width

The digital orthoquads proved to be very difficult to use in measuring channel width. I attempted to measure bankfull, floodplain and valley width. I was able to obtain rough estimates for all three. However, the entire region is heavily vegetated and farms occupy most of the valleys. The DOQs are also in color, which highlights certain features such as farms, roads, changes in vegetation etc., while blurring the edges of valleys. Thus, accurate measurements as they relate specifically to certain tributary junctions are not possible. The DOQs only provide a general idea of width magnitudes and how they increase over long length scales. I also made several attempts at determining the rate at which width is increasing over length from the DOQs. The variation in my results was too great for accurate analysis.

3.2.5 Drainage Area

Along profiles that contained the sawtooth pattern, I collected the ratio of the drainage area of the tributary (A_t) to that of the main stem (A_m). I hypothesized that for a tributary to have a significant affect on the gradient of the main stem, the drainage area of the tributary should scale with drainage area of the main stem. Looking at Figure 11 it appears that tributary drainage basins are all at least one-third the size of the main stem's drainage basin, and the majority are at least half the size of the main stem's. I also compared the ratio to the type of channel response observed in the slope area data to see if a certain type of response was drainage area specific. It appears that this is not the case. The ratio of (A_t / A_m) encompasses the entire range of values where both the main stem and tributary profiles show channel gradient increases at the tributary junction.

4 FIELD METHODS AND ANALYSIS

4.1 Objectives

I conducted a short field venture to obtain a dataset against which observations made from the digital stream profiles could be tested. We collected a longitudinal profile of the German River (corresponds to cowk_29 digital profile, Figures 4, 12) around tributary junctions where the sawtooth pattern in the slope/area data occurred, thereby assessing the accuracy and validity of the profile extracted from the DEM. At these locations we also gathered channel width and grain-size measurements along the main stem, both pre- and post-confluence, and along the tributary. Our reason for collecting grain-size data was twofold: (1) to determine if a pattern of downstream fining existed (as observed by Hack (1957) for the North River and Tye River); (2) to examine if the steepened channel gradient depended upon grain-size differences between the tributary and main stem (Hack had claimed that within his observations that channel gradient will not lower with increasing drainage area if there is a sharp increase in grain-size (1957)). Channel width data is of interest because we wanted to determine if this was an additional method utilized by the main stem in responding to the tributary. The interdependency of channel width and slope could be explored relative to grain-size.

4.2 Methods

The relevant portions of the longitudinal profile of the German River were collected using a laser range finder linked to both a digital compass and GPS. We took

elevation measurements for 500 m along channel above and below every junction to accurately capture any slope changes (Figures 12, 13). Data points were always gathered along one bank at the water's edge. The distance between data points was set by both the sinuosity of the channel and the surrounding vegetation. It should be noted that the see-saw in the slope/area data occurred over a considerably larger scale than that captured in the hand surveys.

To obtain grain-size data, we chose localities that would best characterize the main stem and tributary both before they reached a confluence and about 100 m downstream of where the two joined (Figure 13). Gathering this data proved difficult due to highly variable grain-sizes within short distances along the river. One set of measurements may describe grain-sizes at that particular location but not be representative of the section of channel we wanted to characterize. Where possible we selected localities for measurement that appeared not to be local extremes of grain-size.

We used a method of measuring the grains similar to that used by Hack (1957) for the North River and Middle River because he concluded that it was effective in this area with stream beds dominantly composed of gravels and cobbles. Thus, at chosen points we measured out the bankfull width of a channel with a tape measure. Beginning at one bank, 10 grains were measured across their intermediate axis once every meter along the tape. One person chose grains by pointing a stick at the ground and picking up whatever grain the stick pointed at. Axis measurements were made with a ruler in centimeters and recorded by an assistant. This method was both efficient and appeared to be effective in providing the data sought.

4.3 Results

4.3.1 Longitudinal Profiles

The longitudinal profiles gathered around the tributary junctions of the German River demonstrate that the steepening of the profile is not simply an artifact of the DEM or an error in the profile code. Slopes from each surveyed branch of the river behave exactly as predicted by the slope/area data (Figures 14, 15, 16). The profiles also appeared to be very sensitive to local exposures of bedrock in the channel as well as human influences such as bridges within the resolution at which we collected the data. It should also be noted that bedrock was not exposed to any greater extent in the vicinity of the tributary junctions than other locations in the river. Thus, bedrock exposure can not be the sole cause of the increase in slopes observed in the digital slope/area data.

4.3.2 Grain-size Data

Results from the sediment point counts are mixed. Observationally over short distances, no distinct changes in grain-size exist. However, over the 20 km length scale that we sampled grain-sizes, there is a pattern of downstream fining (Figure 17). This pattern is consistent with finding by Hack (1957) for the North River and certain parts of the Middle River which have their branches sourced in a similar resistant (sandstone) lithology. Within approximately 500 m of the surveyed confluences, we collected several grain-size point counts. These points, however, have no correlation to the steepening of slopes at the confluences.

The profiles of the confluence between the small tributary cowk_35 and the main stem of the German River, cowk_29, show that the tributary's slope remains relatively

constant as it joins with cowk_29 (Figure 14). The main stem slope has just steepened up considerably in response to joining with cowk_32 upstream. During the digital investigation, the assumption was made that short steep tributaries may be bringing in a coarser sediment load and thus steepening the channel. Cowk_35 is just such a tributary. It has a step-pool morphology and is flowing over exposures of bedrock averaging 10 m in length along channel. However, according to the point counts, cowk_29 is carrying a much coarser sediment load than cowk_35. Therefore, the assumption is not entirely true and confirms the observations made from DEM profiles.

At the next examined confluence between cowk_29 and cowk_21, grain-size appears to change very little from the tributary cowk_21 and main stem above the junction to below the confluence (Figure 15). The grain-size data surrounding the final confluence between cowk_29 (main stem) and berg_4 (tributary) reveals the main stem is carrying a much coarser sediment load than the incoming tributary. The channel gradient post-confluence is steeper than expected on both profiles even though there is a large difference in grain-sizes (Figure 16). The lithologic setting for both streams is also equivalent. Thus, while Hack's (1957) data shows that channel gradients are adjusted to grain-size differences between basins, within one longitudinal profile there is no such correlation.

4.3.3 Channel Width

Local channel widths along the German River varied greatly within short distances (Figures 13, 18). Often it was difficult to even determine the bankfull width due to braiding of the streams when in the center of the valleys. We also observed that

channel width was constrained in many locations by two factors: hillsides and human structures. Channels flowing at the base of a hillside were narrower than when a channel flowed through the center of a valley where a channel could braid without the lateral bedrock constraint. Manmade constructions such as bridges, roads, and walls built to protect private properties also forced narrower channel widths. We attempted to avoid such influences when making width measurements, but they undoubtedly have an effect on the local variability of channel width. The data collected at the junctions shows that width does not always instantly increase twofold post-confluence. The sum of the averaged widths from the tributary and main stem upstream does not appear to equal the channel width downstream of the confluence (Figure 18). The main stem only increases in width a small amount with the addition of the tributary.

Comparing the rates at which channel width scales with drainage area within the sandstone of the North River, East Dry Branch, and North Fork shows that all three scale as expected (Figure 19). They are also remarkably similar to the main trunk of the Middle River which lies at much lower elevations, in less resistant lithologies of shales and limestones, and has sinuosity association with alluvial conditions: as opposed to mixed bedrock-alluvial. Whipple (2004) summarizes how such a similarity may be indicative of bedload flux controlling channel width.

5 DISCUSSION

There are two avenues by which to analyze the data I have presented above: (1) evaluate and compare properties such as channel width, lithology etc. only between the tributary and main stem where the oversteepened channel gradients occur; (2) evaluate those same properties between channels and drainage basins to determine why systematic oversteepening occurs in most drainage basins, but not all. Here I will draw together the numerous data sets within the focus of these two contextual frameworks.

I found that width of a channel does not increase to the sum of the tributary's and incoming main stem's widths. Post-confluence widening is much more subtle. Channel width is also highly locally variable depending on proximity to hillsides and human influence. However, widths of both channels with a sawtooth pattern and those without scale within expected values for gravel-bedded alluvial channels (Figure 19) (eg. Hack, 1957; Whipple, 2004).

$$W \propto A^{0.3-0.5}$$

(2)

That these mixed bedrock-alluvial channels scale similarly to alluvial channels is interesting to note as mentioned in Whipple (2004). It is also worth mentioning that the three streams plotted with oversteepened profiles do increase in width at a faster rate than the channel without the pattern. These same streams all contain patterns of downstream fining in sediment size.

Within the scope of the available and collected grain-size data, where the sawtooth pattern occurs in the slope/area data, downstream fining is also present. However, not enough grain-size data is available to claim that downstream fining exists in basins that do not contain oversteepening junctions. Much of Hack's (1957) data was acquired at low elevations where the streams transition to alluvial conditions, and is therefore not useful for the purpose of this study. The data I collected in the higher elevations in the North Fork basin confirms that the sawtooth pattern is not due to local coarsening of the bedload from tributary input.

The lithology of the sediment source appears to be a mildly influencing factor. Inputs of lithologically resistant bedload, such as sandstone clasts, directly to channels underlain by and sourced in less cohesive units like shale have no effect on the channel profile. While most oversteepened junctions are located in sandstone, they can also occur in units like shale or limestone. However, the major branches of the river are found rooted in sandstone; thus, a resistant sediment source.

Sawtooth profiles also have the constraint that the ratio of the tributary's drainage basin to that of the main stem (A_t / A_m) must be over one-third. Despite this and other correlating properties between systematically oversteepened profiles mentioned above, there are several locations with these same properties and have no oversteepened tributary junctions. Therefore, while factors like lithology and the ratio A_t / A_m can be influential, another dominant control must be sought.

Research conducted in both the Blue Ridge Mountains and the Valley and Ridge province, reveals that high-magnitude, low-frequency flooding events (strong storm cells and hurricanes) are responsible for approximately half of the long-term denudation

(Eaton et al., 2003). Eaton describes two different storm events where 43% and 63% of the expected denudation by mechanical load over 3500 yr and 2500 yr periods, respectively, occurred nearly instantaneously. The thousands of debris flows initiated by heavy rainfalls delivered massive amounts of sediment to the drainage network, where in turn it becomes bedload to be transported by the system. These debris flow events have a recurrence interval of approximately 2-4 k.y. Such a situation as this could both possibly account for the oversteepening in the longitudinal profiles and explain why some rivers with similar surrounding properties do not have the sawtooth pattern. This hypothesis is testable with further field work.

Transport-limited channels are defined by channel incision occurring when the transport capacity (Q_c) at any one locality is greater than the sediment flux (Q_s) received from upstream. The channels in this region are incising, albeit at an extremely low rate (Matmon, 2003). This other method of erosion by storm induced debris flows is essentially instantaneously delivering half of the sediment the drainage network must transport out of the mountains for the next several thousand years. Thus, Q_s may be brought to exceed Q_c . Tributaries also experiencing the influx pulse of sediment from debris flows would further increase the need for the main stem to transport out essentially instantly higher sediment loads. The channels must also be incising over time to make up for the other 50% of erosion that the debris flows do not encompass in order to maintain the balance between exhumation and denudation (Matmon, 2003). Therefore, channel slopes respond by steepening at tributary junctions to maintain their dual purpose of transport and incision. More work should be done to determine how much of the sediment introduced into the drainage network by debris flows stays within

the system and is not similarly instantaneously washed out of the system during a storm. Even if this scenario is not precisely the case, debris flows are a promising avenue of research to further constrain the controls on the systematic oversteepening of channel gradients at tributary junctions since no singular influence could be found dominant in the course of this investigation.

6 ACKNOWLEDGEMENTS

I'd like to first thank Kelin Whipple who was ever a patient advisor and kind enough to let me stick around for a fifth year. I learned more about conducting research and thinking beyond a classroom this year than I ever could have hoped. I'd also like to thank all the guys in line for their Ph.D's for their help in solving a variety of computer and IPAQ problems, but especially Joel Johnson and Ben Crosby. Despite their own crushing work loads, they spent ample time helping me with homework, digital troubles, or just teaching me how to handle the locals in my field area. Also, lots of gratitude to Lisa Schultz who came in at the last minute to accompany me on my trek to Virginia.

Thanks to Nick as well for all his emotional support. If he wasn't there to cook mac and cheese for me during late nights of work, I probably would have starved (or at least lost some weight).

Last I'd like to thank my parents. It wasn't just their financial contribution that drove me to stay for another degree, but their emotional support and the ambition they instilled in me when I was young to work hard at life (and homework) even when it becomes impossibly hard.

7 REFERENCES

- Baldwin, J.A., K.X. Whipple, and G.E. Tucker, Implications of the shear stress river incision model for the timescale of postorogenic decay of topography, *J. Geophys. Res.*, 108(B3), 2158, 2003.
- Denton, G.H., and T.H. Hughes, 1981. *The Last Great Ice Sheets*. Wiley-Interscience, New York, 484 p.
- Eaton, L.S., B.A. Morgan, R.C. Kochel, A.D. Howard, Role of debris flows in long-term landscape denudation in the central Appalachians of Virginia, *Geology*, 31(4), 339-342, 2003.
- Flint, J.J., Stream gradient as a function of order, magnitude, and discharge, *Water Resour. Res.*, 10, 969-273, 1974.
- Hack, J.T., Studies of longitudinal stream profiles in Virginia and Maryland, *U.S. Geol. Surv. Prof. Pap.*, 294-B, 42-97, 1957.
- Kirby, E., K. Whipple, Quantifying differential rock uplift rates via stream profile analysis, Geological Society of America, *Geology*, 29, p.415, 2001.
- Hack, J.T., Geomorphology of the Shenandoah Valley, Virginia and West Virginia, and origin of the residual ore deposits, *U.S. Geol. Surv. Prof. Pap.* 484, 84 p., 1965.
- Hatcher, R.D., Jr., Tectonic synthesis of the U.S. Appalachians, in Hatcher, R.D., Jr., Thomas, W.A., and Viele, G.W., eds., *The Appalachian-Ouachita orogen in the United States; The Geology of North America: Boulder Colo.*, Geological Society of America, v. F-2, 511-535, 1989.
- Matmon, A., P.R. Bierman, J. Larsen, S. Southworth, M. Pavich, M. Cafee, Temporally and spatially uniform rates of erosion in the southern Appalachian Great Smoky Mountains, *Geology*, 31(2), 155-158, 2003.
- Montgomery D.R., N. Finnegan, A. Anders, B. Hallet, Downstream adjustment of channel width to spatial gradients in rates of rock uplift at Namche Barwa, *Abstr. Progr. Geol. Soc. Am.* 34:241, 2002.
- Pazzaglia, F.J., and M.T. Brandon, Macrogeomorphic evolution of the post-Triassic Appalachian mountains determined by deconvolution of the offshore basin sedimentary record, *Basin Res.*, 8, 255-278, 1996.

- Pinet, P., and M. Souriau, Continental erosion and large-scale relief, *Tectonics*, 7(3), 563-582, 1988.
- Roe, G.H., D.R. Montgomery, and B. Hallet, Effects of orographic precipitation variations on the concavity of steady-state river profiles, *Geology*, 30(2), 143-146, 2002.
- Snyder, N., K.X. Whipple, G.E. Tucker, and D. Merritts, Landscape response to tectonic forcing: Digital elevation model analysis of stream profiles in the Mendocino triple junction region, northern California, *Geol. Soc. of Am. Bul.*, 112, 1250-1263, 2000.
- Stock, J.D., W.E. Dietrich, Valley incision by debris flows: evidence of a topographic signature, *Water Resour. Res.*, 39 (3), p. 25, 2003.
- Whipple, K.X., and G.E. Tucker, Implications of sediment-flux-dependent river incision models for landscape evolution, *J. Geophys. Res.*, 107(B2), 2039, 2002.
- Whipple, K.X., Bedrock rivers and the geomorphology of active orogens, *Annu. Rev. Earth Planet. Sci.* 32, 151-185, 2004.
- Wobus, C., K.X., Whipple, E. Kirby, N. Snyder, J. Johnson, K. Spyropolu, B. Crosby, D. Sheehan, Tectonics from topography: Procedures, promise and pitfalls, *in press*.

8 FIGURES

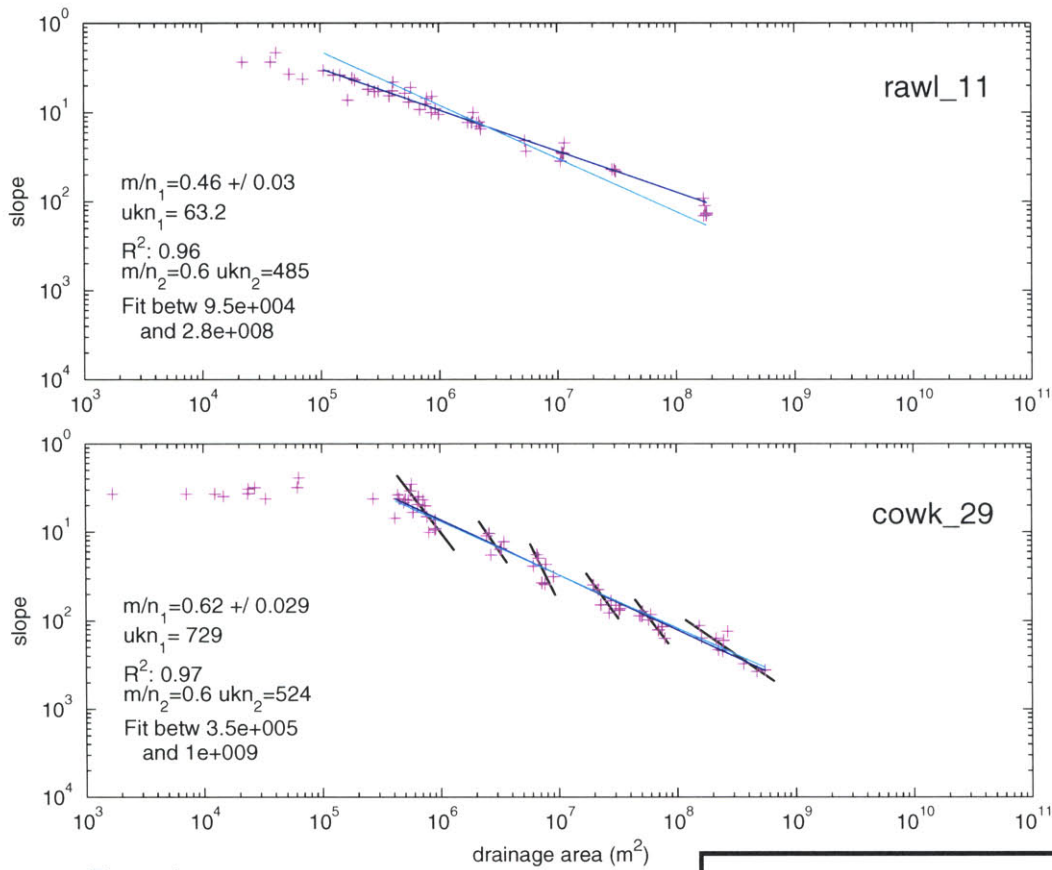
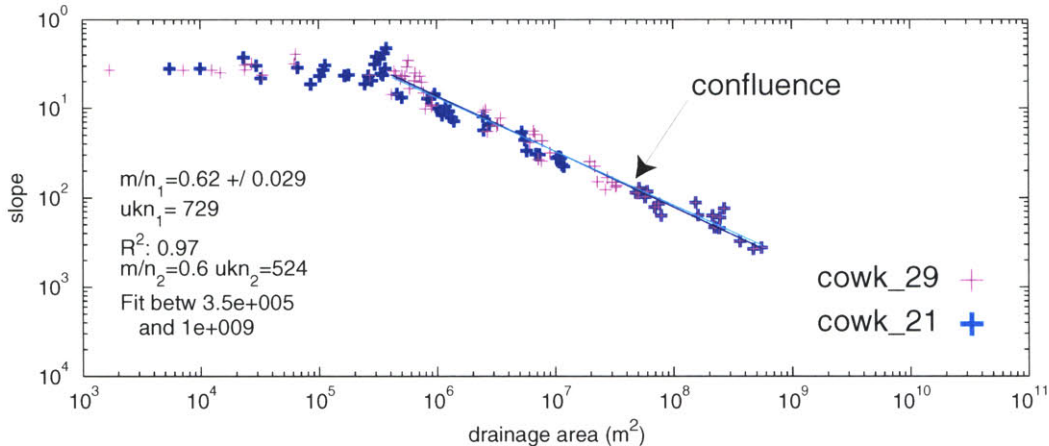
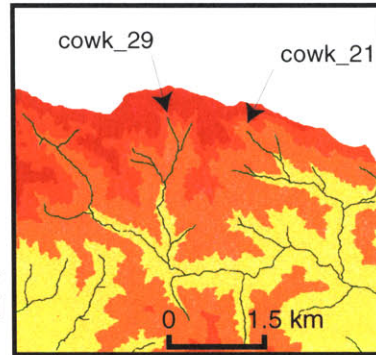


Figure 1:

The first plot of rawl_11 slope/area data is linear as expected from a log log transform of Flint's Law. The middle plot of cowk_29 shows the systematic oversteepening of the channel. Below is an example of how to interpret where two channels converge. When cowk_29 and cowk_21 join, the slope of cowk_29 increases. To the right is a DEM showing the path of the conjoining streams.



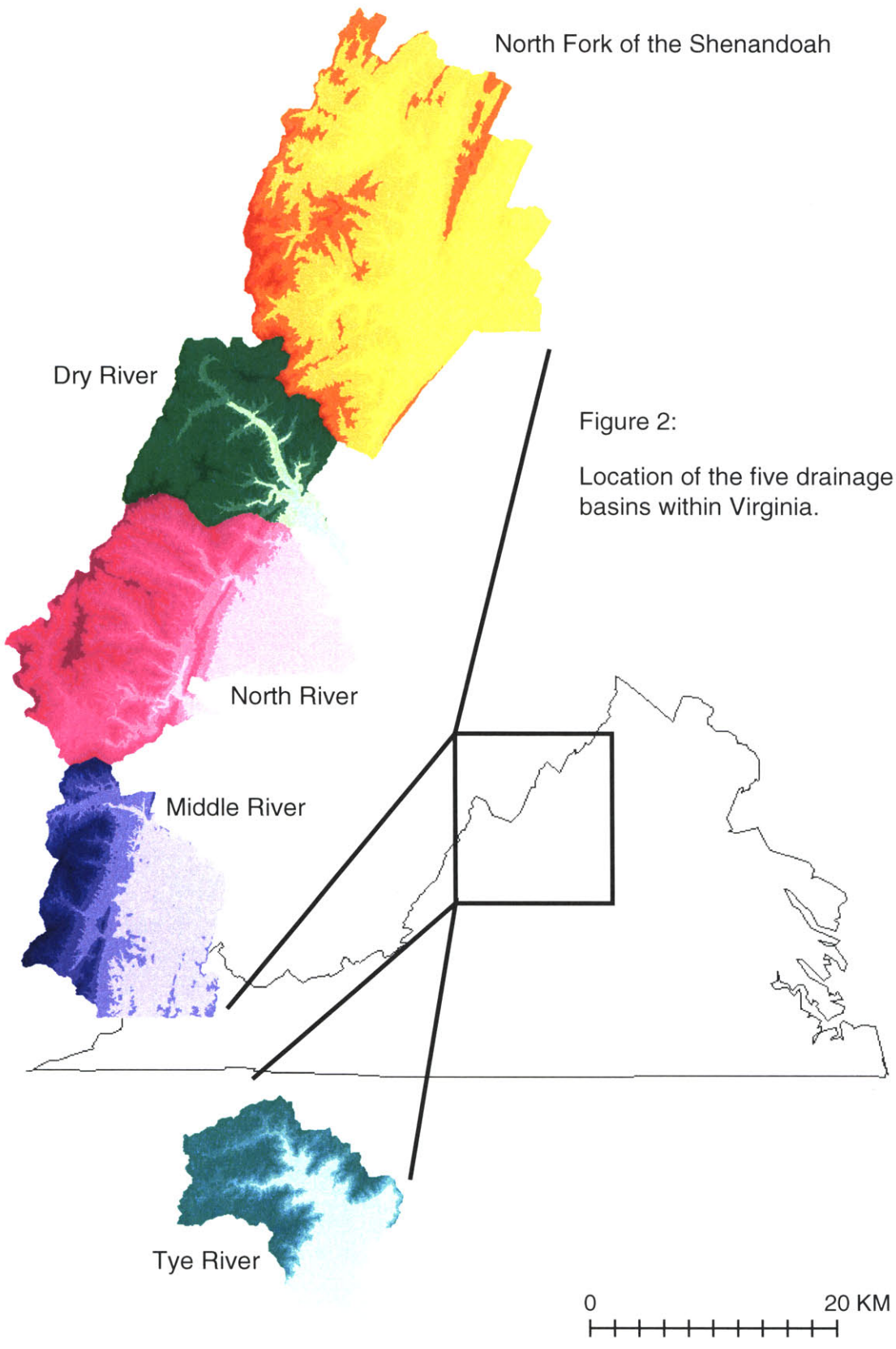


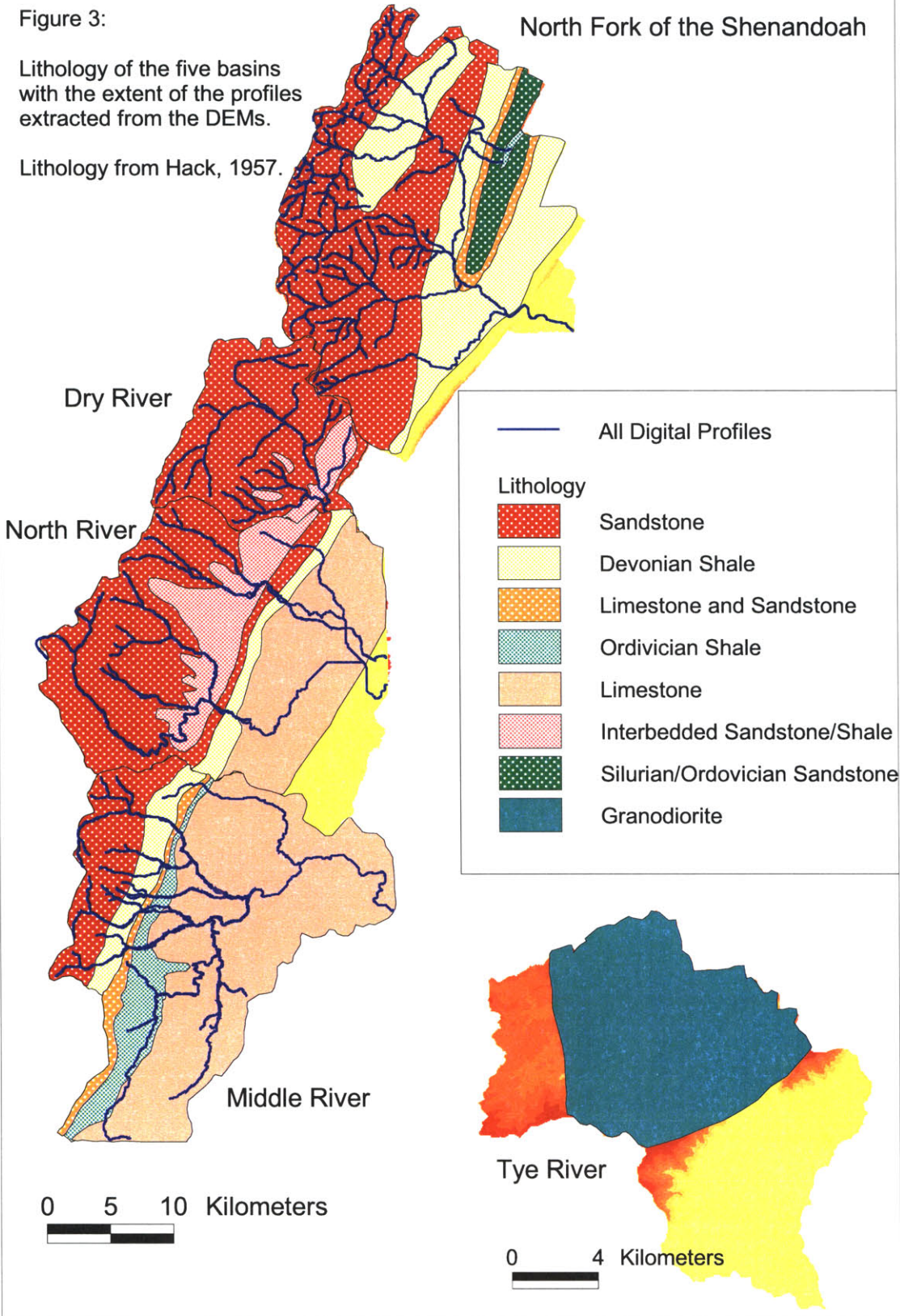
Figure 2:
Location of the five drainage
basins within Virginia.

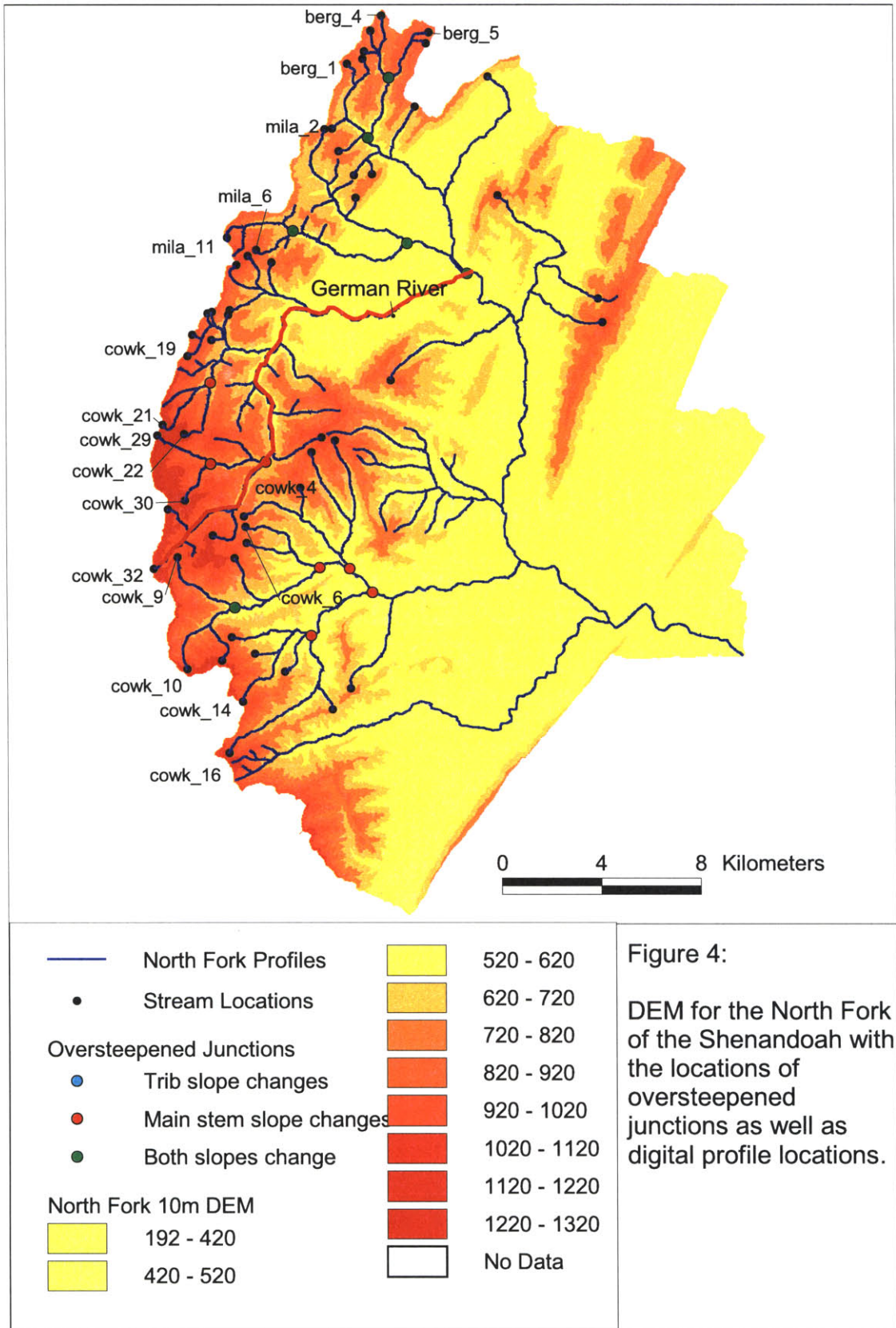
Figure 3:

Lithology of the five basins with the extent of the profiles extracted from the DEMs.

Lithology from Hack, 1957.

North Fork of the Shenandoah





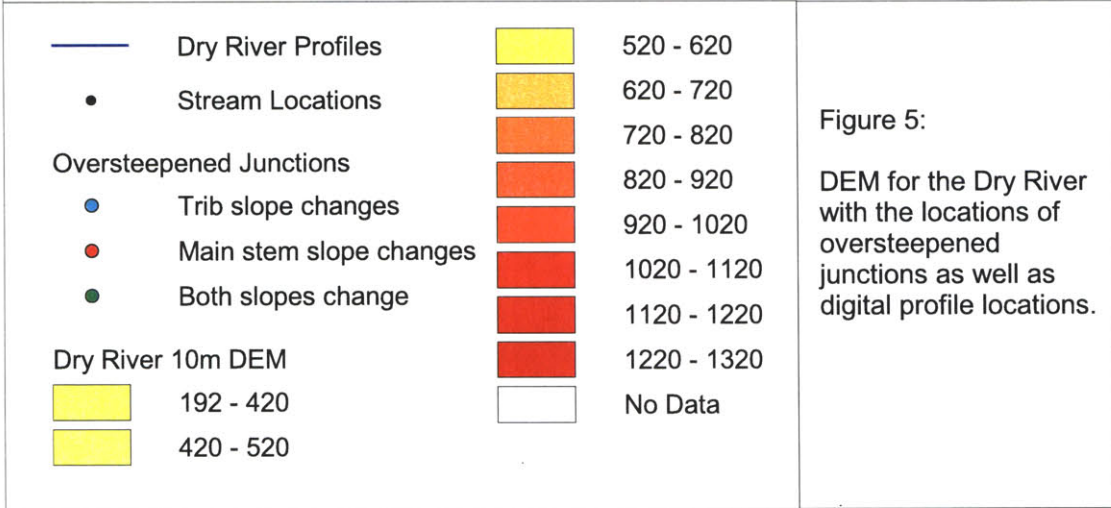
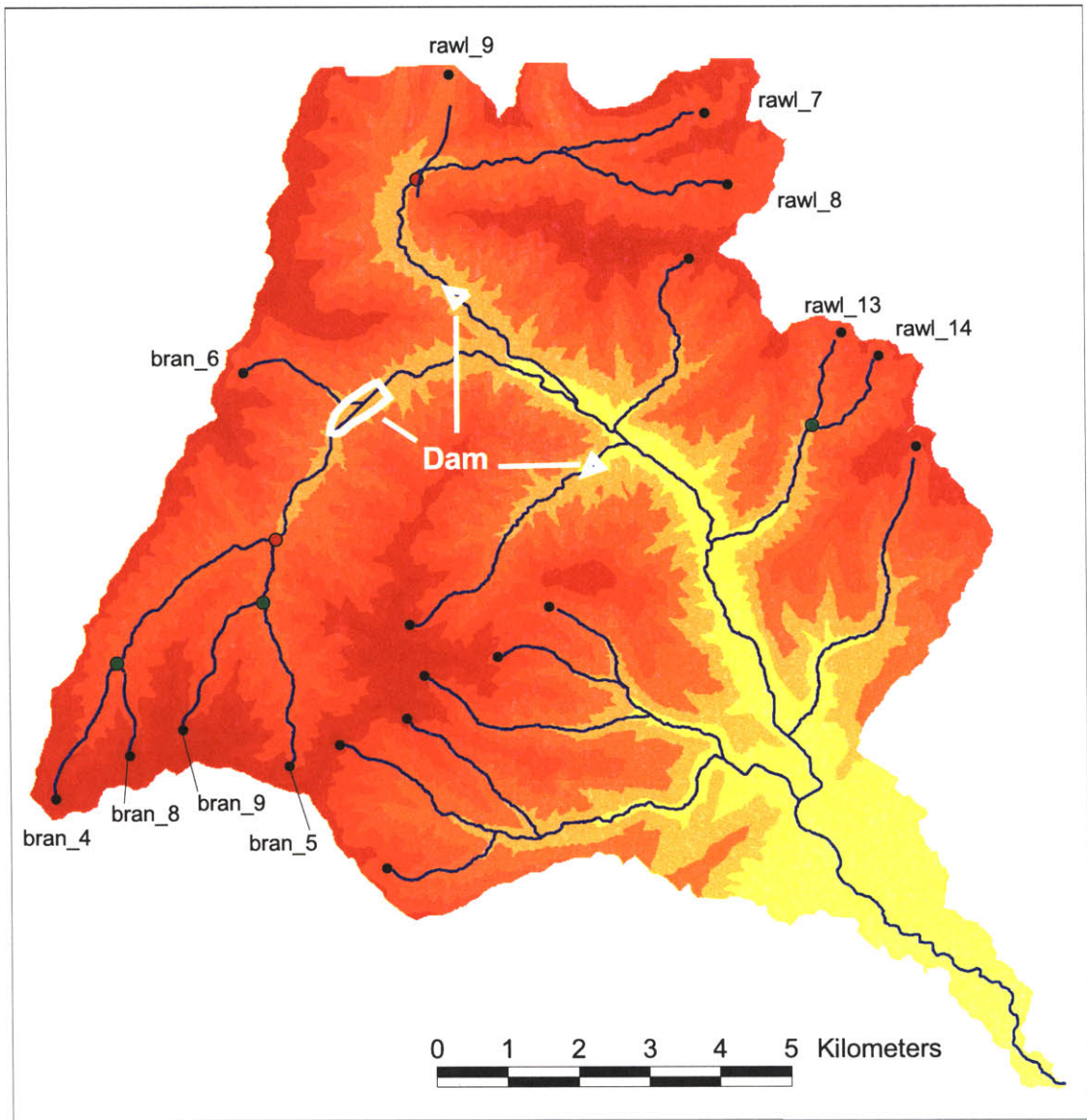


Figure 5:
DEM for the Dry River with the locations of oversteepened junctions as well as digital profile locations.

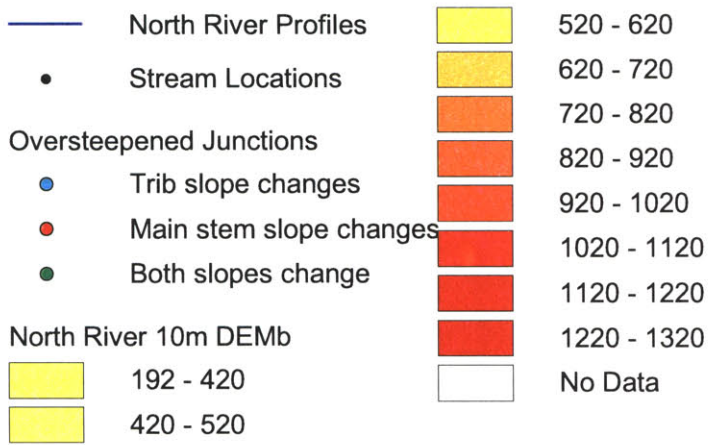
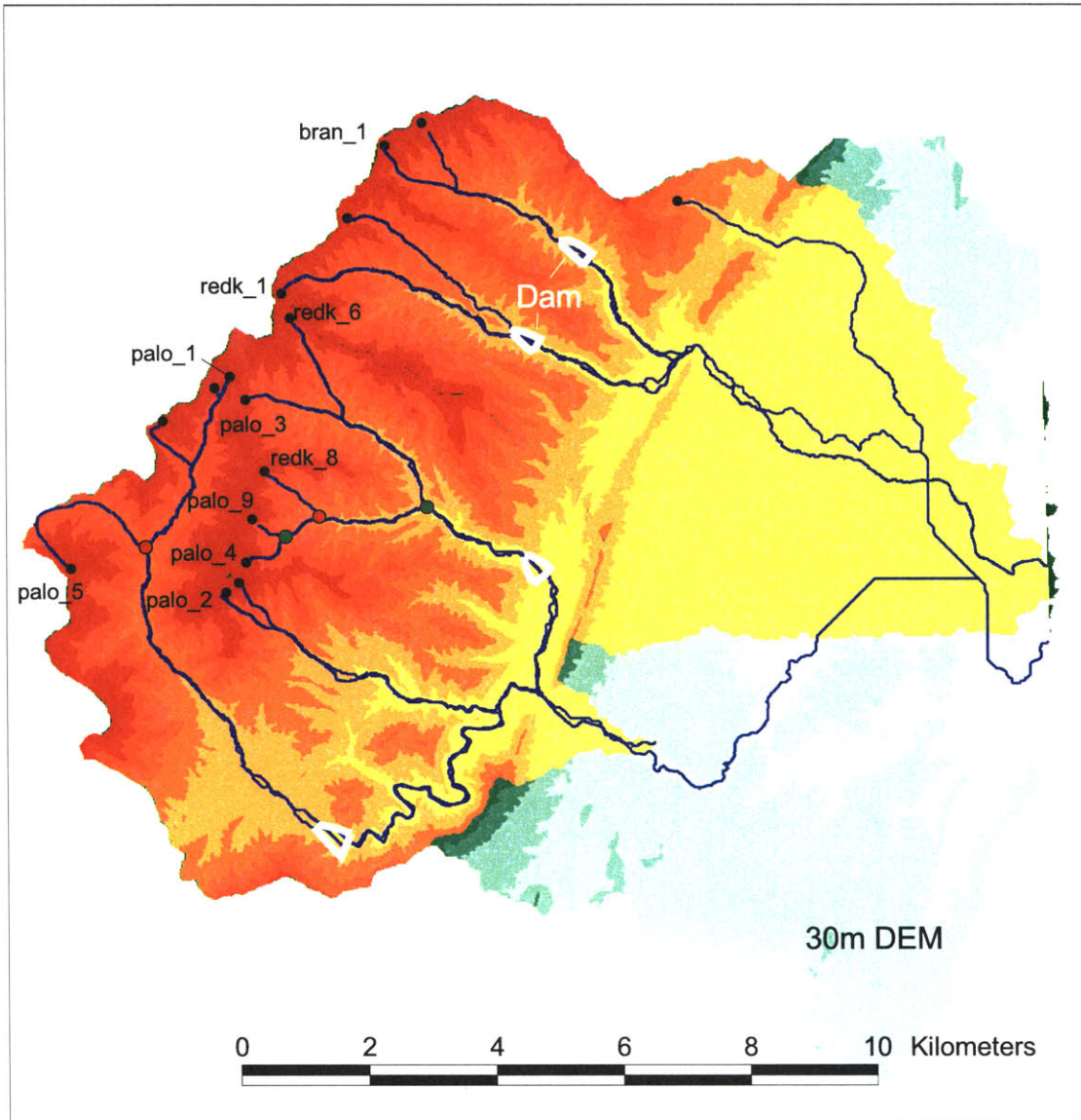


Figure 6:
DEM for the North River with the locations of oversteepened junctions as well as digital profile locations. Also shows the extent of the 10m DEM vs. the 30m DEM.

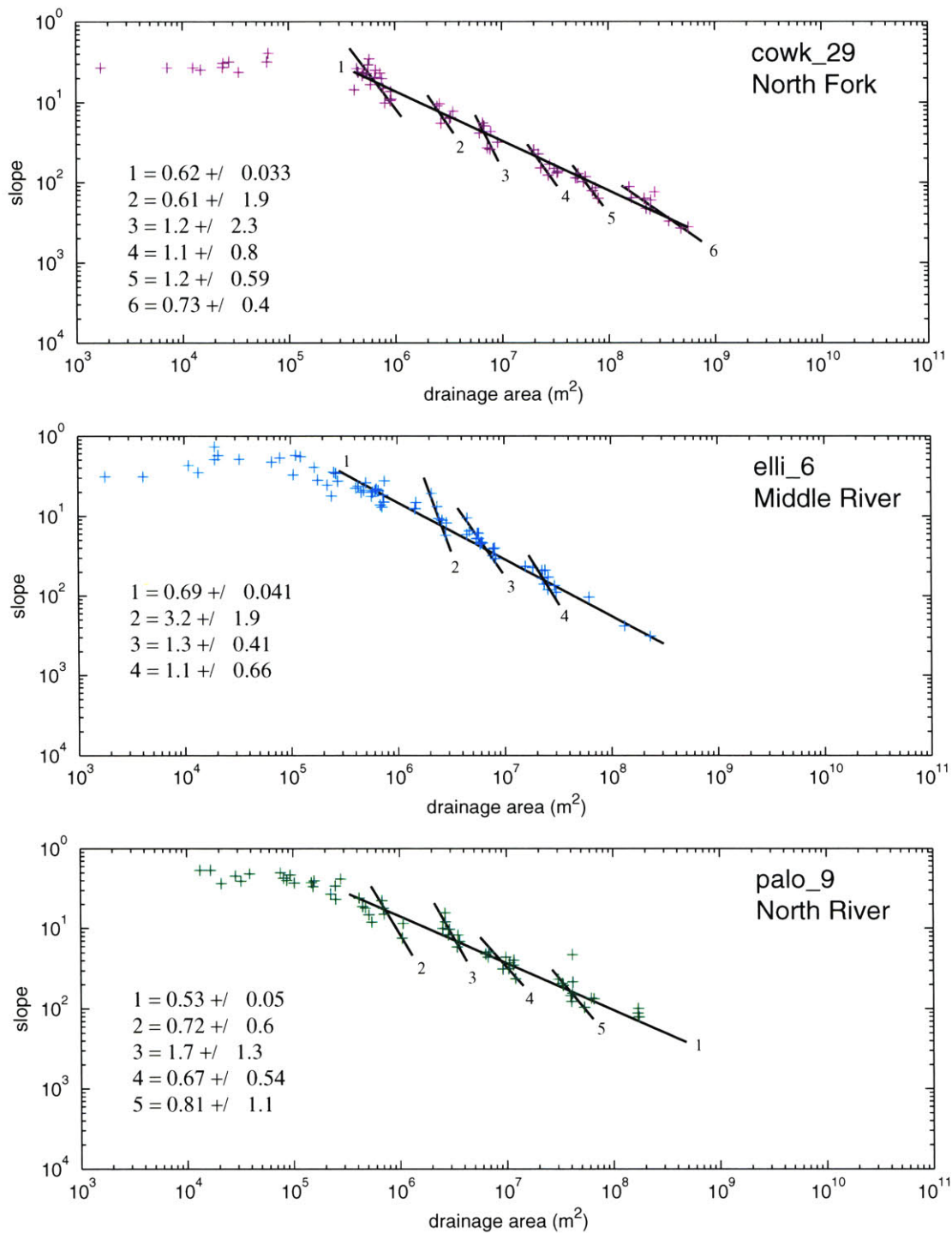


Figure 8:

The concavity of these three profiles shows similarity across all three drainage basins. Fits made through the individual steepened sections vary but show consistently high local concavities between tributary junctions.

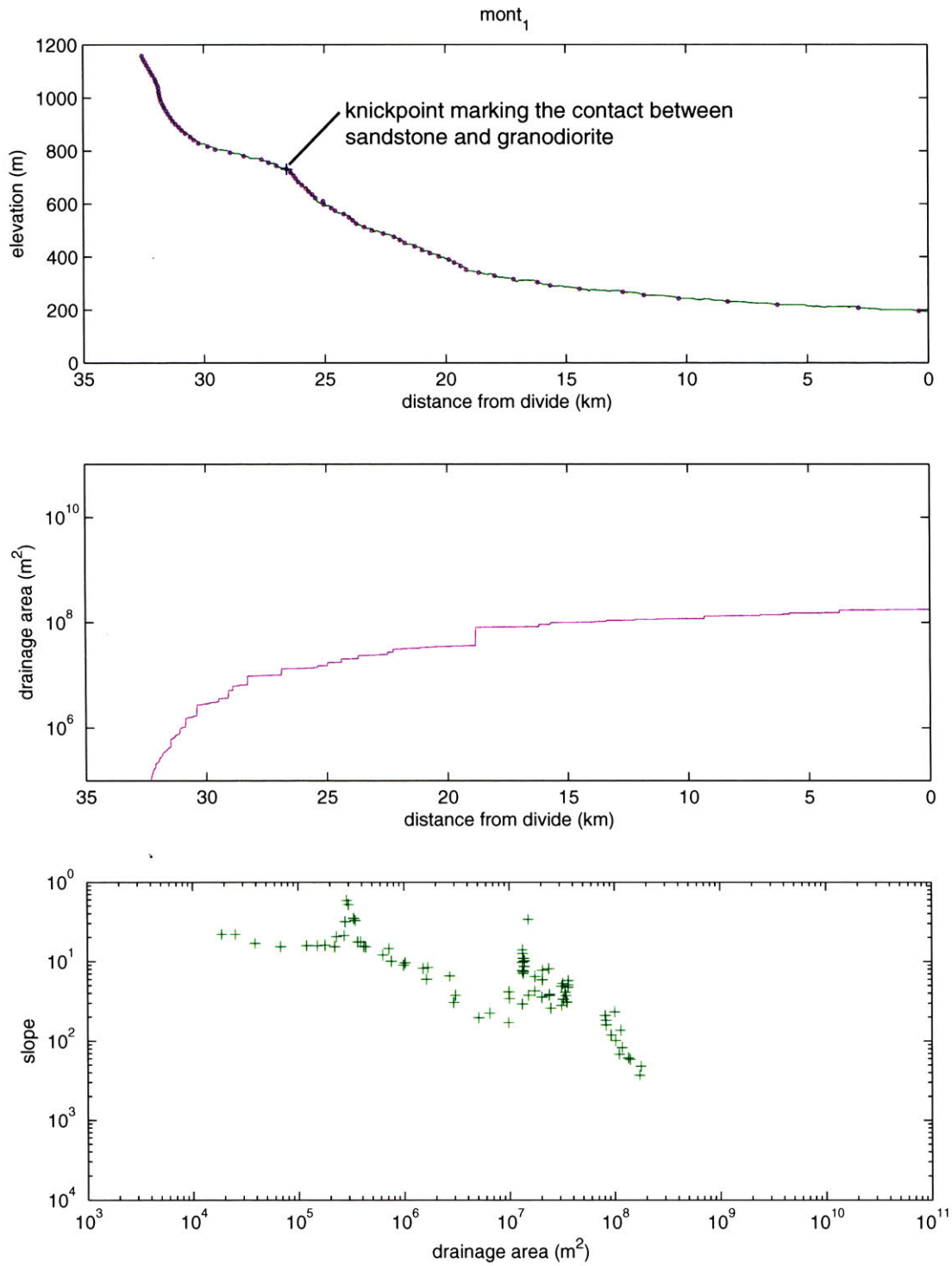


Figure 9:

Shows how the lithologic knickpoint registers in the slope/area data making any interpretation or occurrence of the see-saw pattern impossible.

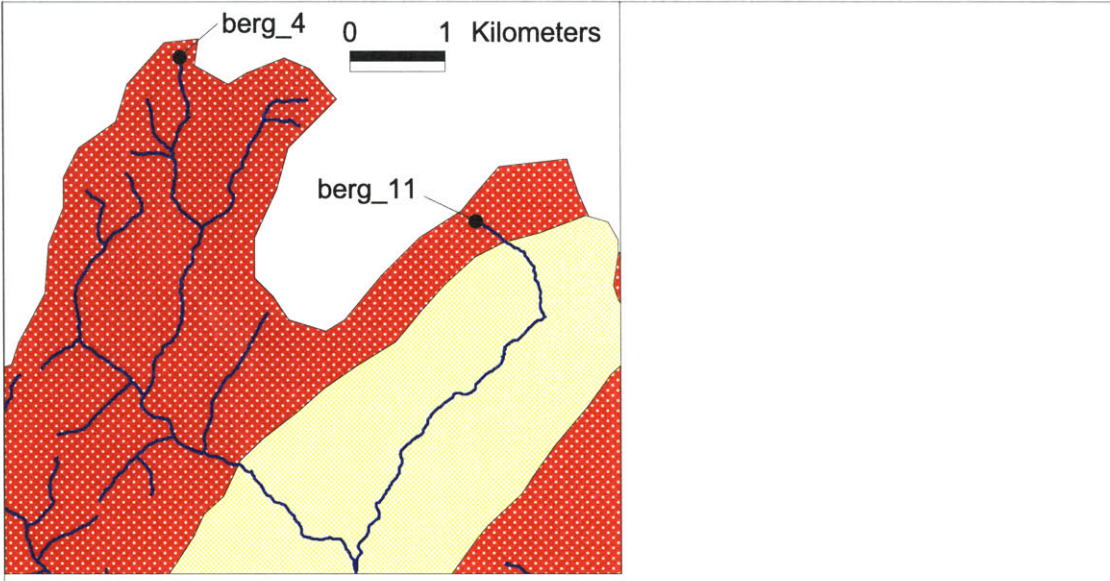
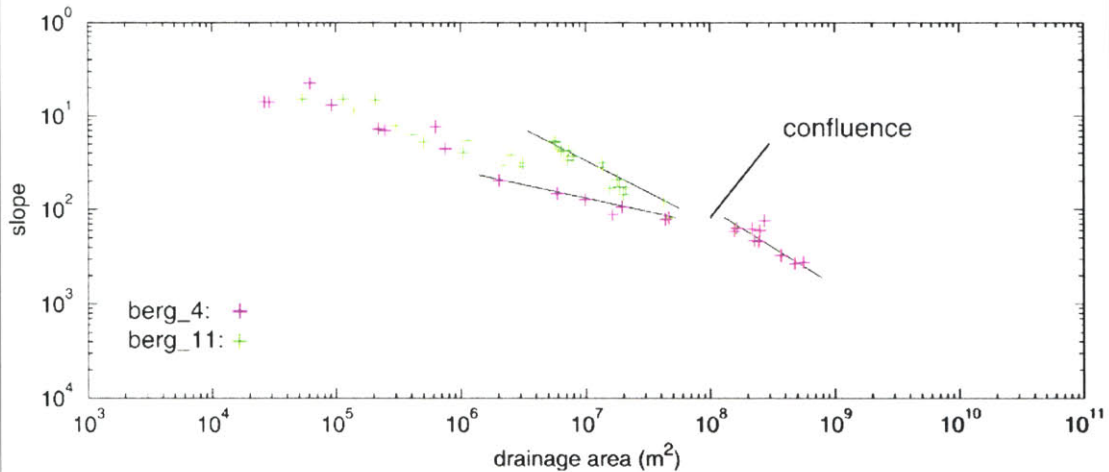
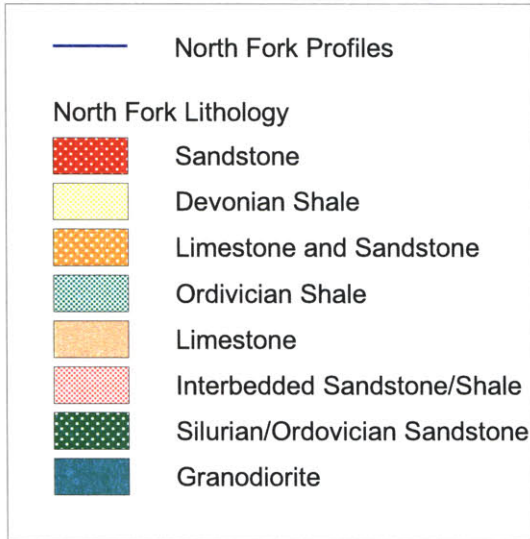


Figure 10:

Slope/area and lithologic data from berg_4 (main stem) and berg_11 (tributary). Demonstrates how berg_11 is less steep as it flows through a less resistant lithology (shale) until it joins with berg_4 which is steeper and originates in a more cohesive unit (sandstone).



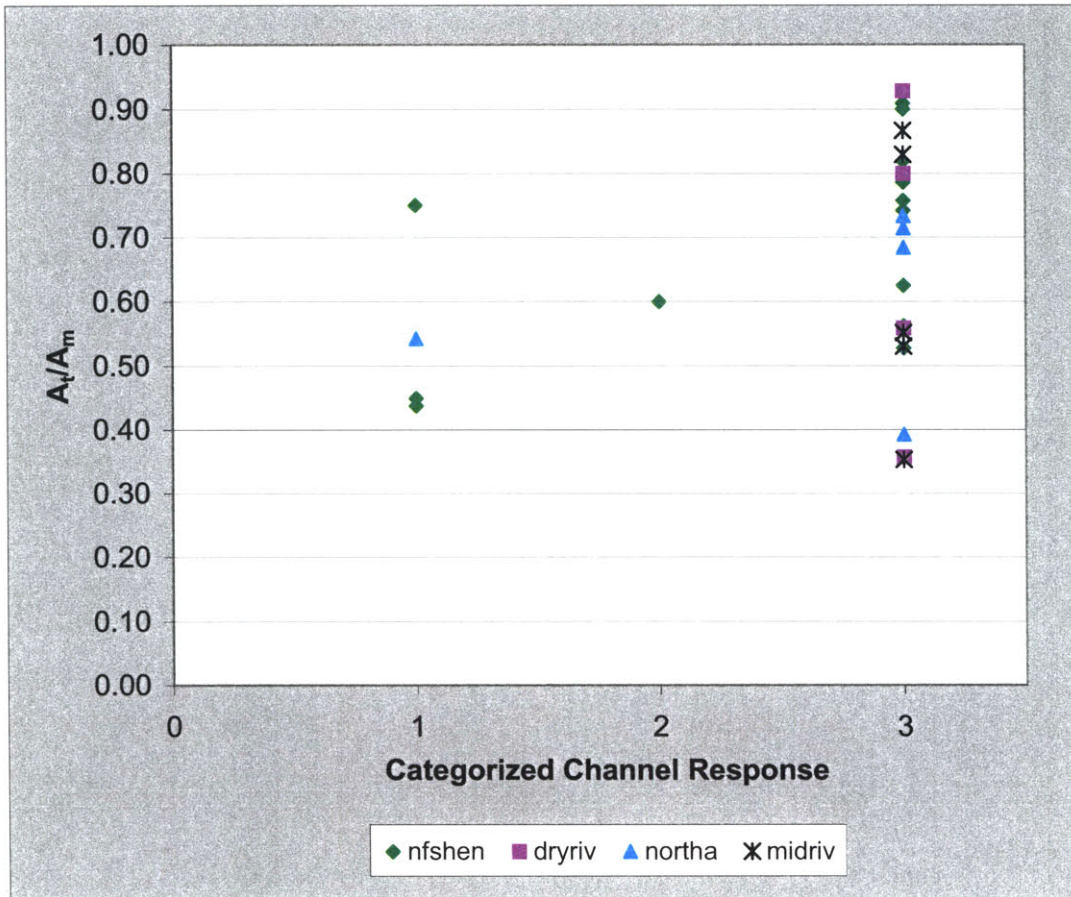


Figure 11:

Plot showing the ratio of the tributary's drainage area to that of the main stem and categorized by channel response at the confluence. The ratios don't appear to influence channel response. Neither is any basin limited to one type of channel response or grouped around a ratio value.

Channel Response Categories:

1. Only the main stem profile steepens at confluence
2. Only the tributary profile steepens
3. Both the main stem and tributary profiles increase in slope, or slope remains constant not decreasing with increasing drainage area

Basins:

1. nfshen – North Fork of the Shenandoah
2. dryriv – Dry River
3. northa – North River
4. midriv – Middle River

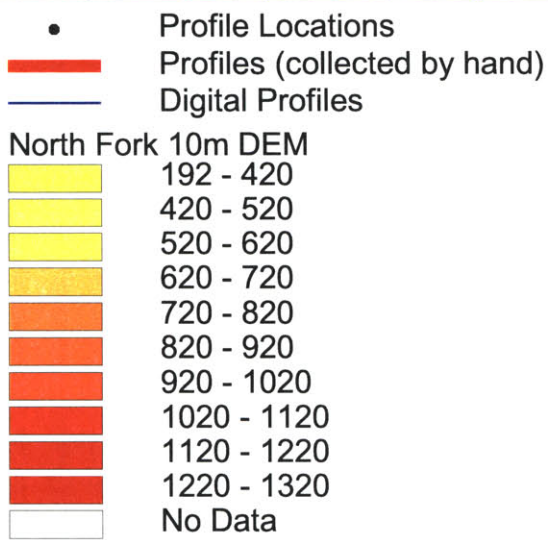
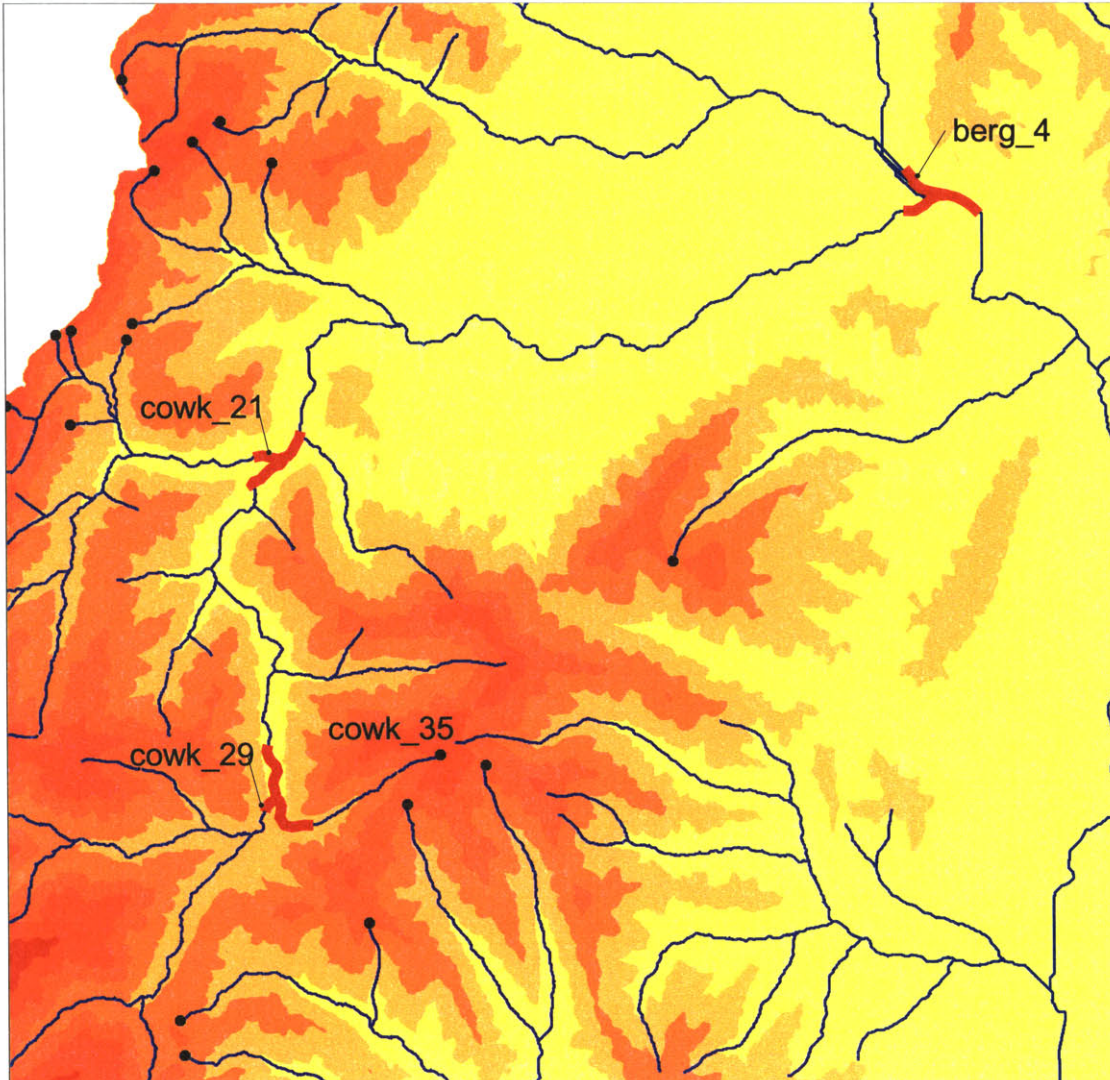
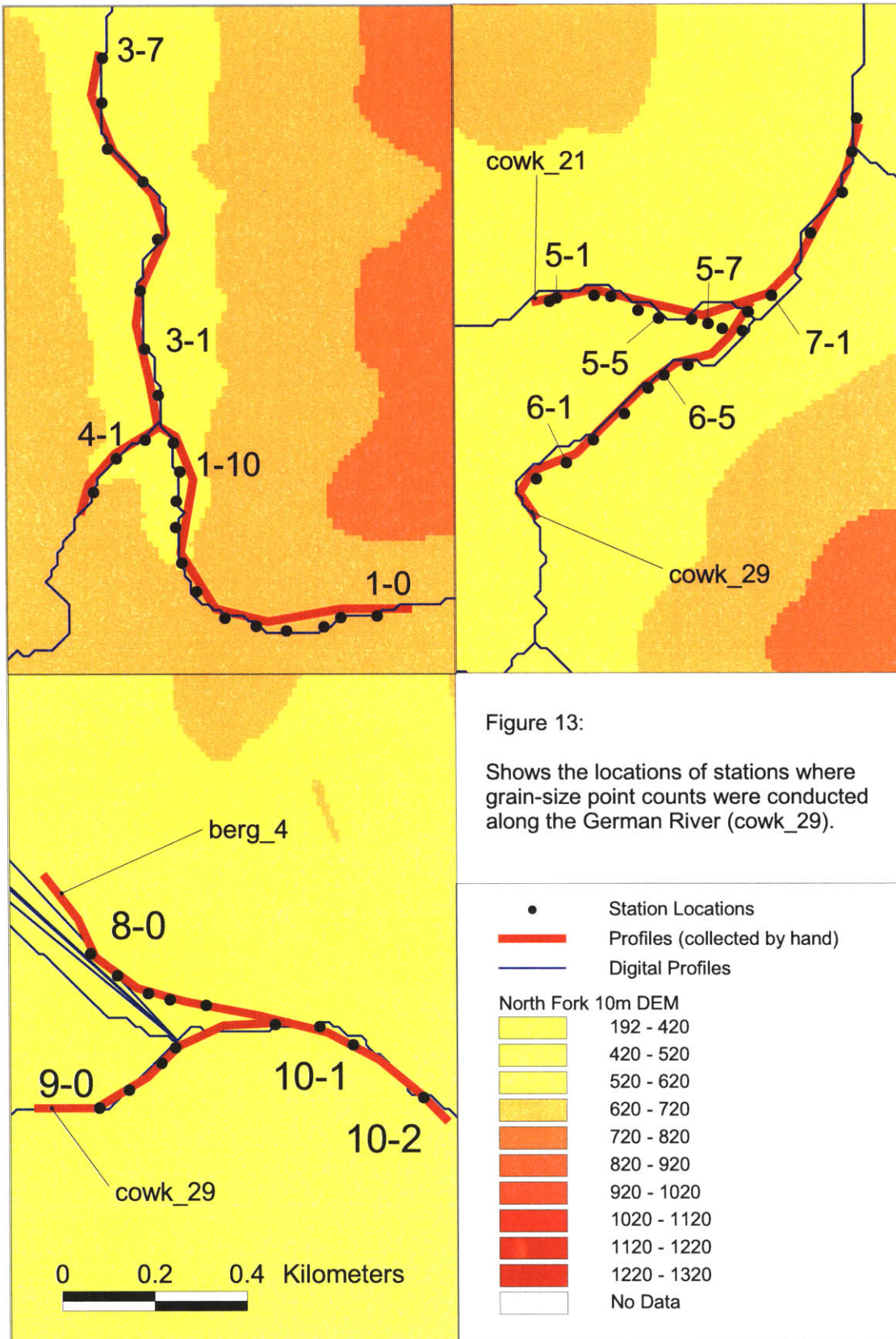
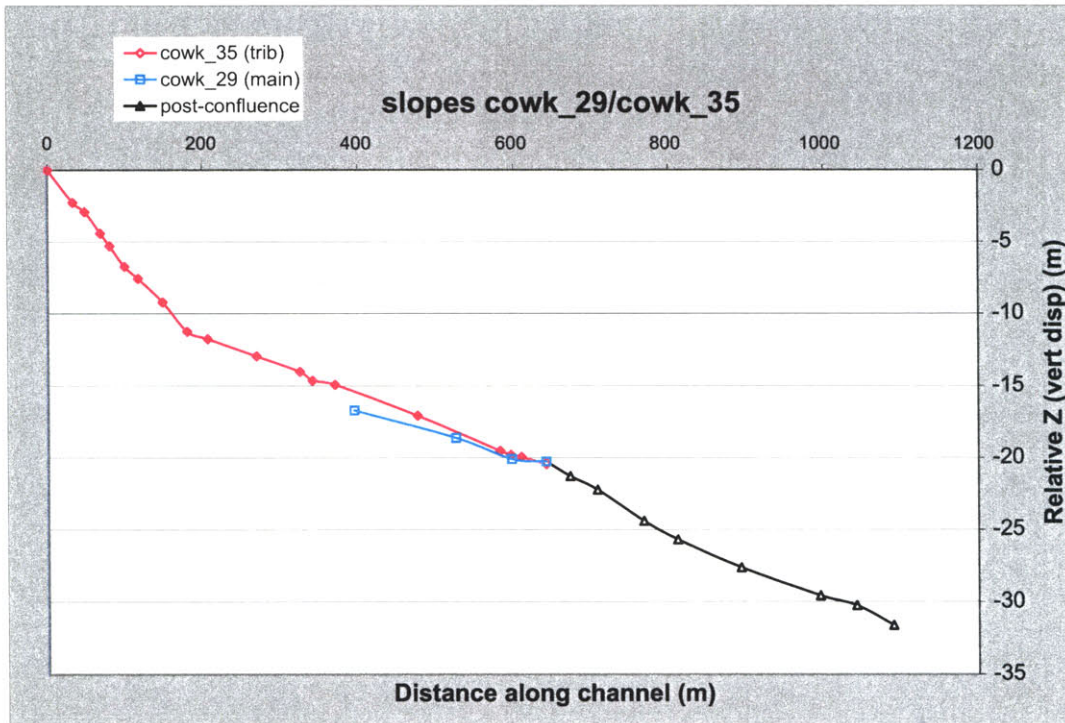
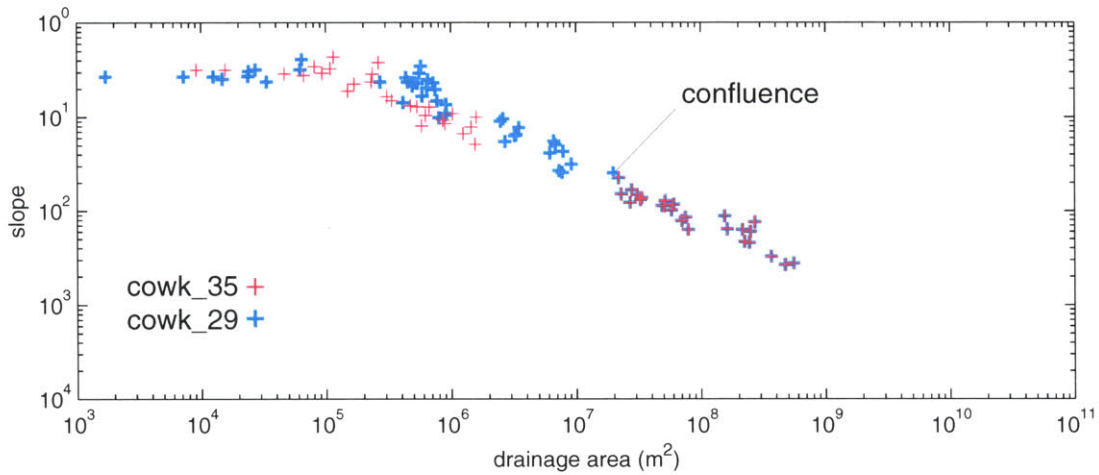


Figure 12:

Shows the locations of the hand collected profiles around oversteepened tributary junctions along the German River (cowk_29). Distance from first junction to third is approximately 20km.

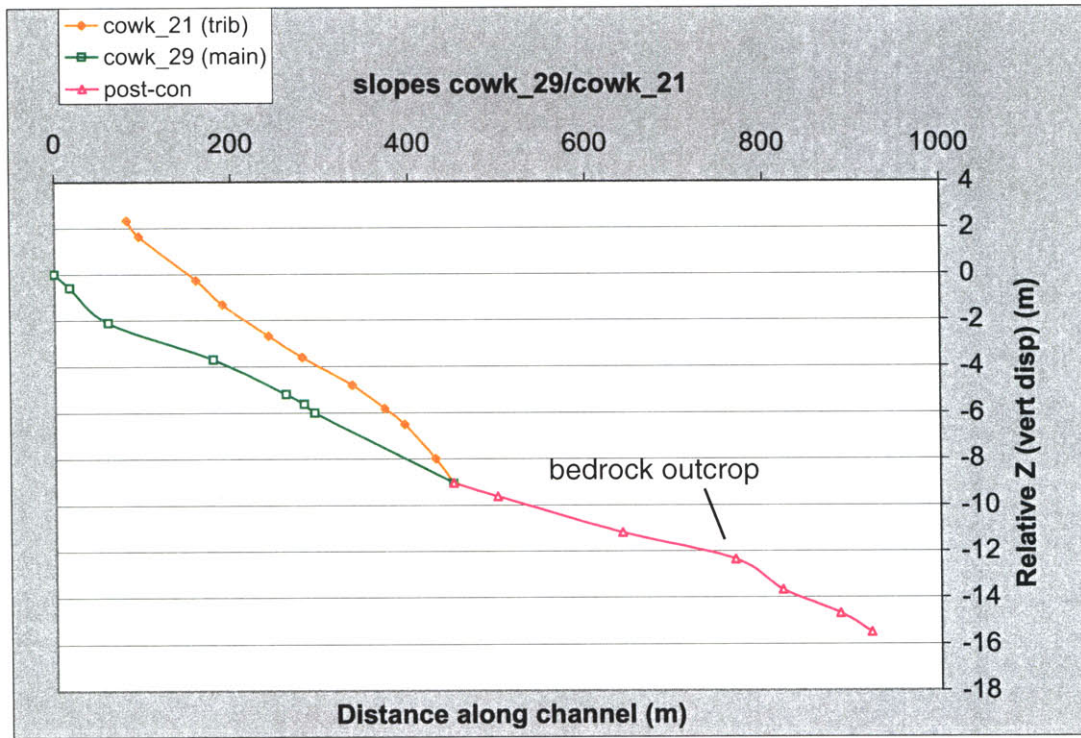
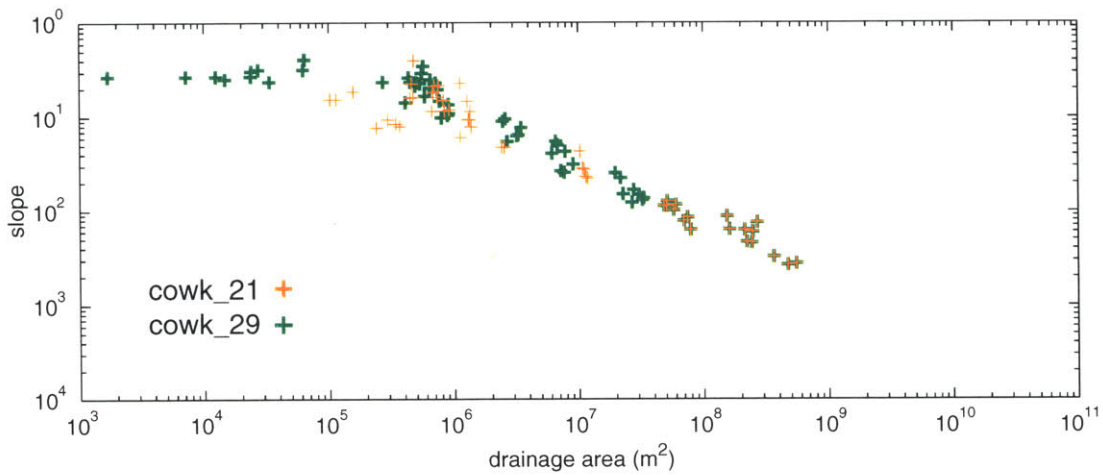




	cowk_29	cowk_35	cowk_35	post-con	post-con
mean (cm)	8.29	5.29	5.74	7.45	5.82
median	6.00	3.00	3.75	6.75	5.00
mode	5.50	0.50	1.00	1.00	0.10

Figure 14:

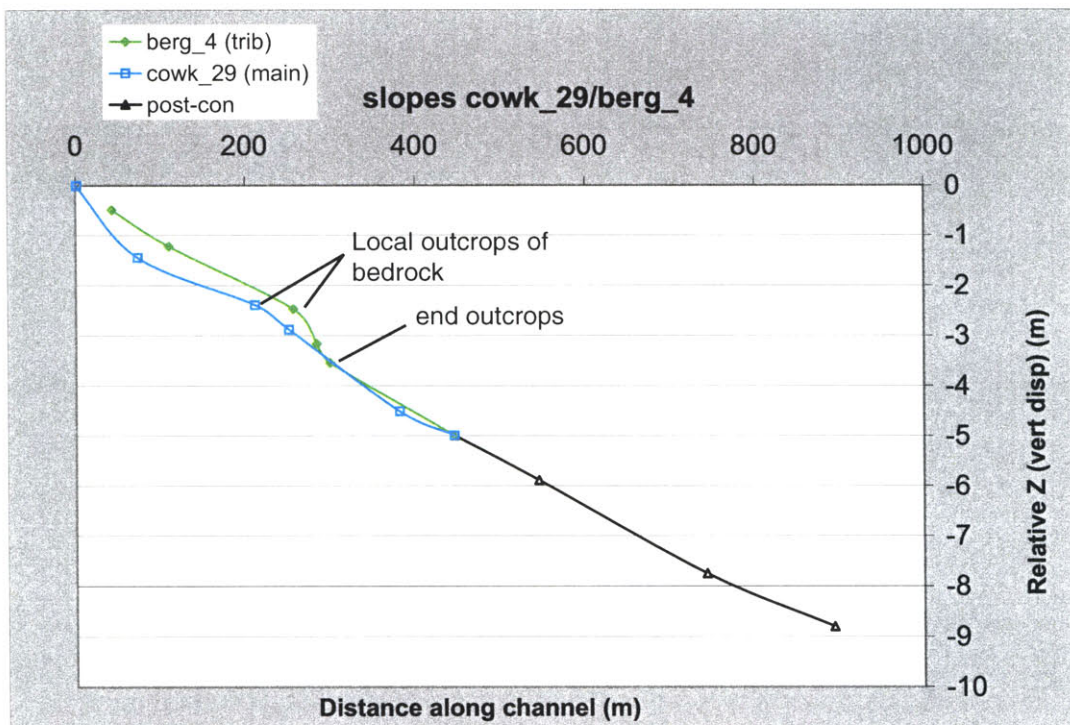
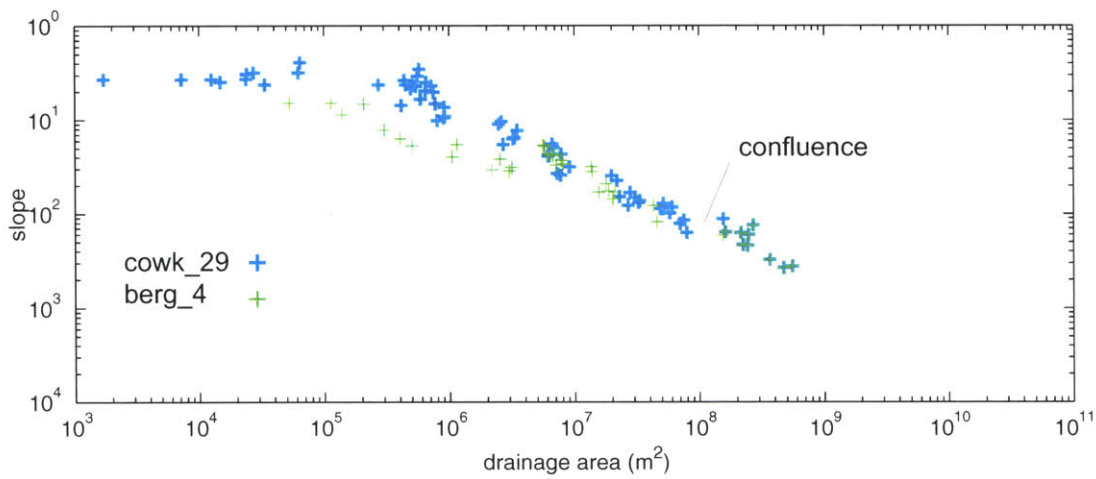
The profiles mapped by hand positively correlate to the slope/area data extracted from the DEM. Grain-size data is charted moving downstream from right to left. Comparison to the profiles reveals no obvious interdependence.



	cowk_21	cowk_21	cowk_21	cowk_29	cowk_29	post-con
mean (cm)	8.63	5.46	11.36	9.97	7.78	8.19
median	6.75	4.00	9.75	8.25	7.00	6.00
mode	8.00	0.10	18.00	11.00	8.00	0.10

Figure 15:

These profiles continue to display the same properties as at the previous confluence.



	berg_4	cowk_29	post-con	post-con
mean (cm)	5.02	8.19	4.09	5.87
median	3.00	6.00	2.75	4.50
mode	0.10	0.10	0.10	0.10

Figure 16:

Profiles steepen in response to local out crops of bedrock. At oversteepened trib junctions, bedrock was not exposed to any greater extent than anywhere else along the channel. Grain-size data at this location also confirmed a pattern of downstream fining.

Figure 17: Structure of Average Grain-size: German River (cm)

Station	Main stem	Trib.	Description	
Sta 4-1	8.29		cowk_29(main)	upstream
avg	8.29			
Sta 1-0		5.29	cowk_35 (trib)	
Sta 1-10		5.82	cowk_35 (trib)	
avg		5.56		
Sta 3-1	7.45		cowk_29 (post-con)	
Sta 3-7	5.82		cowk_29 (post-con)	
avg	6.64			
Sta 6-1	9.97		cowk_29 (main)	
Sta 6-5	7.78		cowk_29 (main)	
avg	8.88			
Sta 5-1		8.63	cowk_21 (trib)	
Sta 5-5		5.46	cowk_21 (trib)	
Sta 5-7		11.36	cowk_21 (trib)	
avg		8.49		
Sta 7-1	8.19		cowk_29 (post-con)	
avg	8.19			
Sta 8-0		5.02	berg_4 (trib)	
avg		5.02		
Sta 10-1	4.09		cowk_29 (post-con)	downstream
Sta 10-2	5.87		cowk_29 (post-con)	
avg	4.98			

*post-con: post confluence

Structure of Median Grain-size Variations: German River (cm)

Station	Main stem	Trib.	Description	
Sta 4-1	6		cowk_29(main)	upstream
avg	6.00			
Sta 1-0		3	cowk_35 (trib)	
Sta 1-10		3.75	cowk_35 (trib)	
avg		3.38		
Sta 3-1	6.75		cowk_29 (post-con)	
Sta 3-7	5		cowk_29 (post-con)	
avg	5.88			
Sta 6-1	8.25		cowk_29 (main)	
Sta 6-5	7		cowk_29 (main)	
avg	7.63			
Sta 5-1		6.75	cowk_21 (trib)	
Sta 5-5		4	cowk_21 (trib)	
Sta 5-7		9.75	cowk_21 (trib)	
avg		6.83		
Sta 7-1	6		cowk_29 (post-con)	
avg	6.00			
Sta 8-0	3		berg_4 (trib)	
avg				
Sta 10-1		2.75	cowk_29 (post-con)	downstream
Sta 10-2		4.5	cowk_29 (post-con)	
avg		3.625		

Figure 18: Width Structure (m)

Station	Main stem	Trib.	Description	
Sta 4-1	12.35		cowk_29 (main)	upstream
avg	12.35			
Sta 1-0		4.63	cowk_35 (trib)	
Sta 1-1		3.29		
Sta 1-3		2.60		
Sta 1-5		3.87		
Sta 1-6		3.97		
Sta 1-8		5.02		
Sta 1-11		8.80		
Sta 2-3		9.25		
avg		3.90		
Sta 3-0	6.86		cowk_29 (post-con)	
Sta 3-2	8.37			
Sta 3-4	10.40			
avg	8.54			
sum	16.25			
Sta 6-0	5.88		cowk_29 (main)	
Sta 6-6	9.67			
avg	7.78			
Sta 5-2		7.21	cowk_21 (trib)	
Sta 5-3		5.63		
Sta 5-5		6.83		
Sta 5-7		3.40		
avg		5.77		
Sta 7-1	20		cowk_29 (post-con)	
Sta 7-4	10			
avg	15.00			
sum	13.54			
Sta 9-0	13.98		cowk_29 (main)	
	13.98			
Sta 8-0		12.73	berg_4 (trib)	
Sta 8-1		15.78		
Sta 8-4		12.44		
		13.65		
Sta 10-1	23.38		cowk_29 (post-con)	
Sta 10-2	13.65			
avg	18.52			
sum	27.63			downstream

*sum: sum of incoming channel widths

**post-con: post confluence

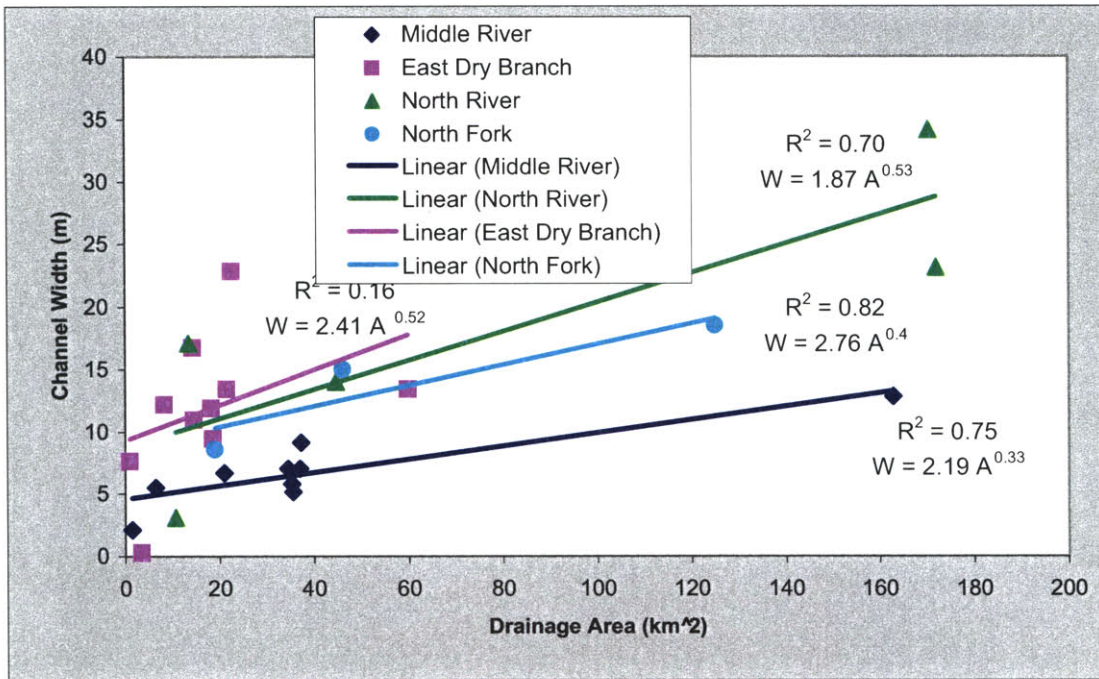


Figure 19:

Channel widths for the major streams in the region scale as expected with drainage area. However, the three profiles that have oversteepened tributary junctions do scale faster than the lower portion of the Middle River. Width data for the North River, East Dry Branch, and Middle River is all taken from Hack (1957).

9 APPENDIX

Appendix 9.1

Hack (1957) Principal measurements at selected localities

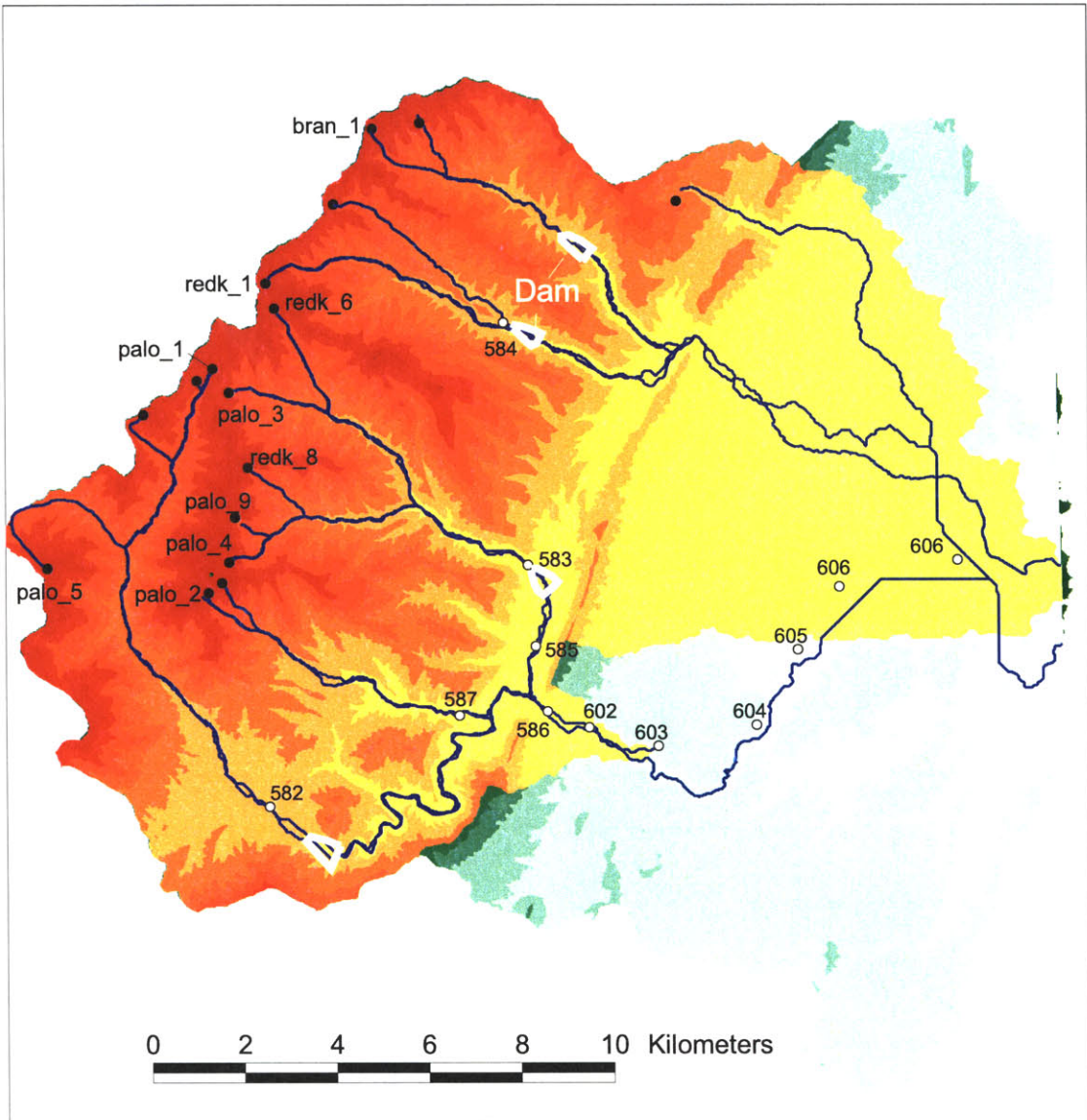
Appendix 9.1.1 Data Tables

Locality	Basin	River	Length (km)	Area (km ²)	Median grain-size (mm)	Trask sorting	Width (m)
569B	Middle River	East Dry Branch	1.931	2.590	100	6.00	
643		do	4.506	8.288	166	1.90	12.19
642		trib	1.046	0.311	128	2.50	3.35
612		trib	1.287	0.906	76	2.60	7.62
610		do	7.725	14.245	80	2.10	16.76
607		do	7.886	14.504	98	2.00	10.97
608		do	9.012	18.285	62	1.60	11.89
609		do	9.978	18.648	60	1.60	9.45
611		do	11.265	21.497	83	1.60	13.41
614		do	12.714	22.533	69	1.70	22.86
613		do	14.323	59.829	62	1.90	13.41
624		Middle River	17.703	110.074	22	2.10	
623		do	25.910	162.910	142	2.20	12.80
622		do	29.612	253.042	74	2.10	23.16
615		do	37.337	354.051	45	2.10	17.98
575		do	39.107	383.059	58	2.30	27.43
576		do	39.429	382.800	105	2.50	29.57
589		do	40.073	383.836	59	2.70	40.84
588		do	40.234	384.613	50	1.80	48.77
592		do	42.326	390.052	110	1.60	27.74
591		do	42.809	391.088	81	1.10	17.98
597		do	45.223	465.939	49	2.60	31.39
593		do	46.188	467.493	110	2.00	25.30
596		do	46.993	468.529	91	1.40	23.77
619		do	50.212	478.630	65	1.30	26.82
617		do	51.016	478.889	80	2.25	25.60
599		do	55.361	498.573	64	1.50	
649		Edison Creek	1.609	1.399			2.13
648		do	3.621	6.475	7	4.50	5.49
647		do	8.851	20.979	18	2.00	6.71
639		do	12.553	34.447	16	2.20	7.01

Appendix 9.1.1 Data Tables cont.

Locality	Basin	River	Length (km)	Area (km ²)	Median grain-size (mm)	Trask sorting	Width (m)
638	Middle River	Edison Creek	12.875	34.965	16	2.20	
637		do	13.358	35.224	42	2.30	5.79
634		do	13.679	35.483	66	2.10	5.18
635		do	14.484	37.037	38	1.70	7.01
636		do	14.806	37.296	10	2.25	9.14
582	North River	North River	15.933	44.548	107	1.70	14.02
585		trib	3.862	3.108	100	1.90	10.67
584		trib	5.955	8.547	66	2.15	17.07
587		trib	8.208	17.094	77	2.50	13.41
583		trib	11.104	40.922	80	1.70	41.76
586		do	29.773	170.421	130	1.70	34.14
602		do	31.060	171.975	110	2.00	23.16
603		do	33.796	176.378	95	1.50	31.09
604		do	36.693	199.792	66	1.60	54.86
605		do	39.107	211.602	64	1.60	32.31
606A		do	41.199	216.523	48	1.70	24.38
606B		do	45.223	263.661	42	4.20	38.71
579	Tye River	Tye River	6.116	15.281	380	2.40	9.75
578		do	8.530	31.080	500	3.00	13.41
580		do	10.300	34.965	350	6.00	11.58
577		do	13.840	82.880	230	2.50	24.99
581		trib	3.219	5.957	630	3.20	4.88

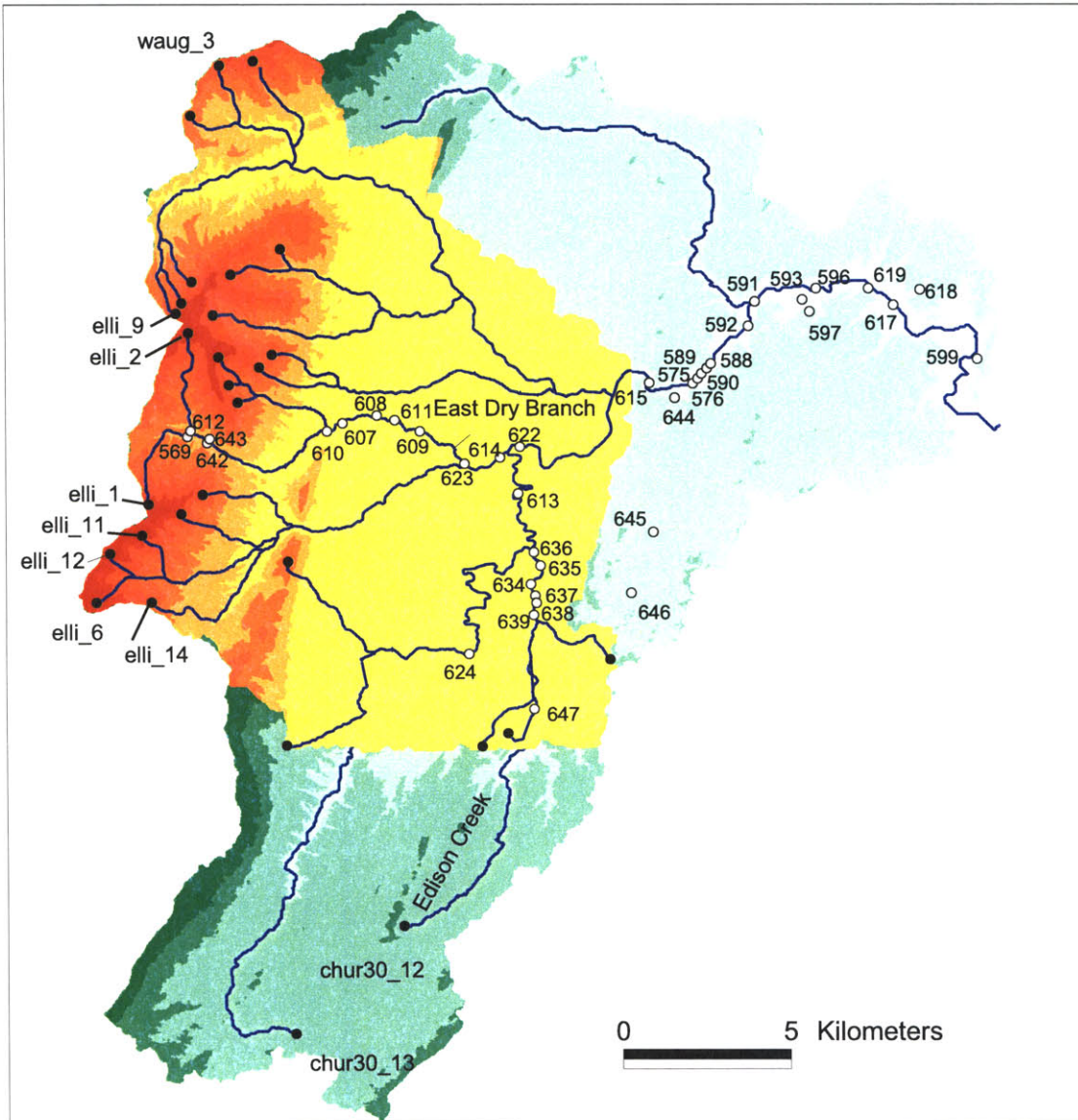
9.1.2 Data Locations



- North River Profiles
- Stream Locations
- Hack Data Locations

Appendix 9.1.2.1:

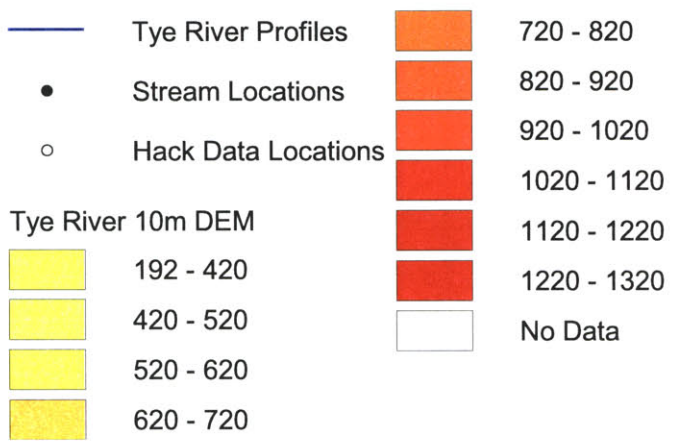
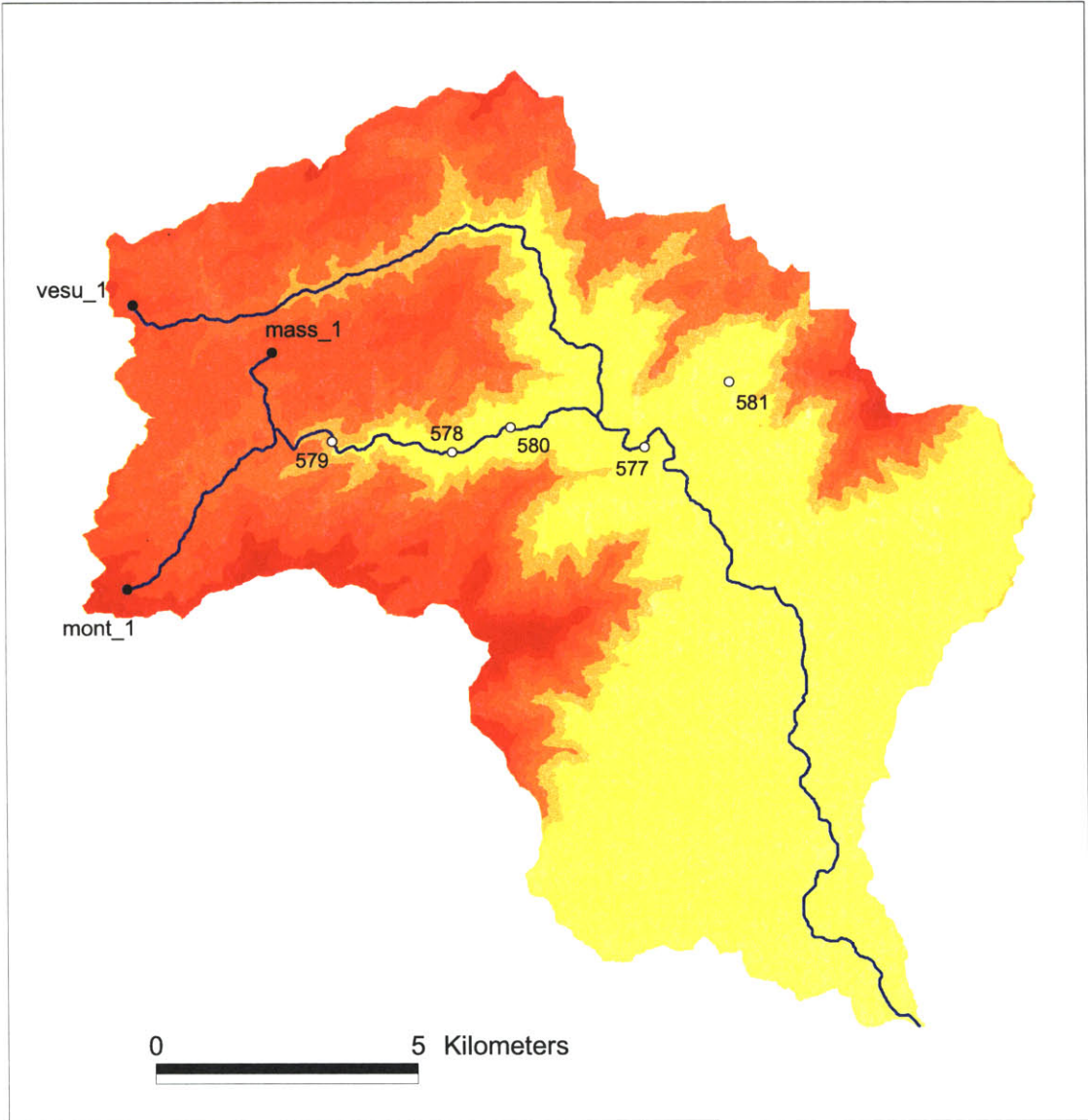
Shows locations of Hack's (1957) grain-size data. It is also possible to see where the channels increase in sinuosity at lower elevations perhaps indicating a transition from mixed bedrock-alluvial conditions to a fully alluvial regime.



-  Middle River Profiles
-  Stream Locations
-  Hack Data Locations

Appendix 9.1.2.2:

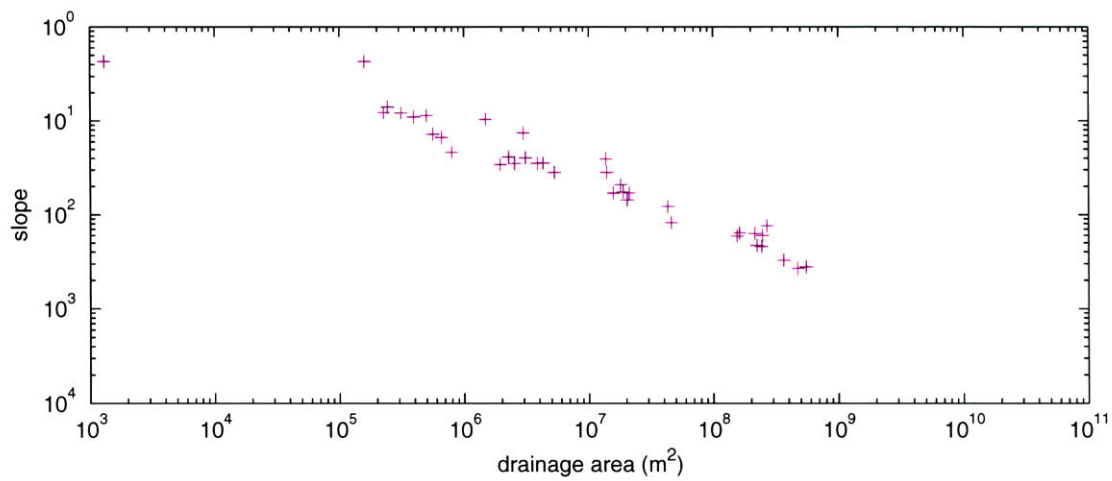
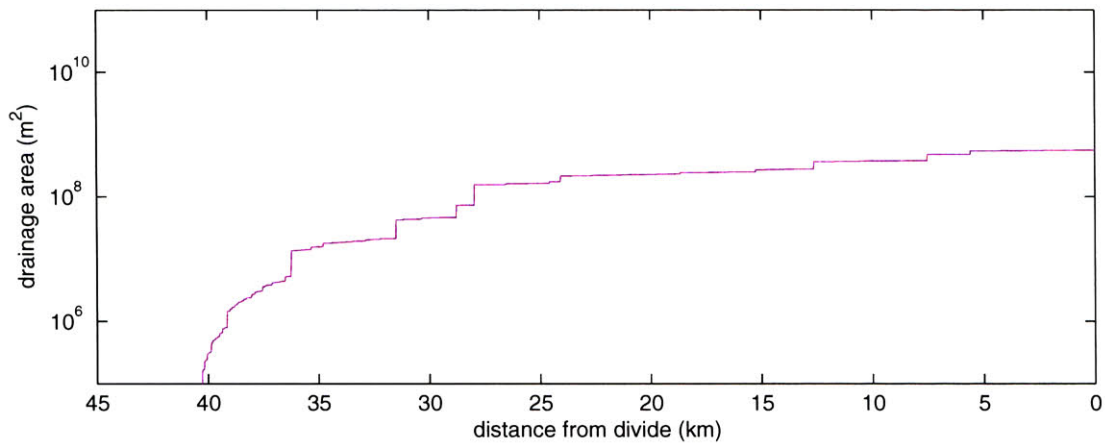
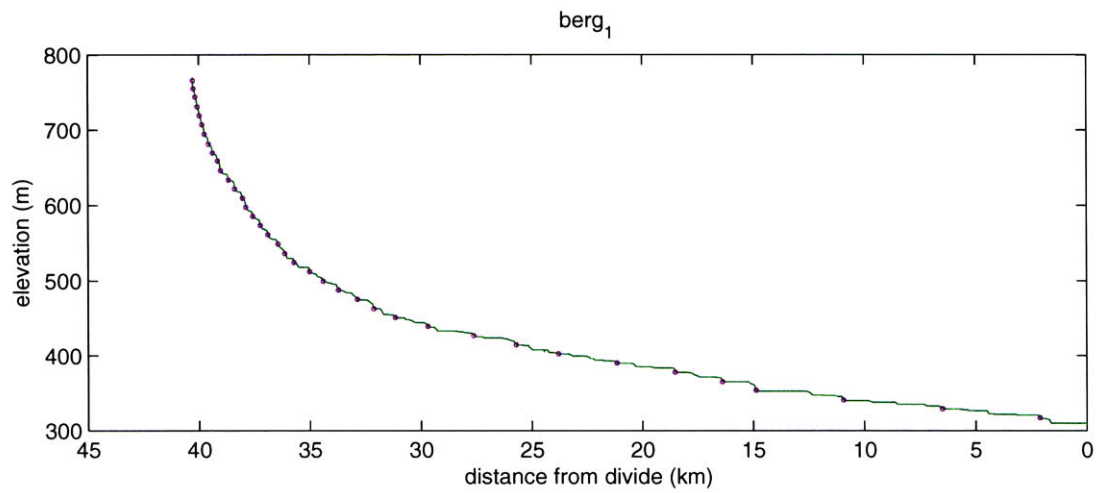
Shows locations of Hack's (1957) grain-size data. It is also possible to see where the channels increase in sinuosity at lower elevations perhaps indicating a transition from mixed bedrock-alluvial conditions to a fully alluvial regime.

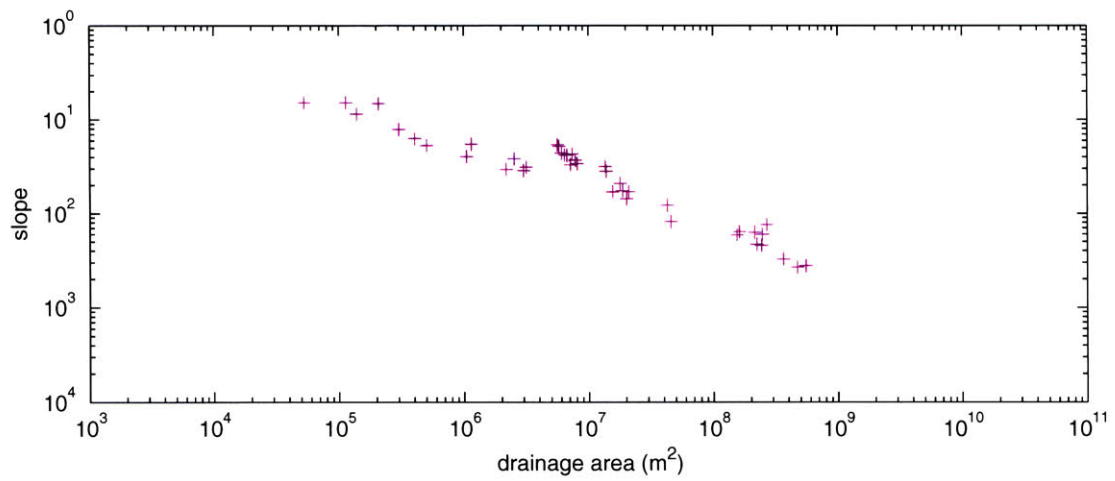
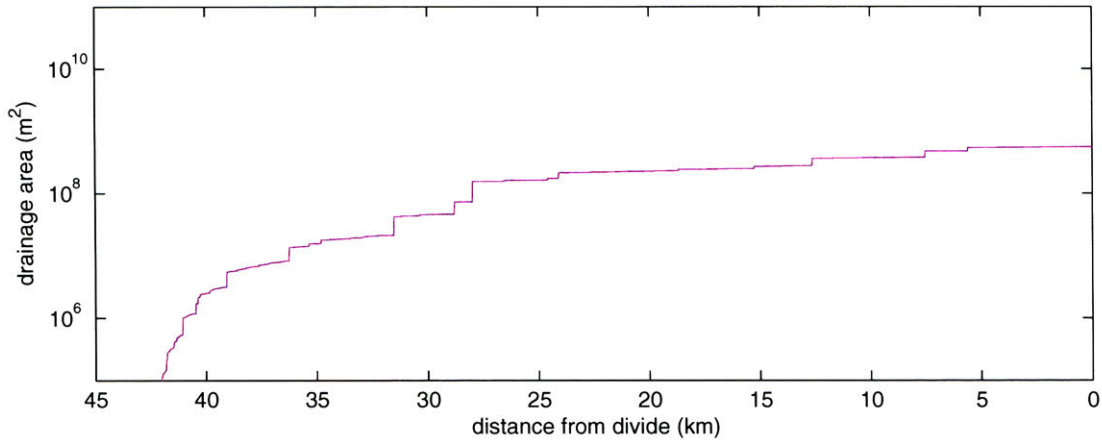
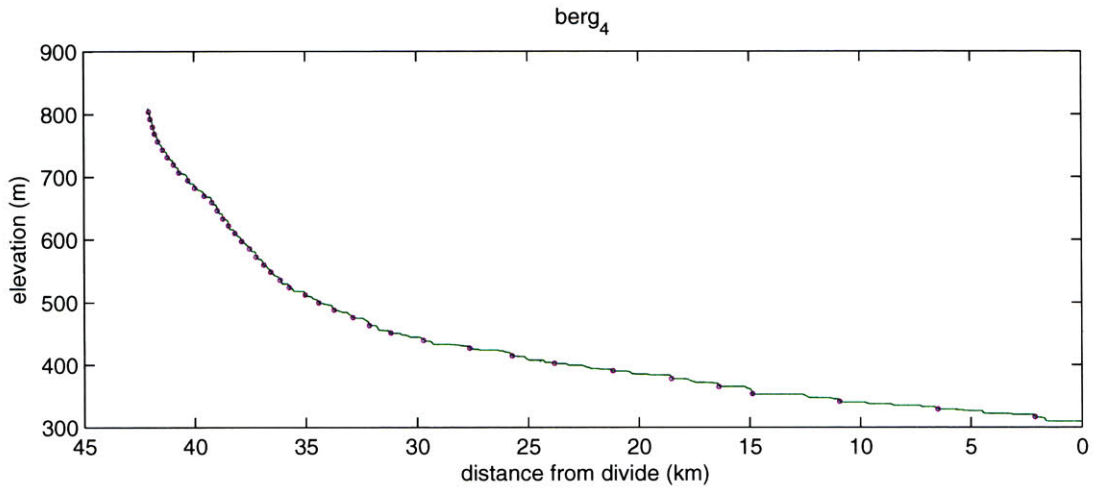


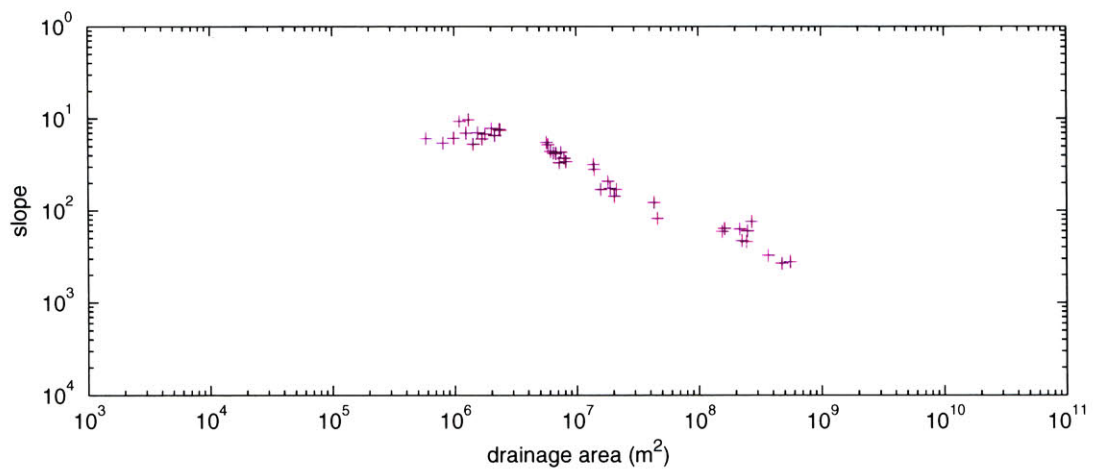
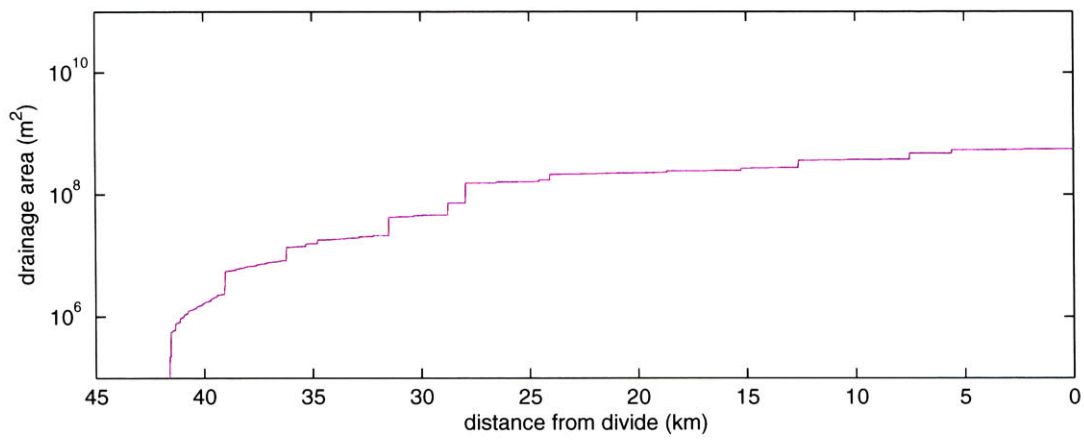
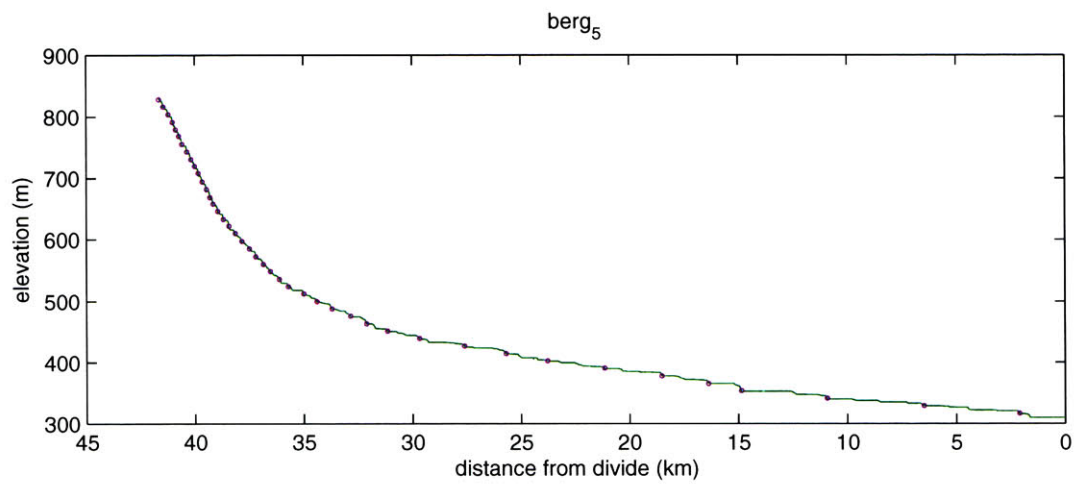
Appendix 9.1.2.3:
Shows locations of Hack's grain-size data (1957).

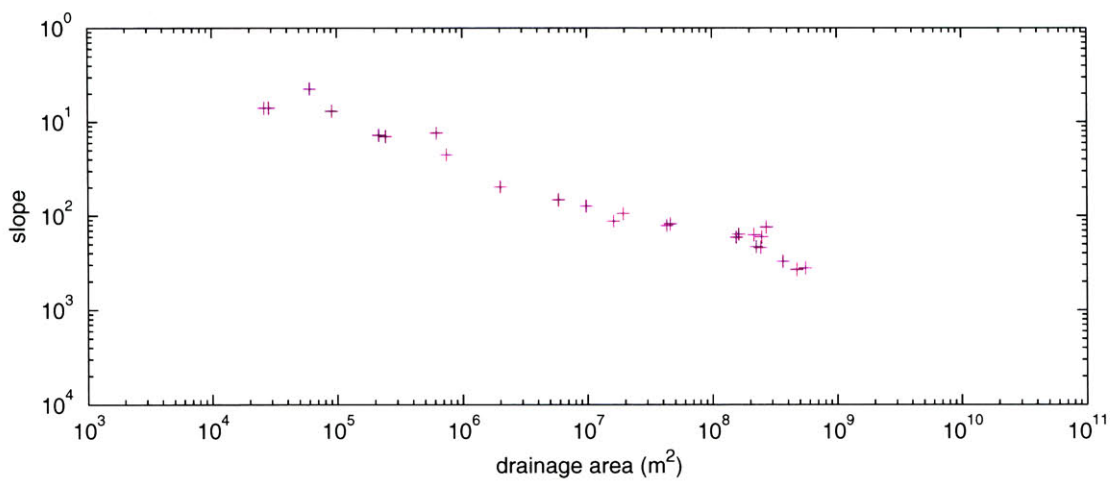
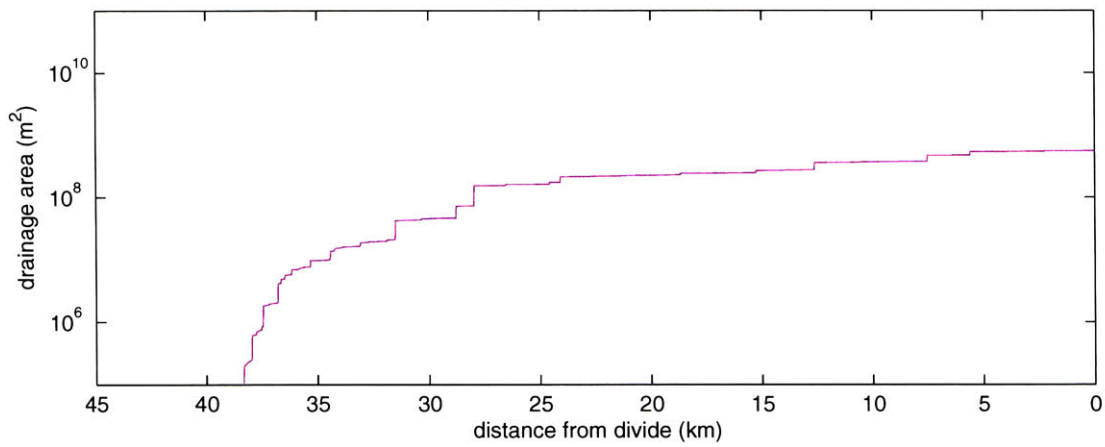
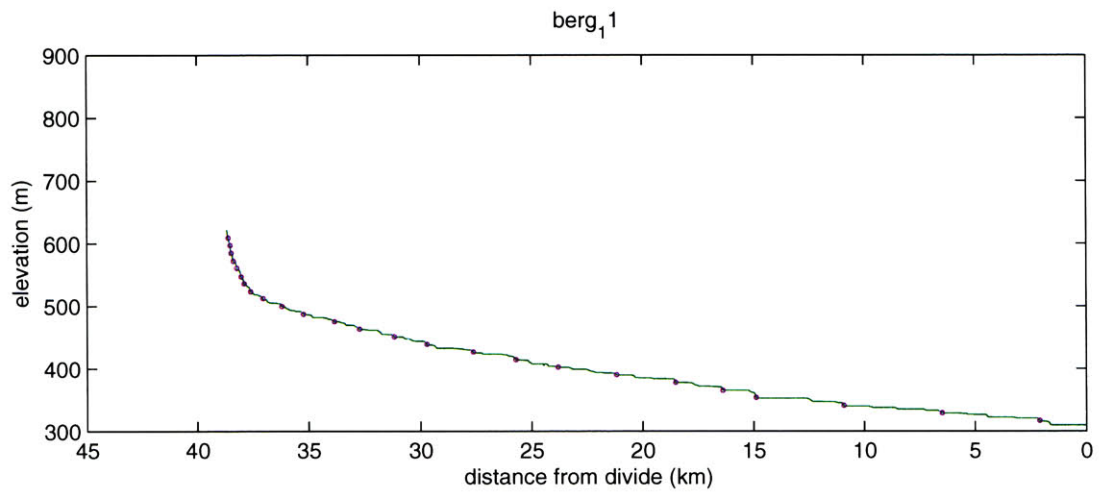
9.2 Related Longitudinal Profiles

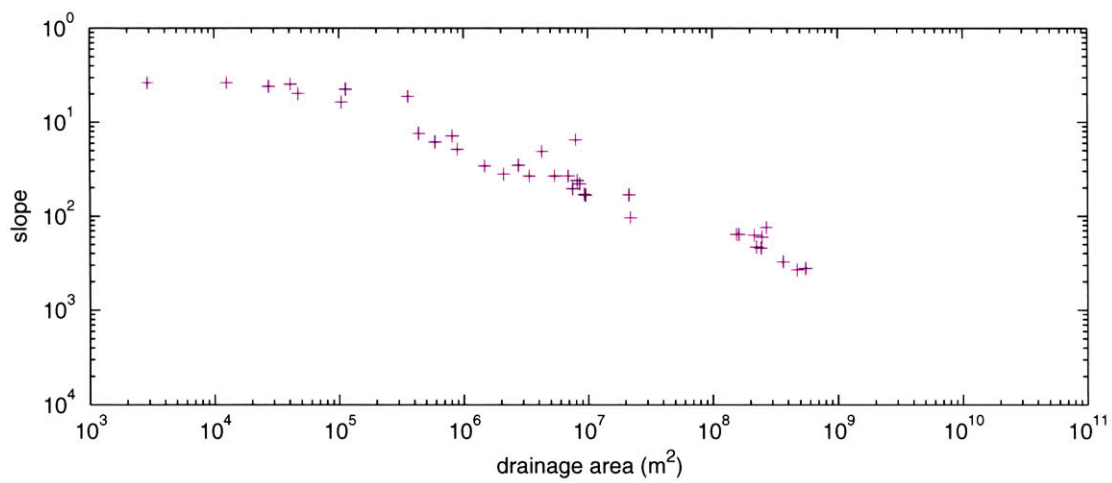
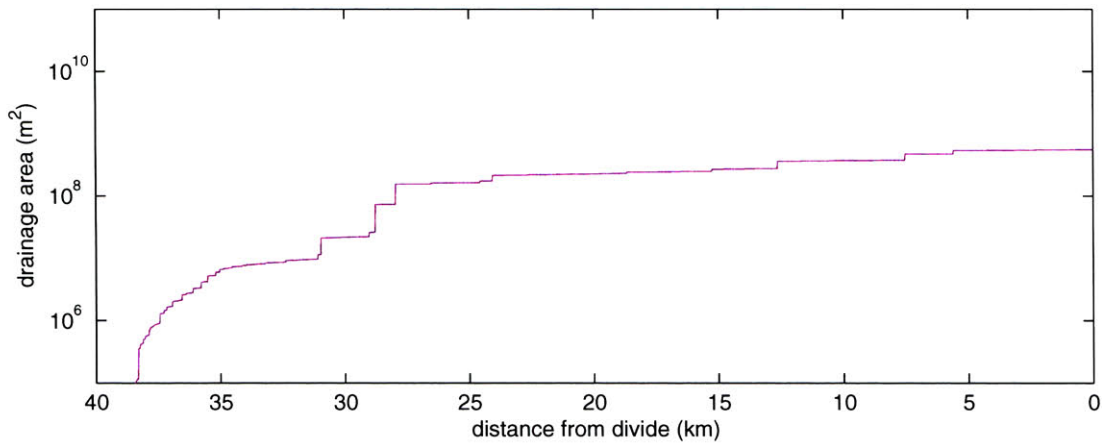
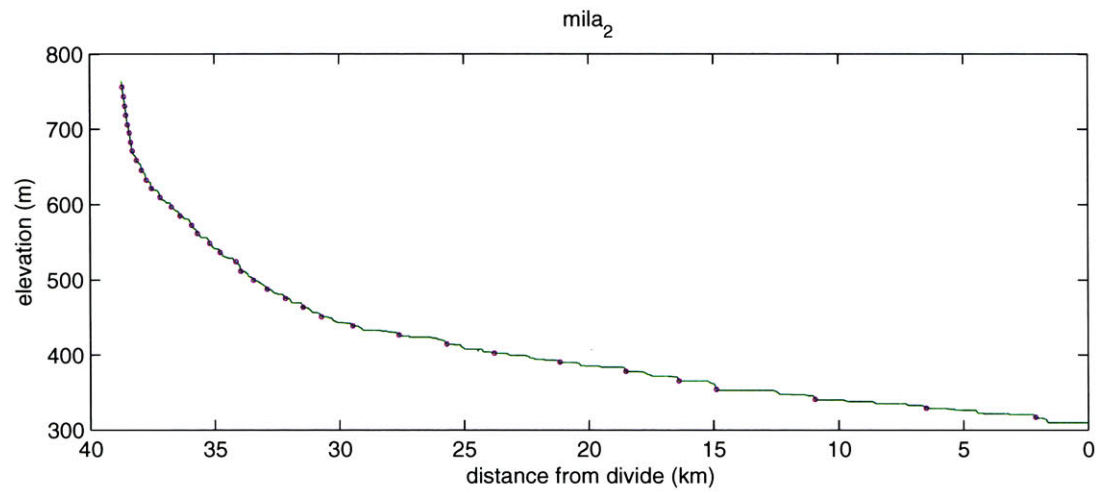
9.2.1 North Fork of the Shenandoah Basin

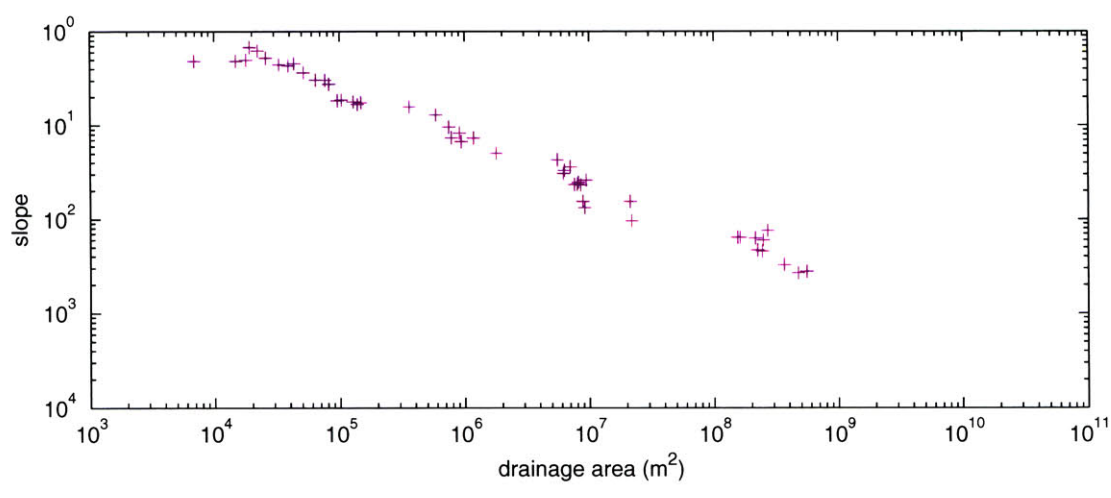
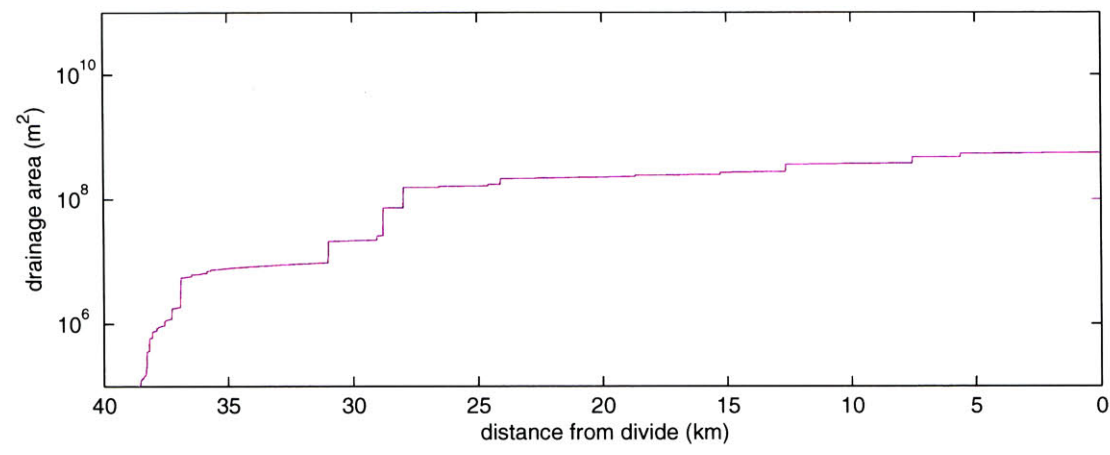
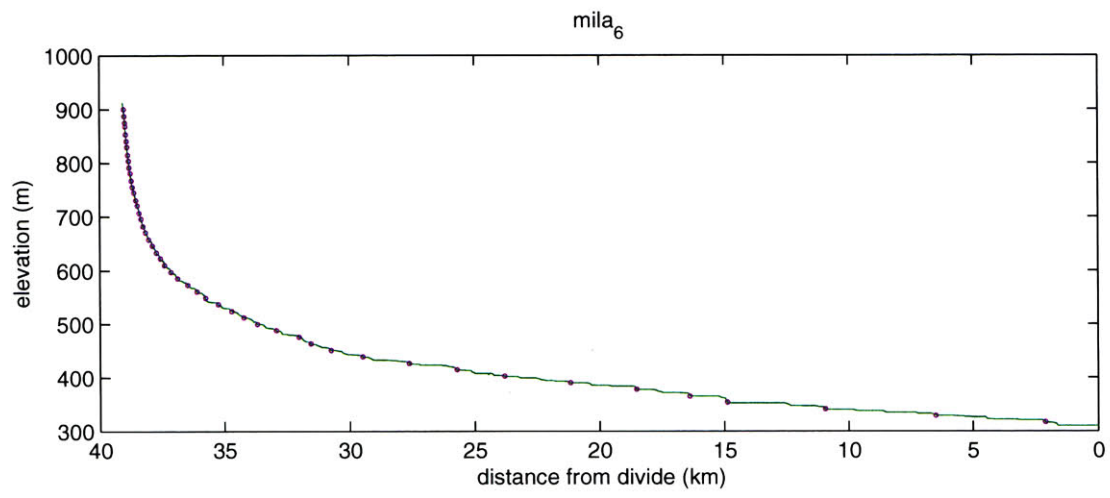


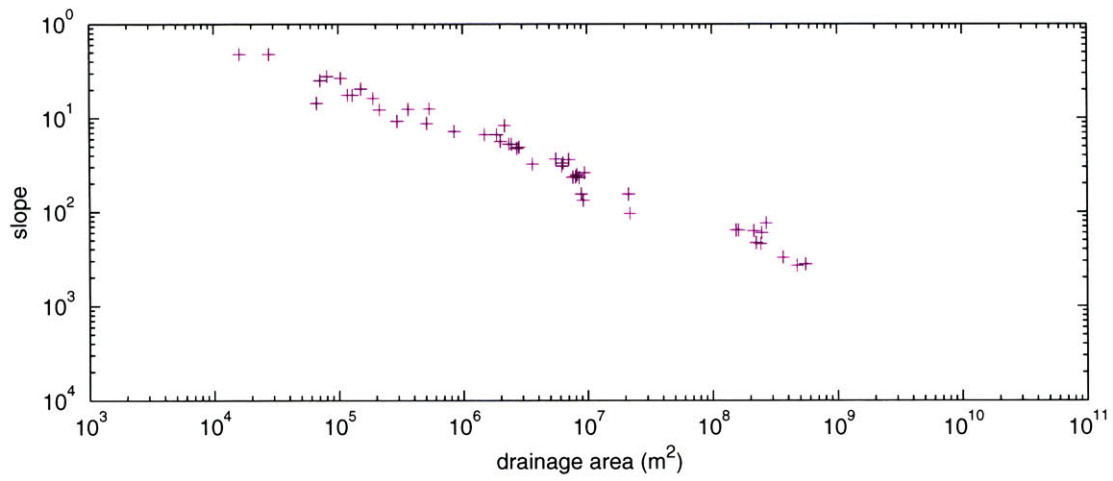
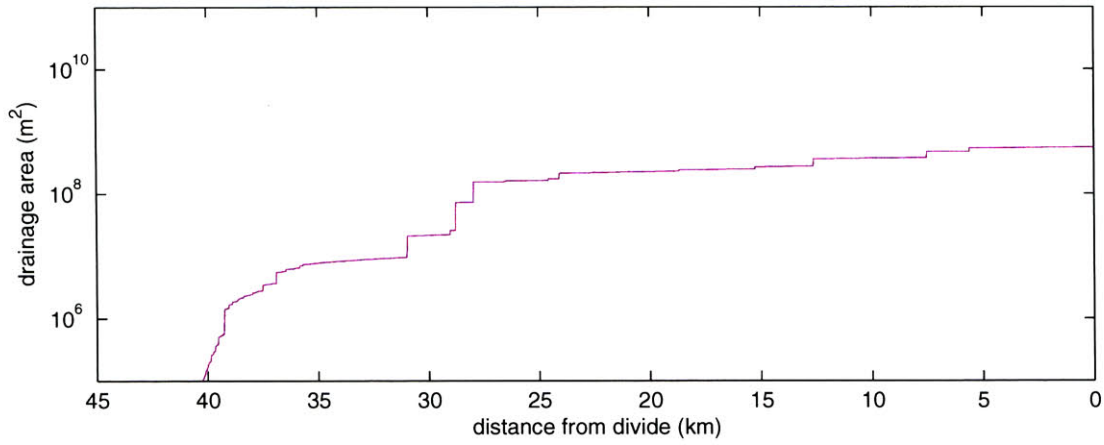
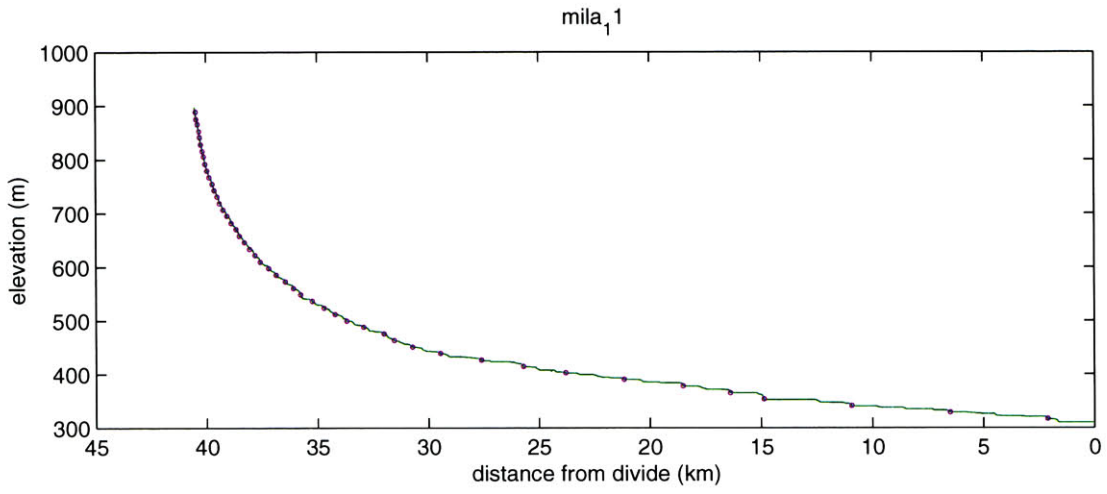


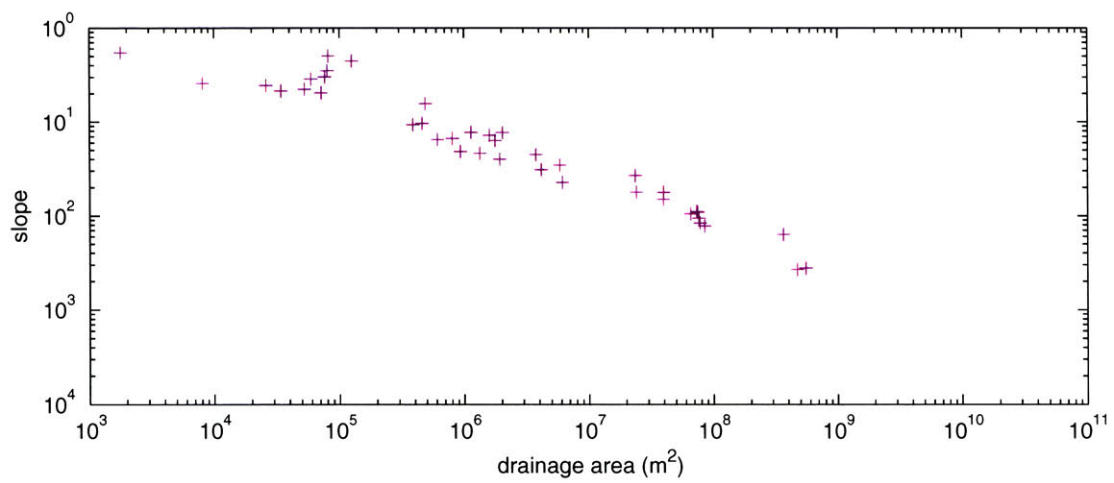
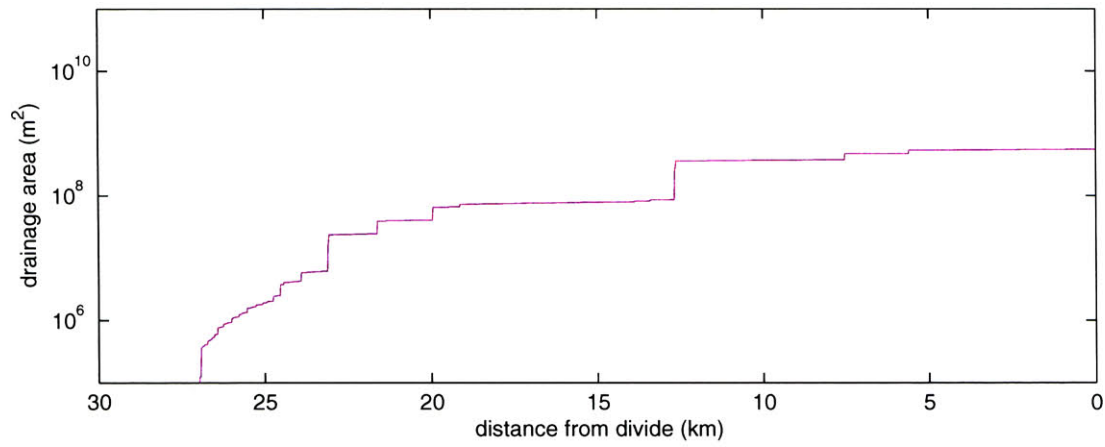
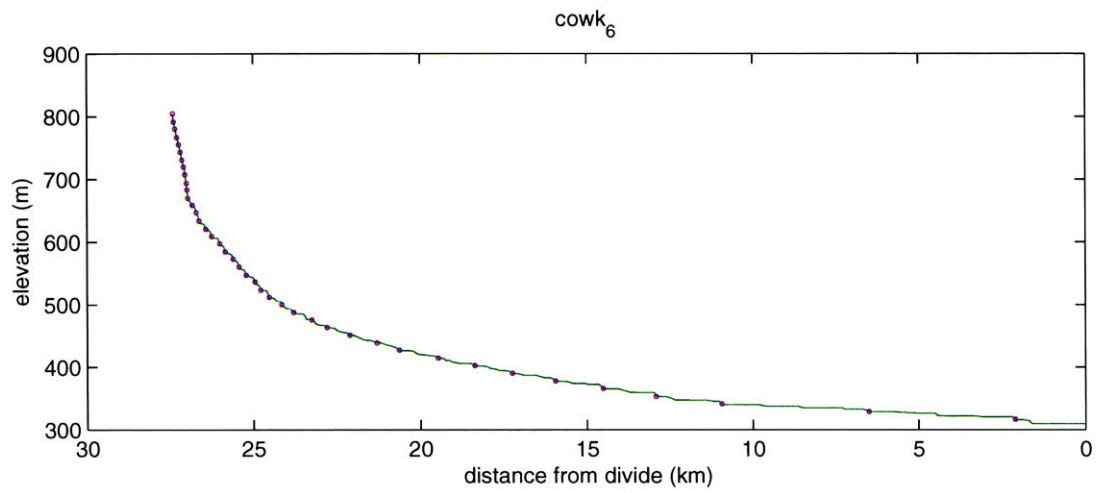


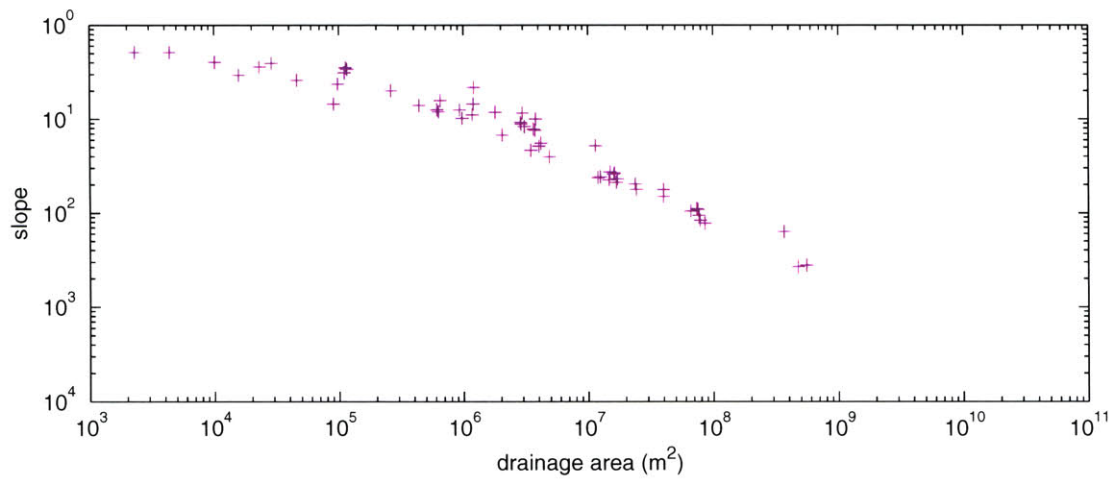
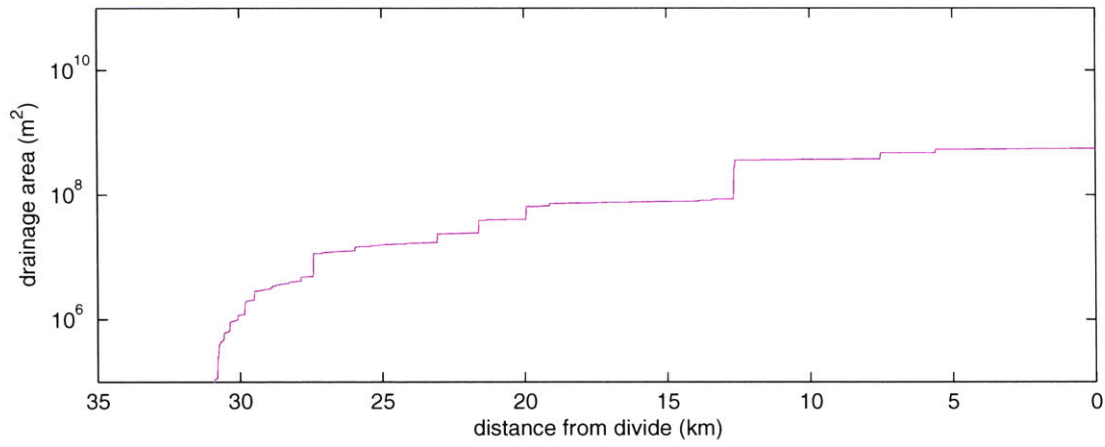
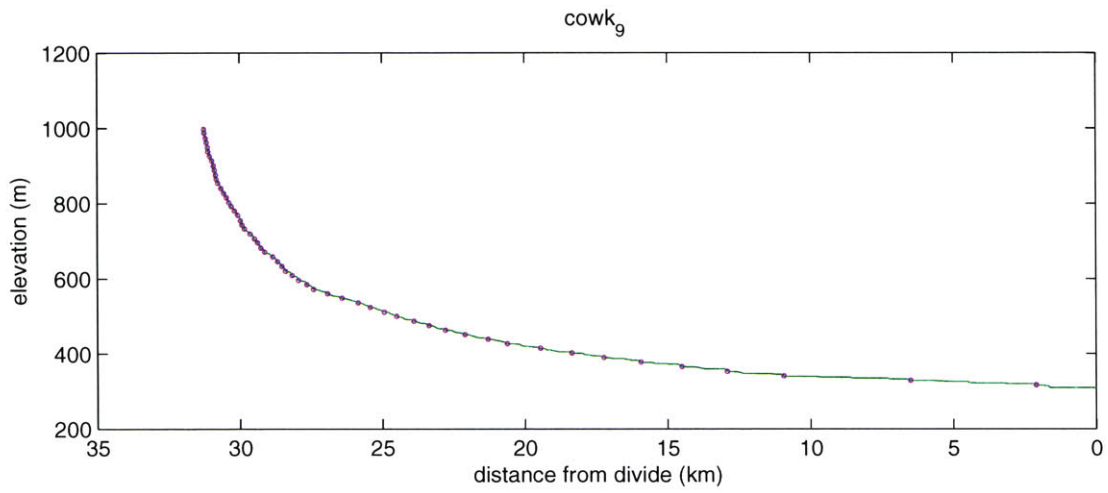


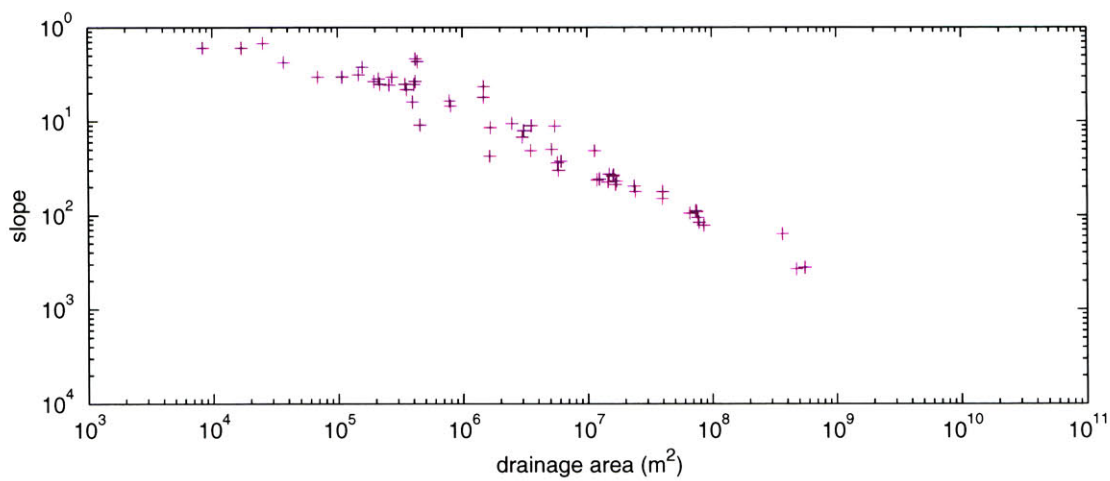
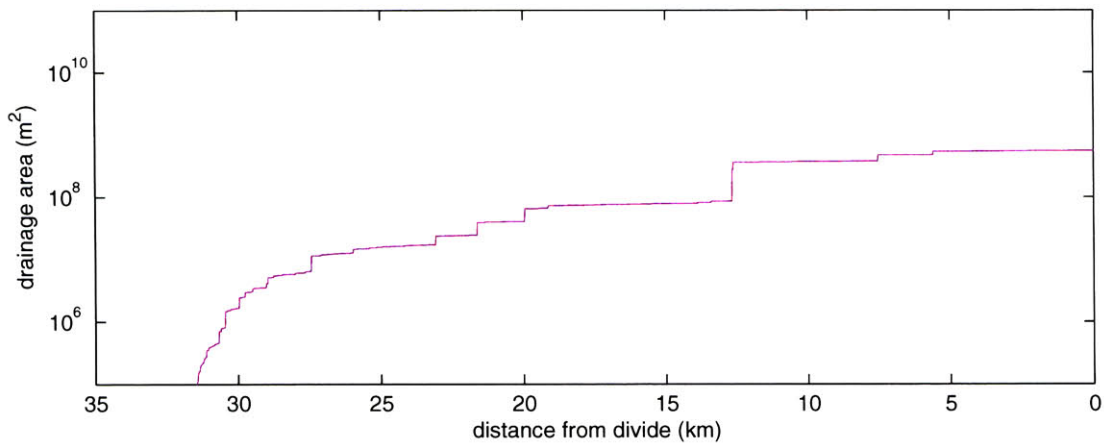
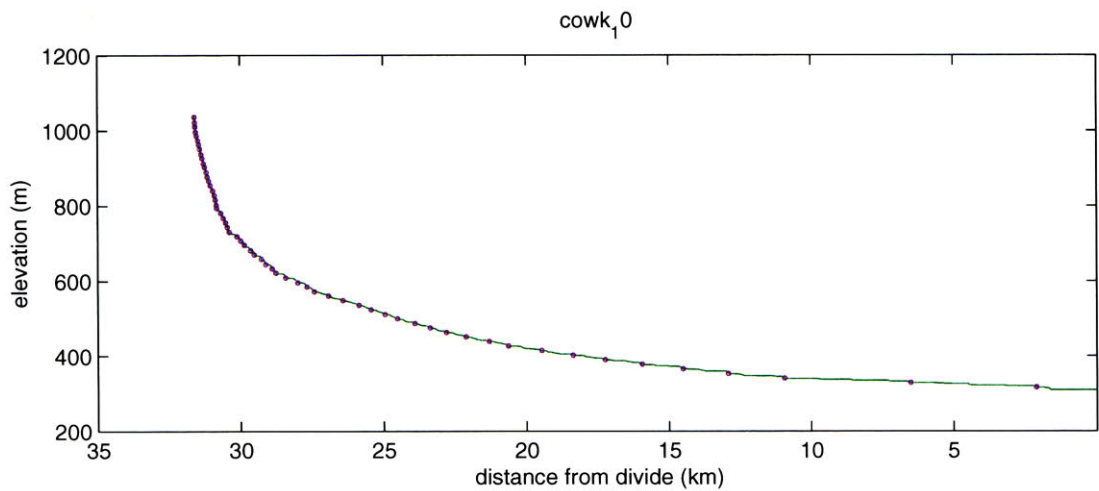


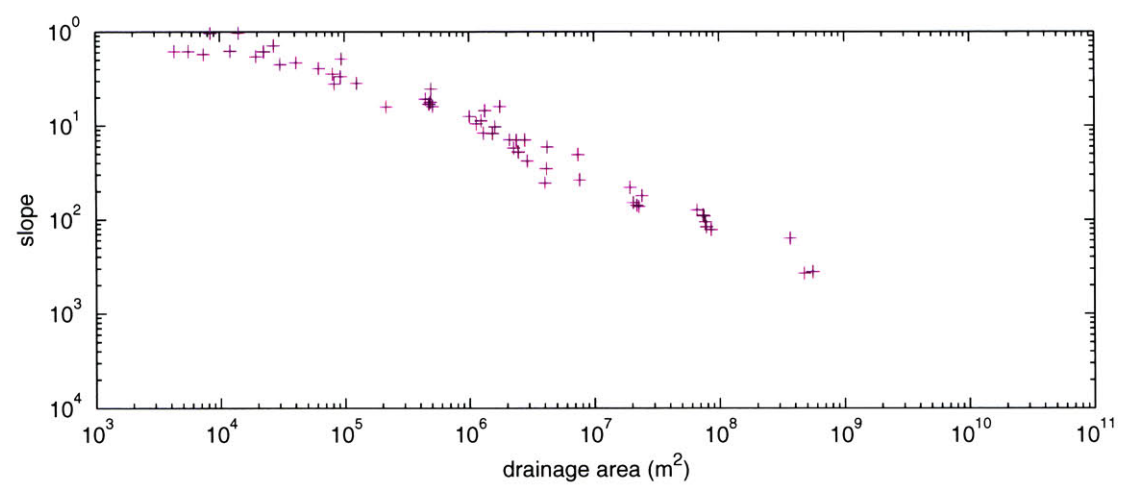
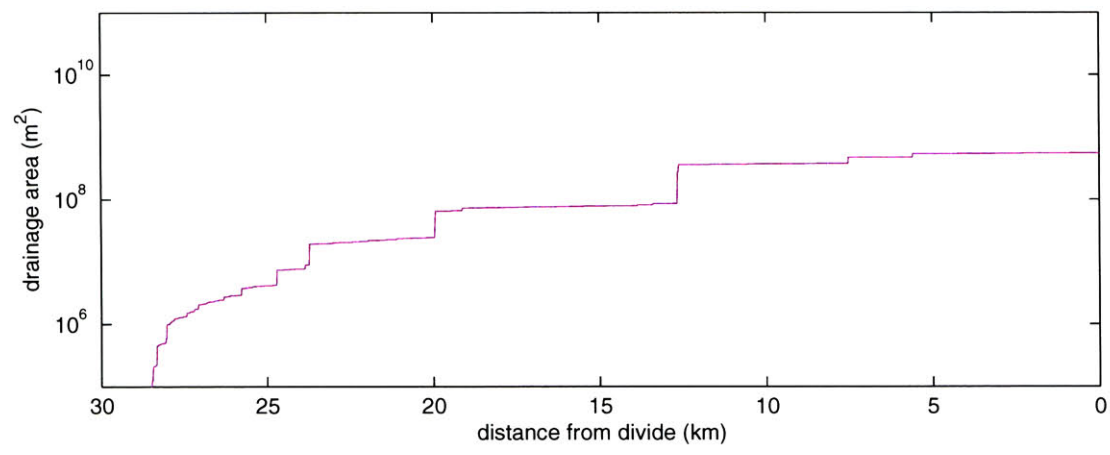
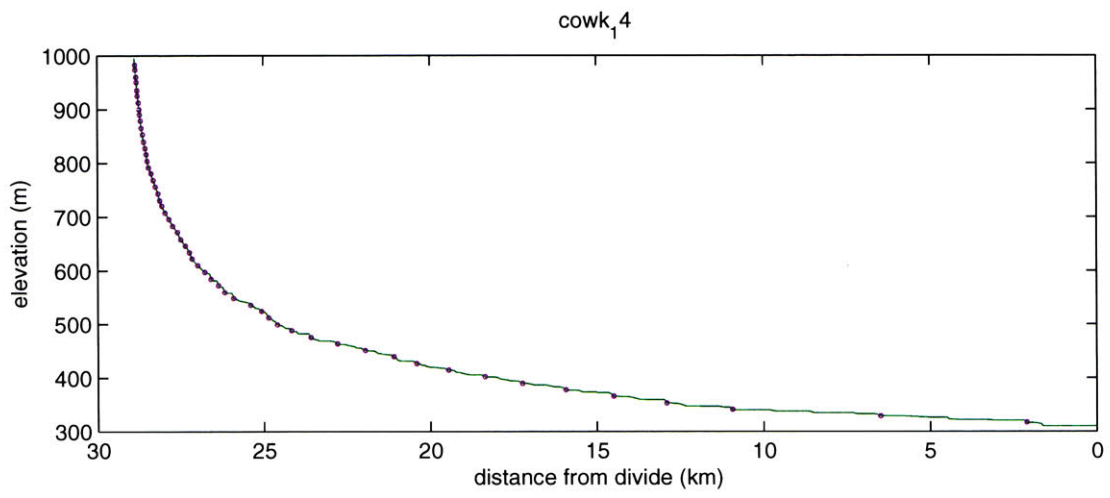


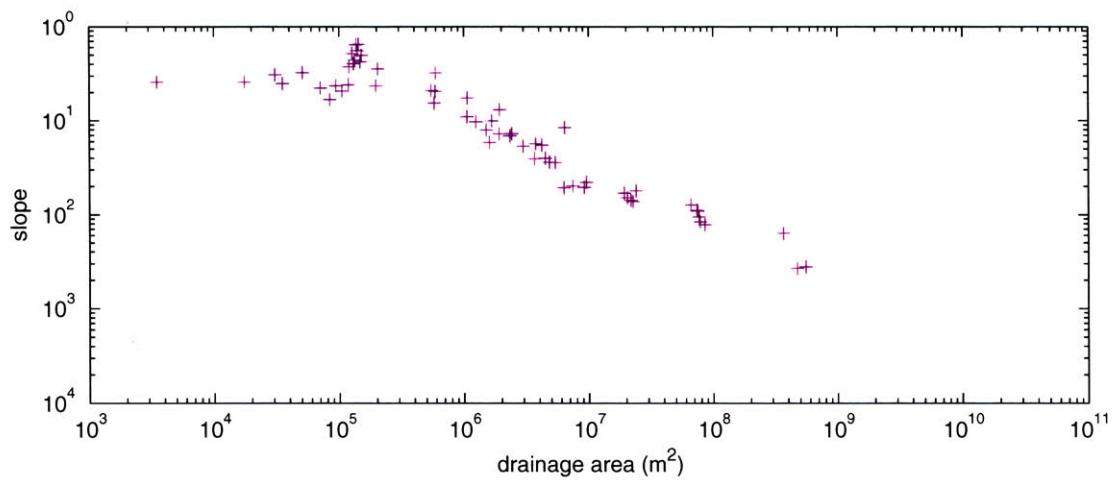
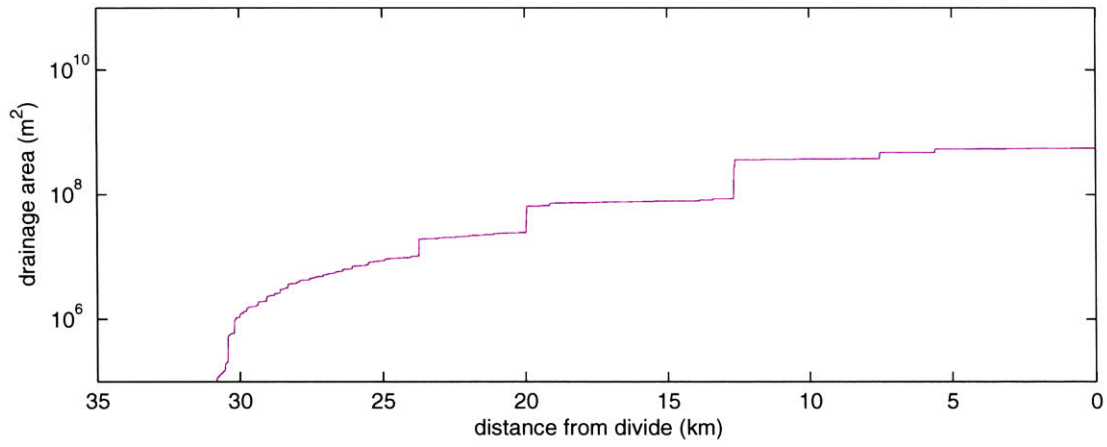
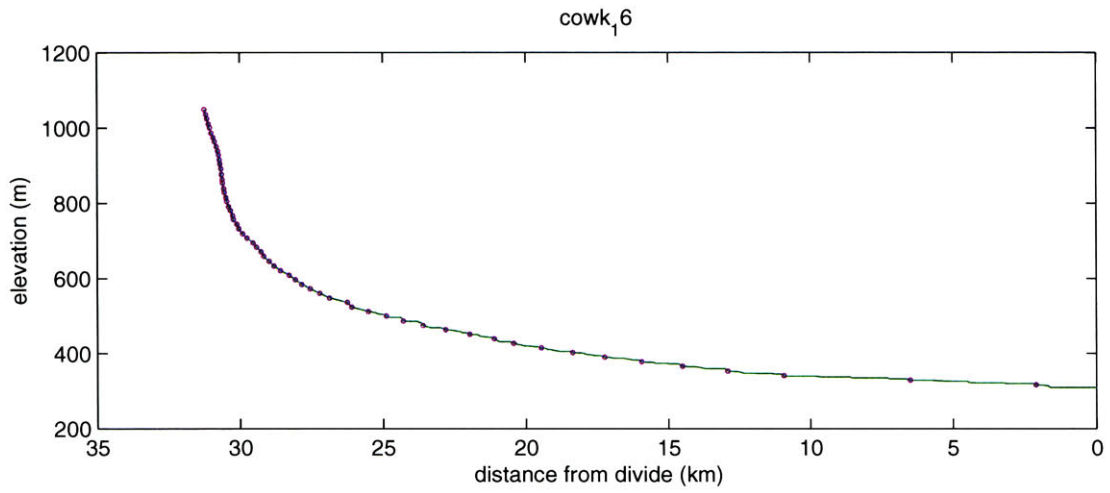


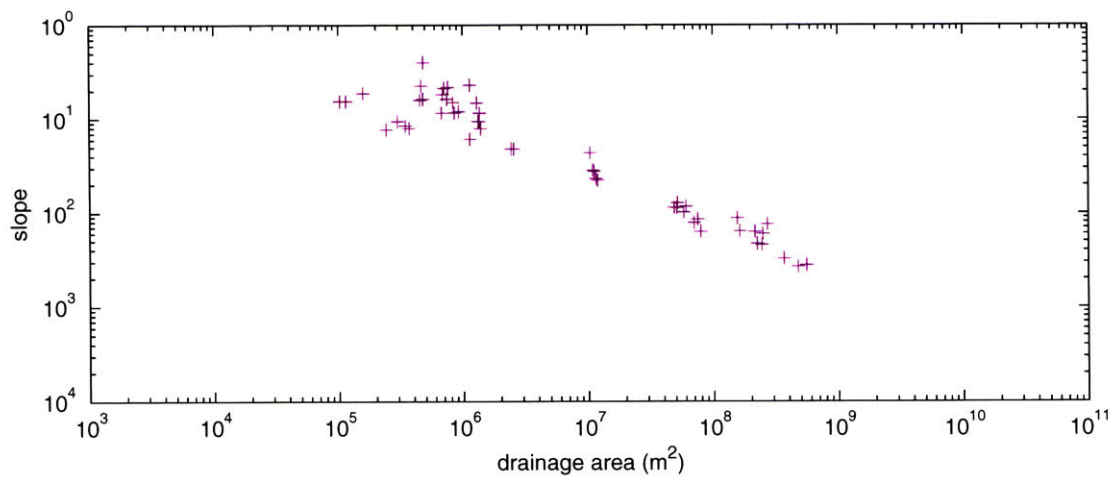
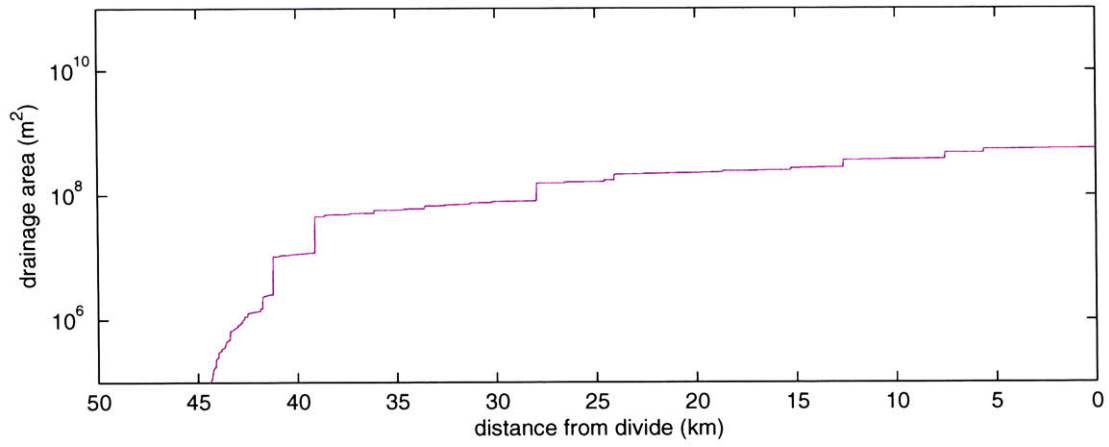
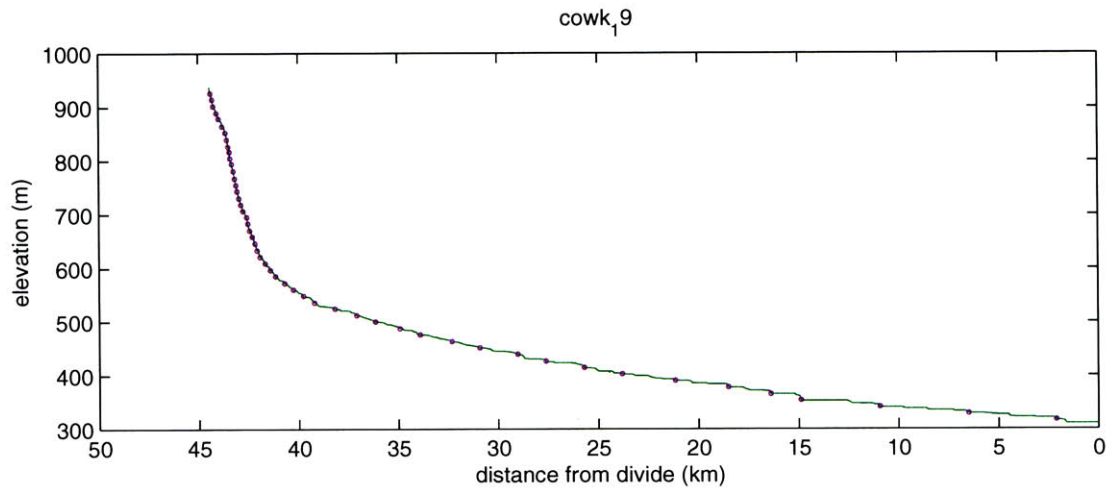


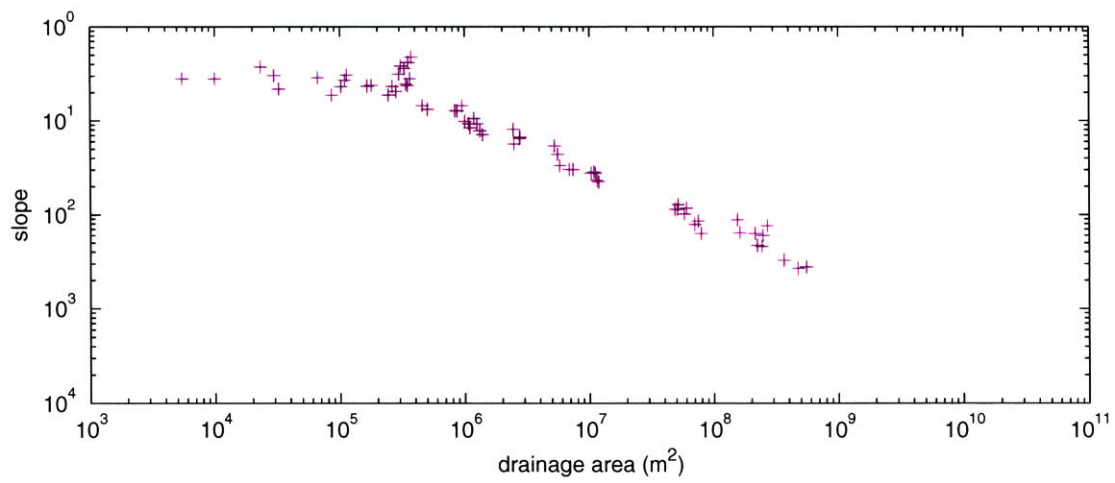
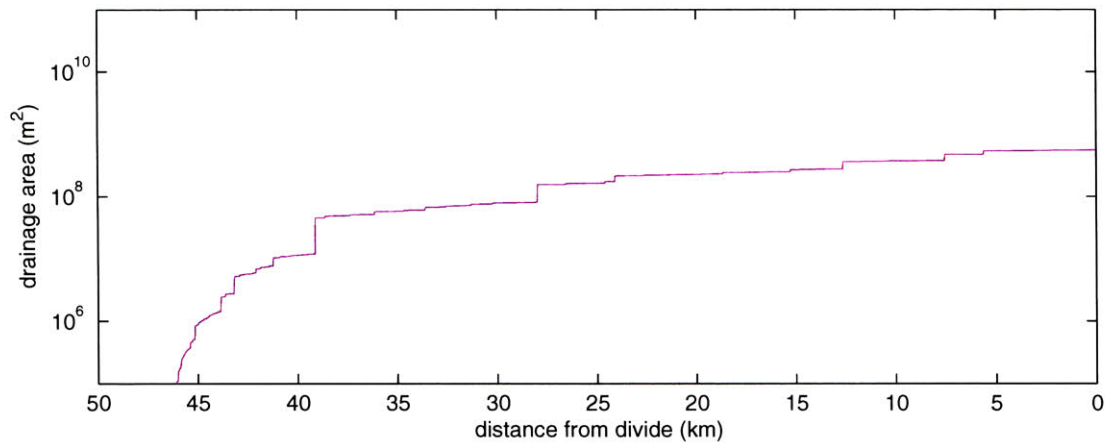
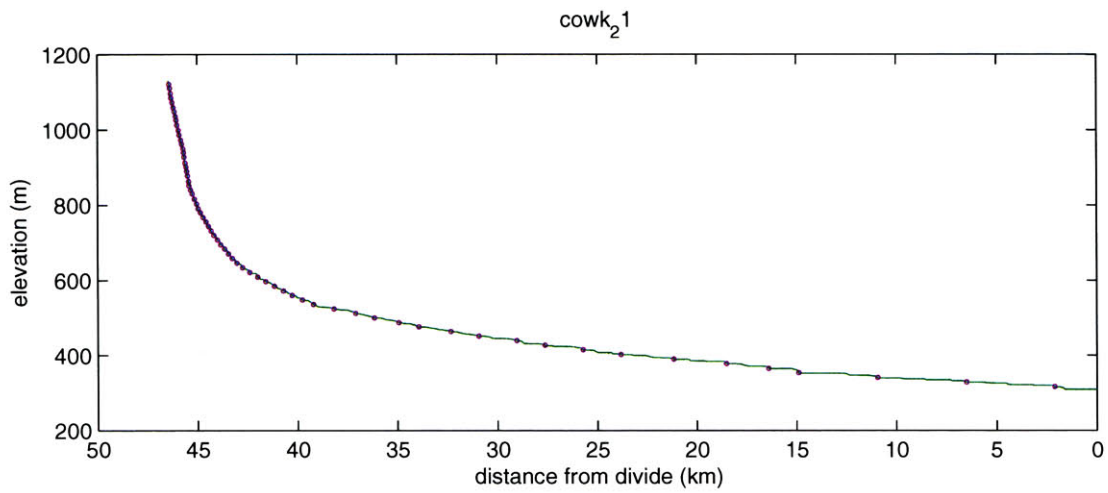


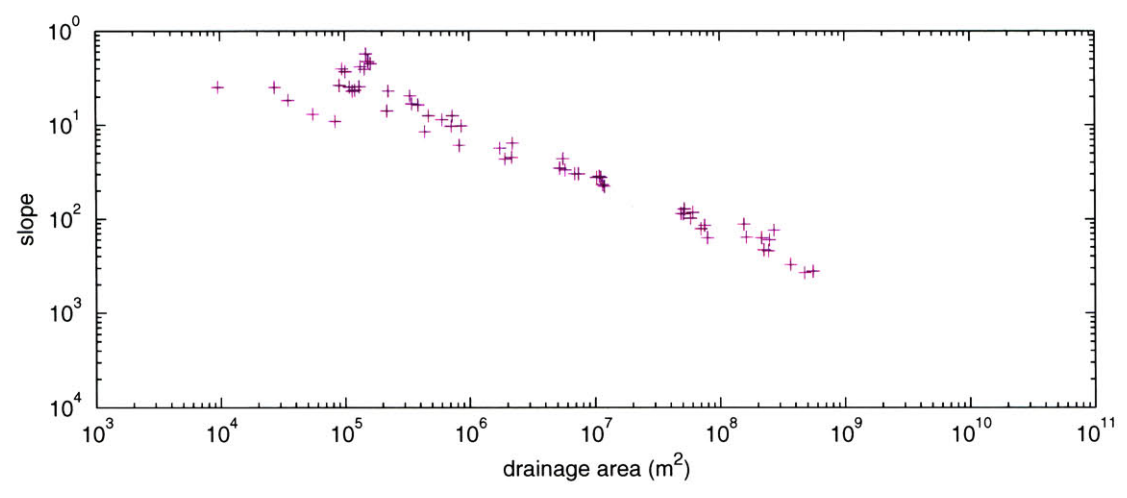
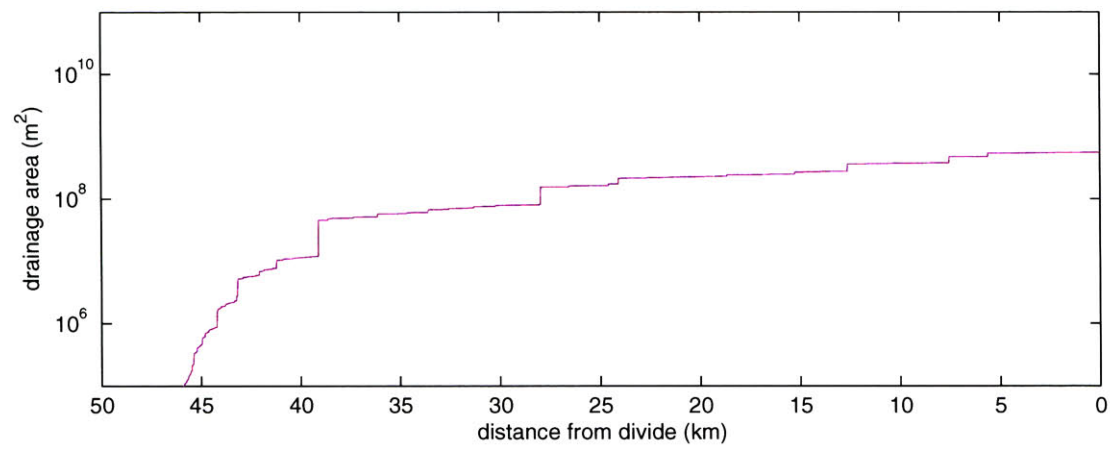
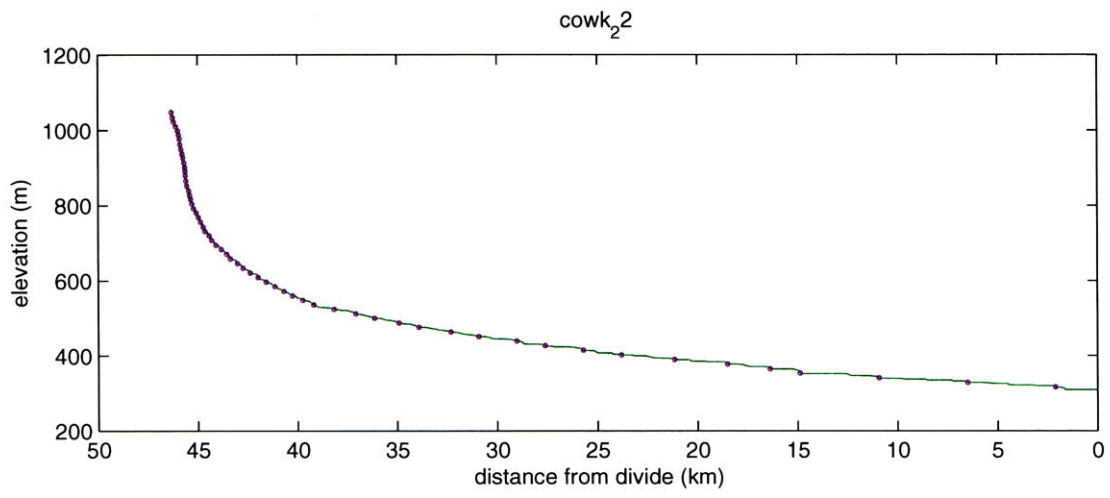


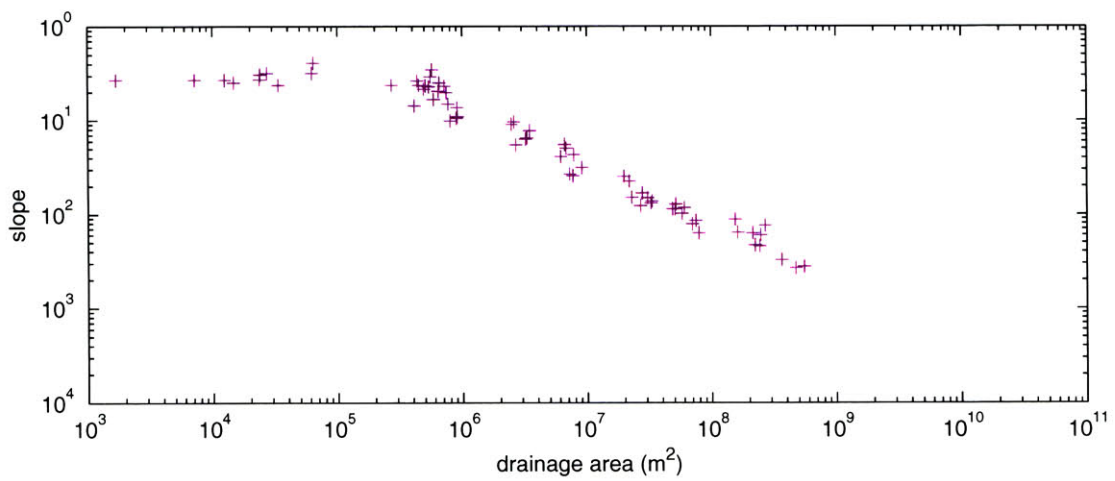
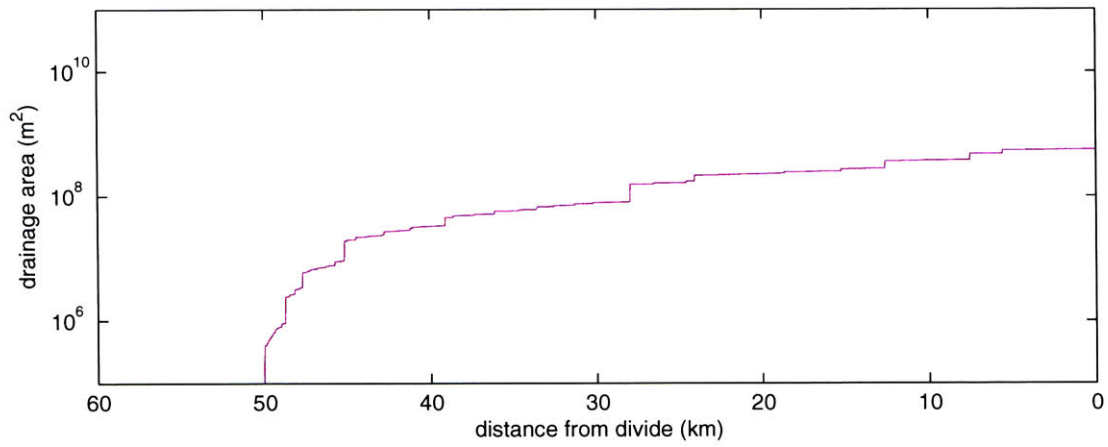
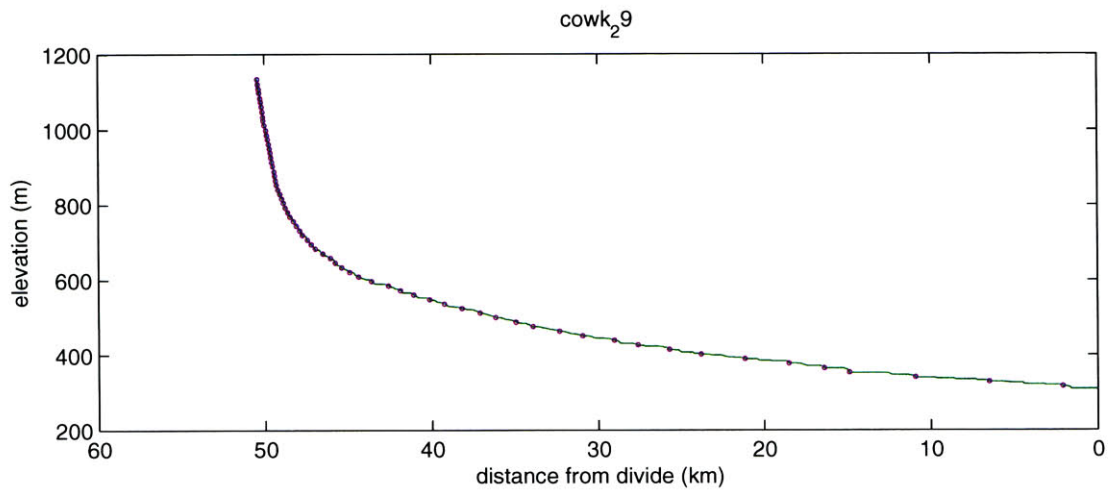




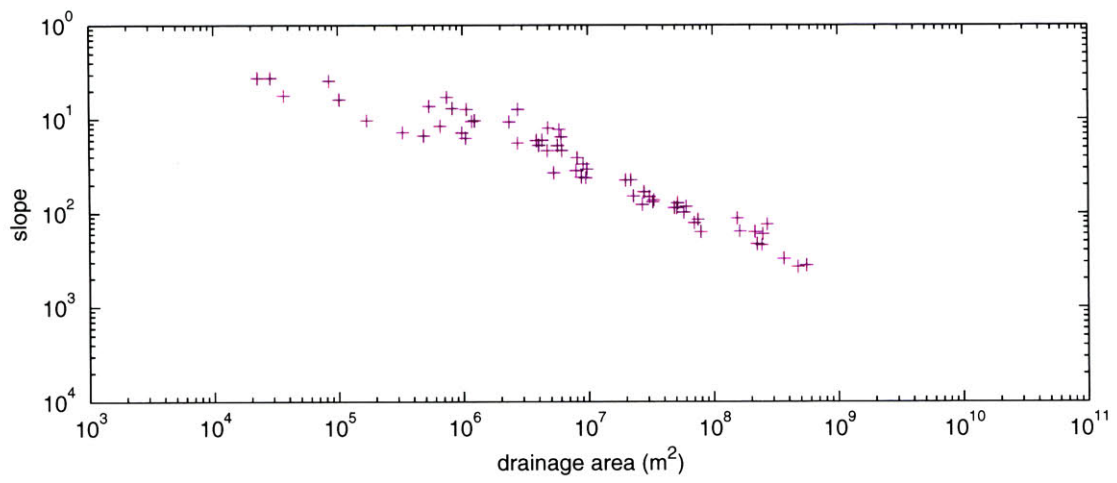
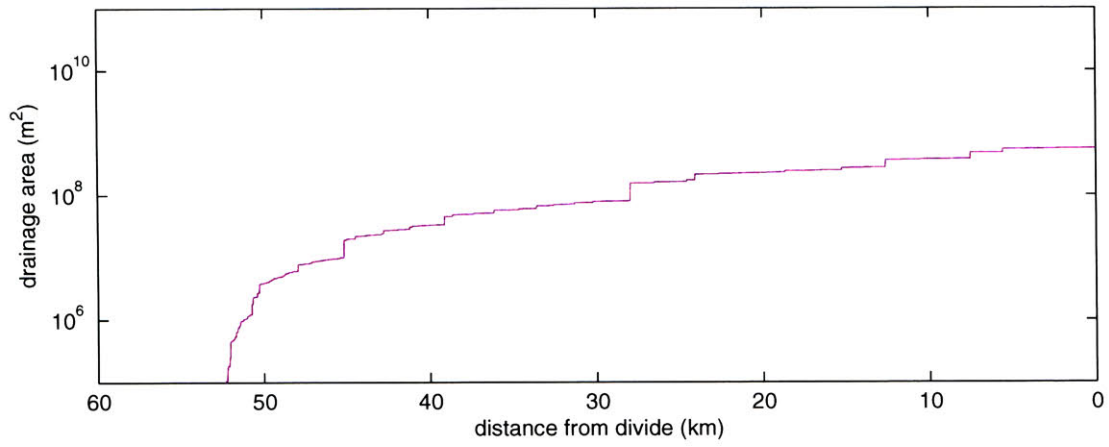
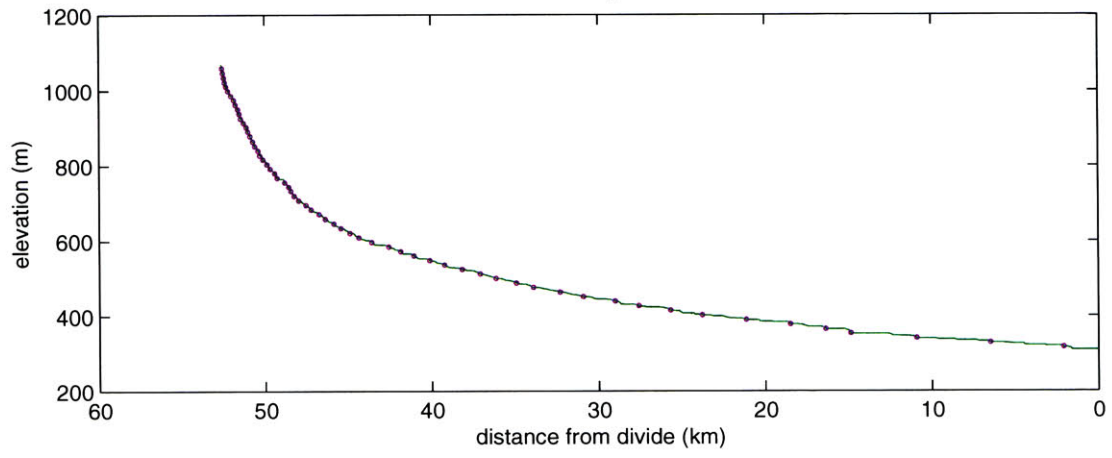


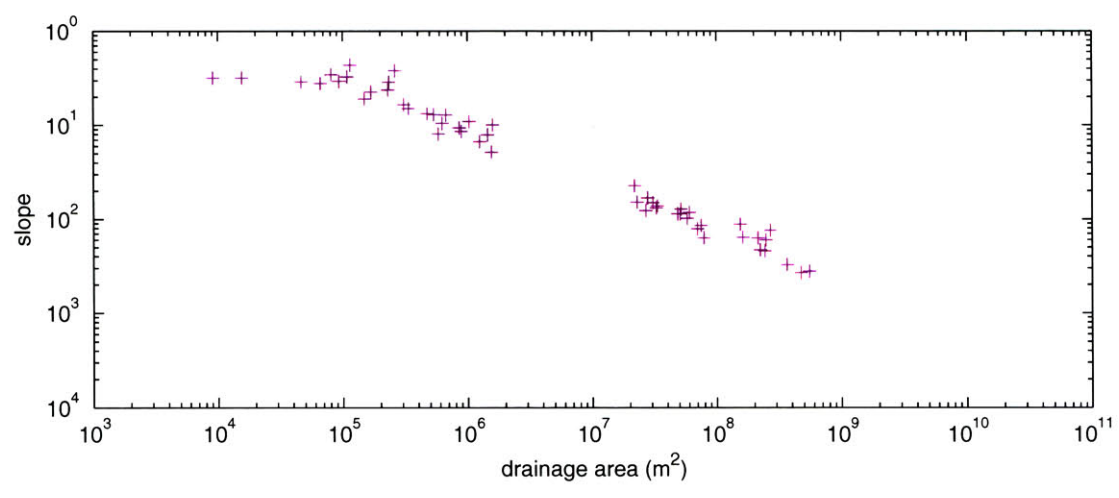
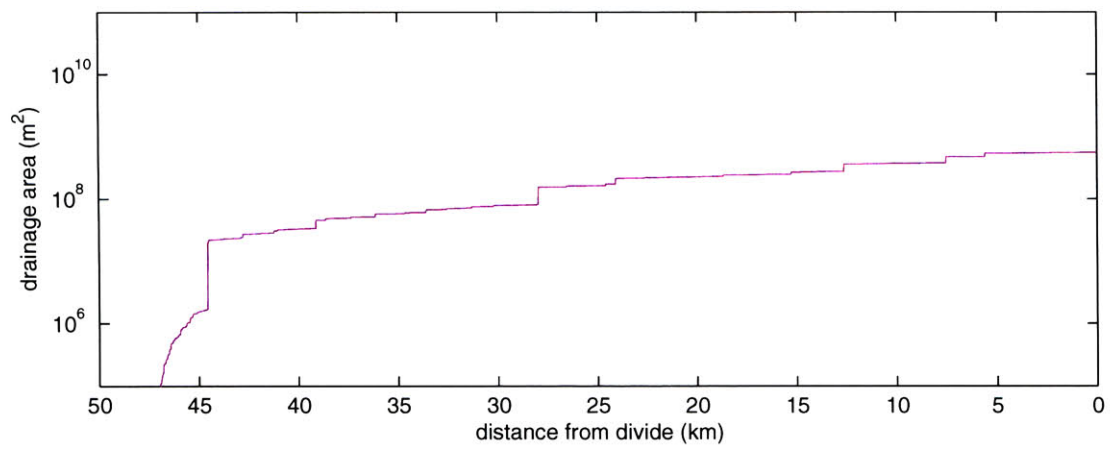
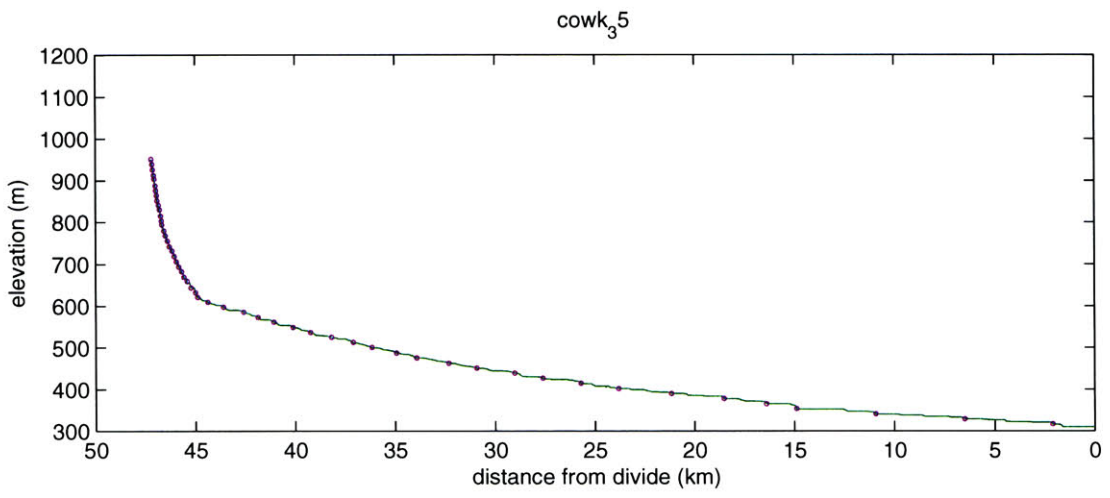




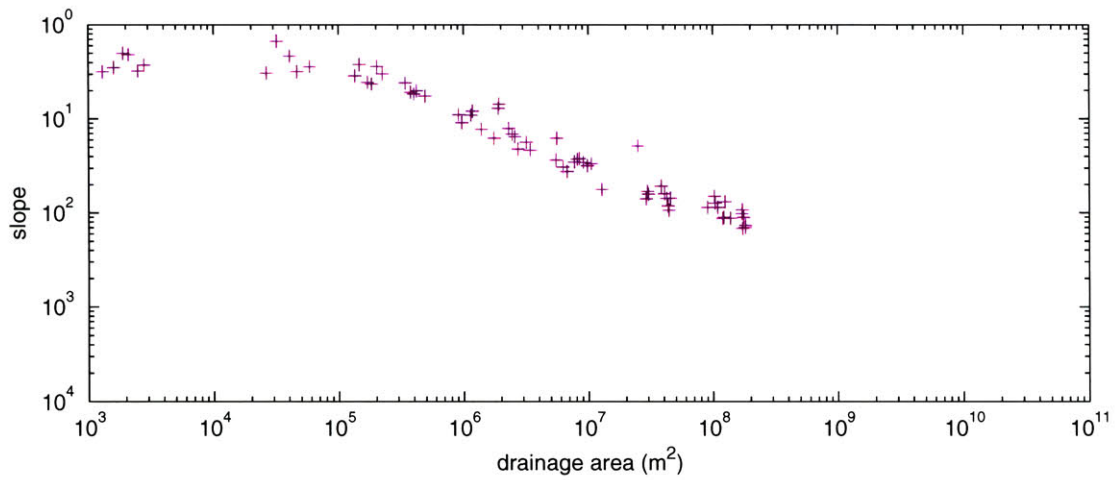
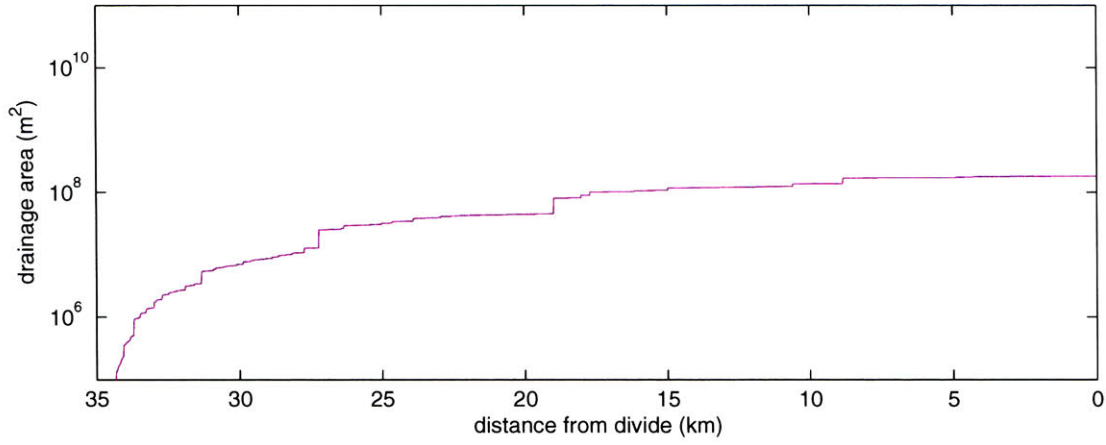
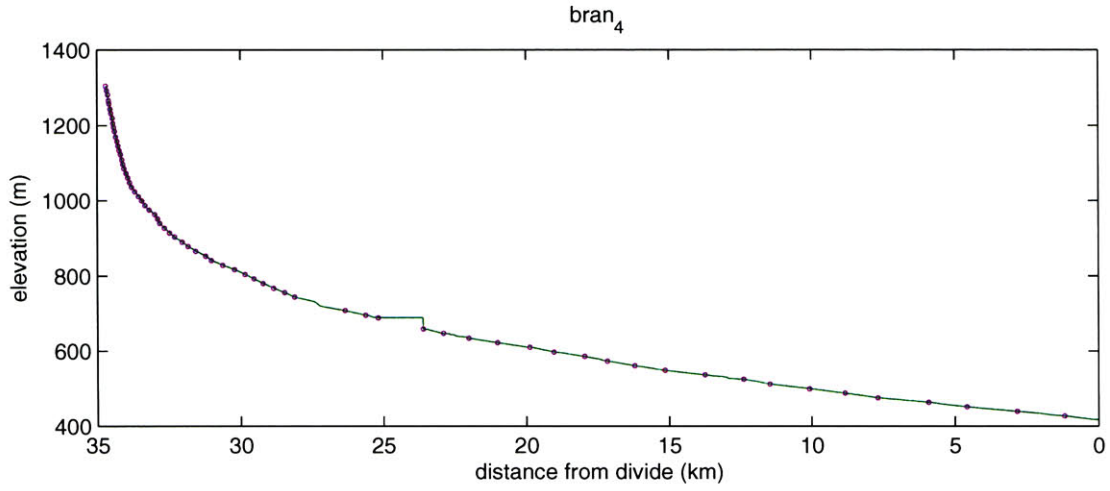


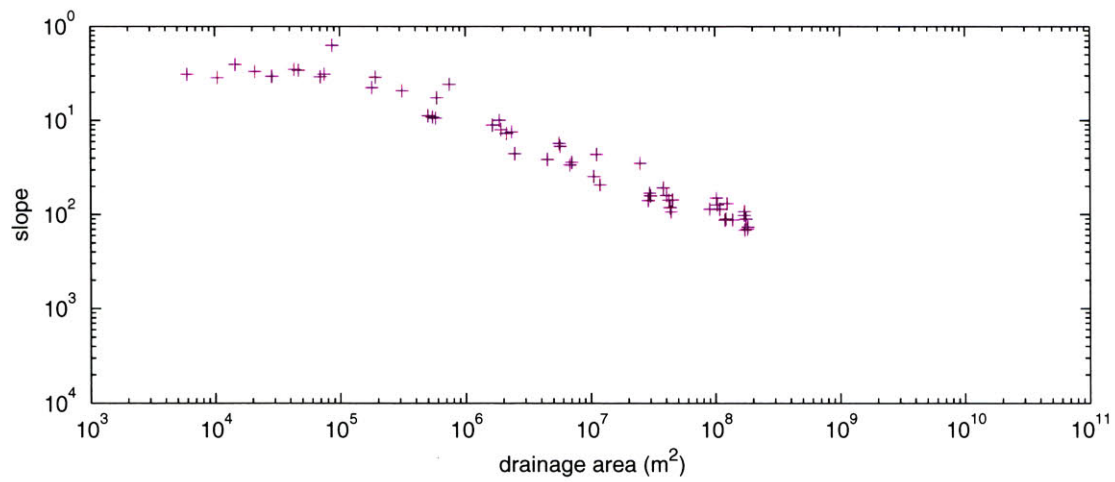
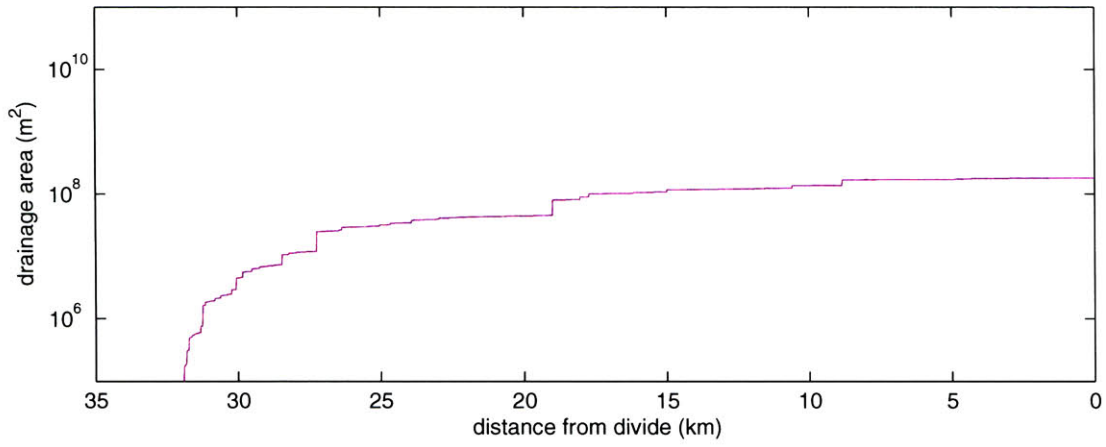
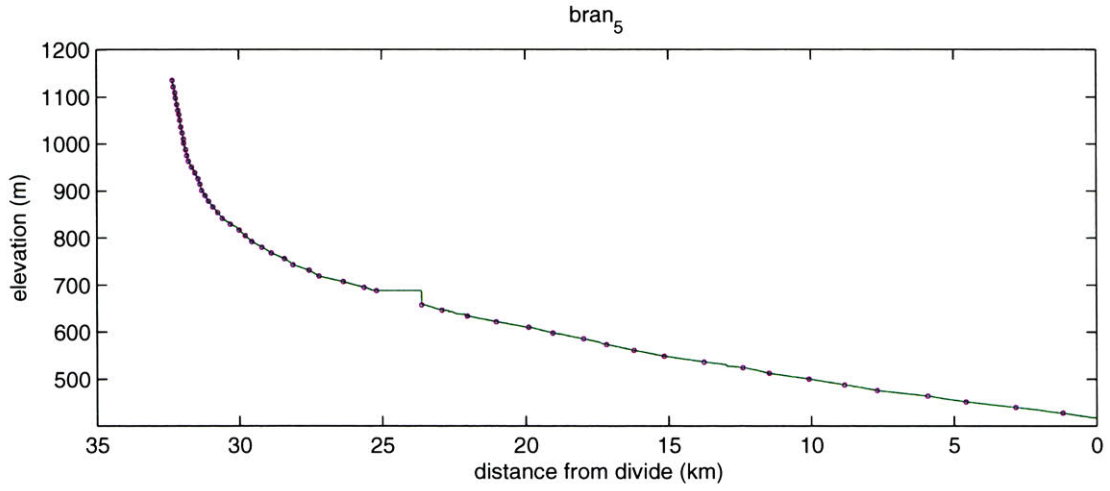
cowk₃2

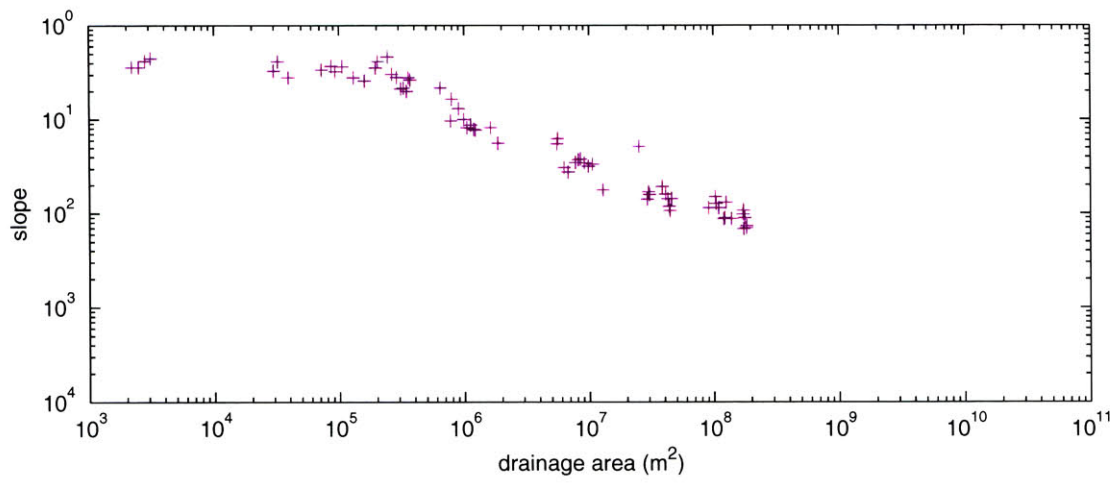
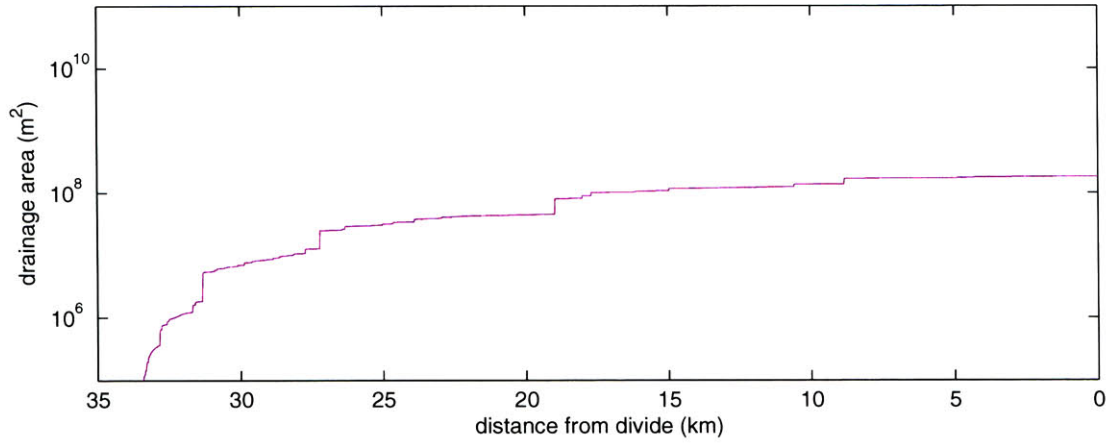
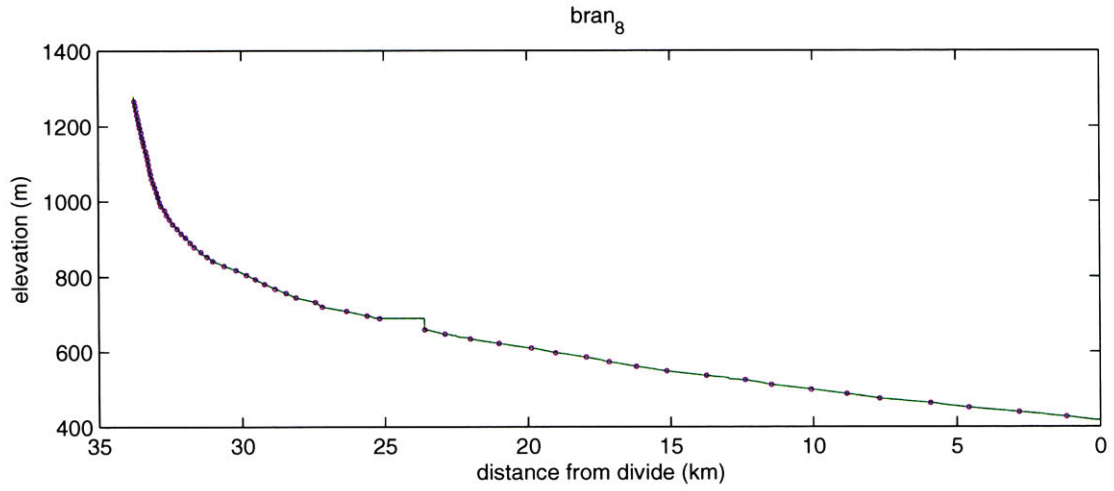


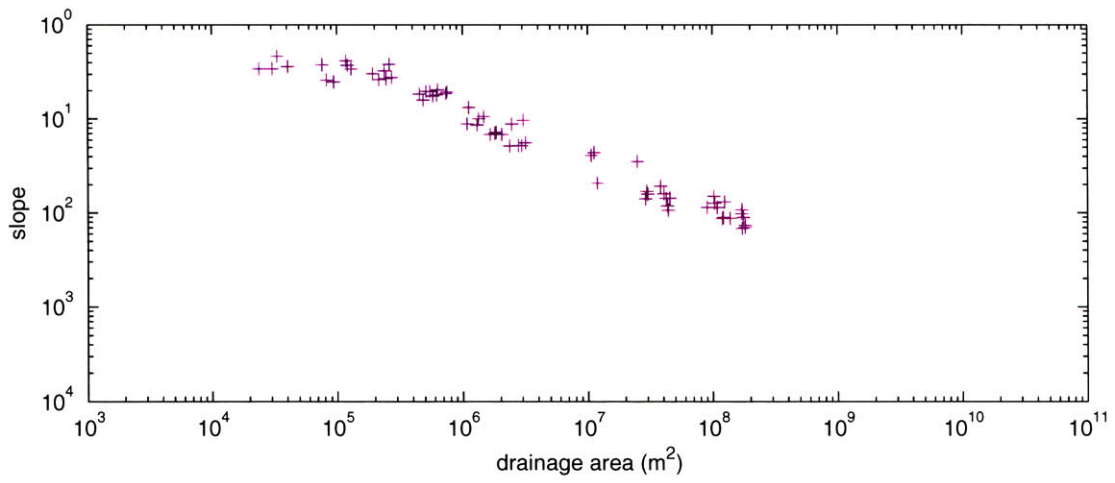
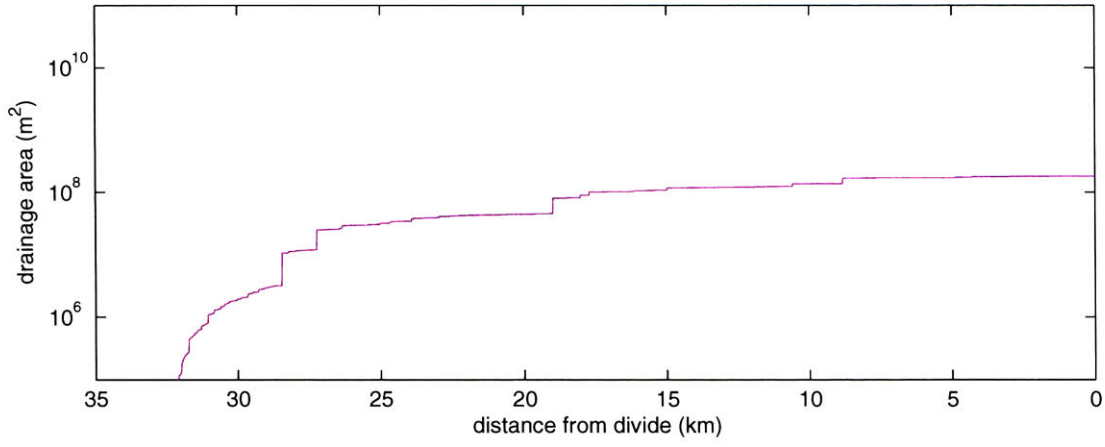
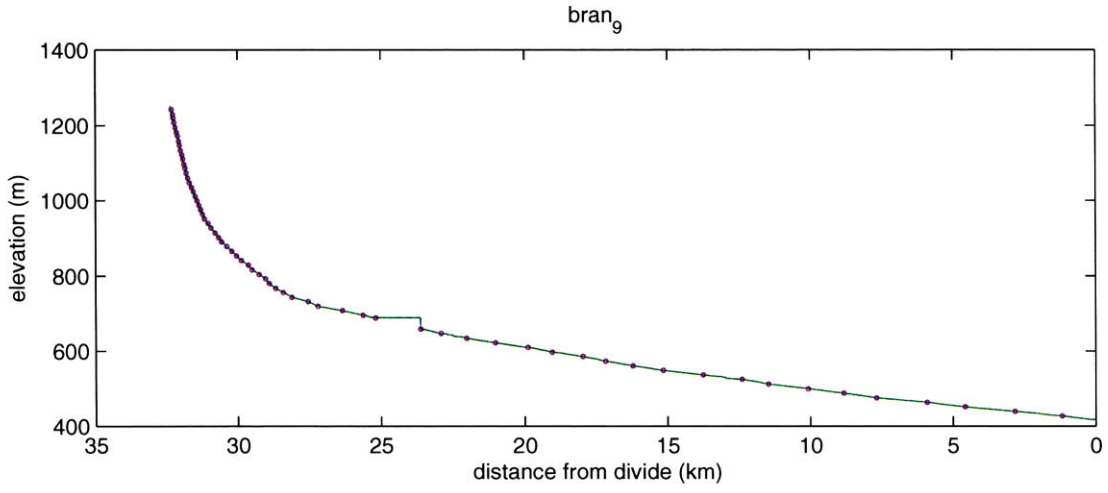


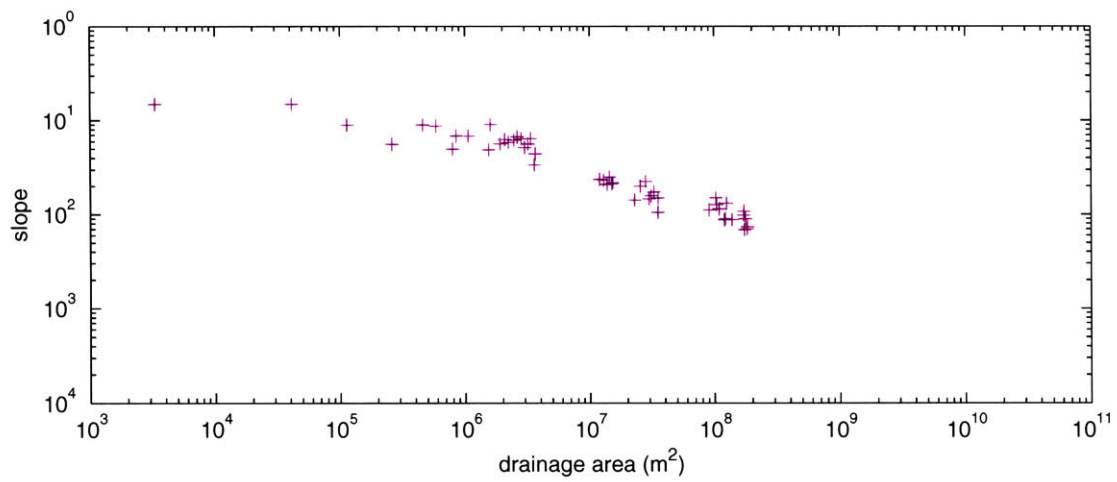
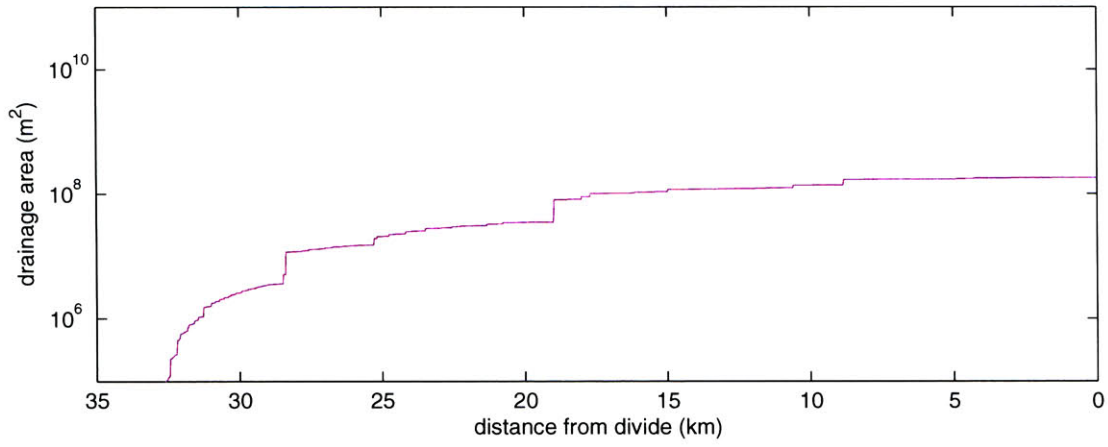
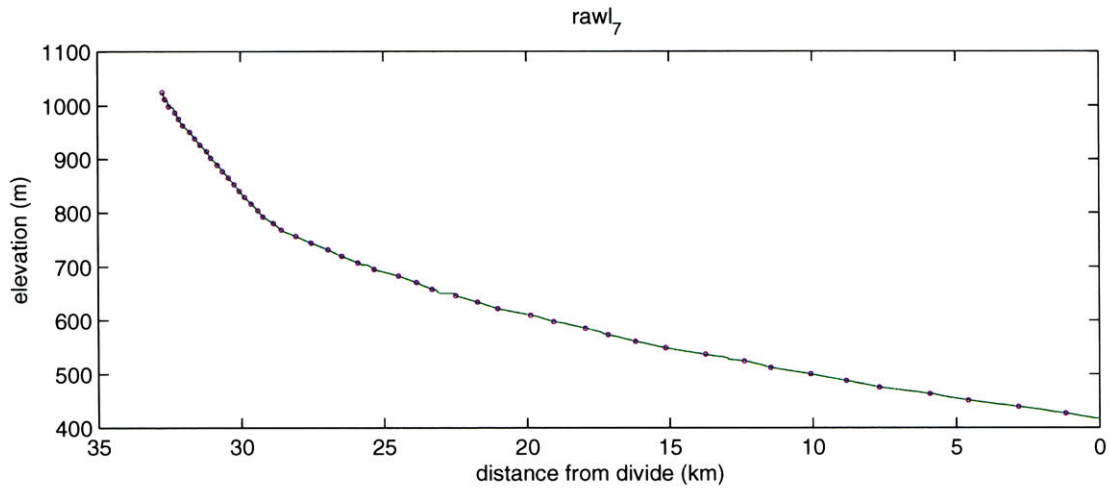
9.2.2 Dry River Basin

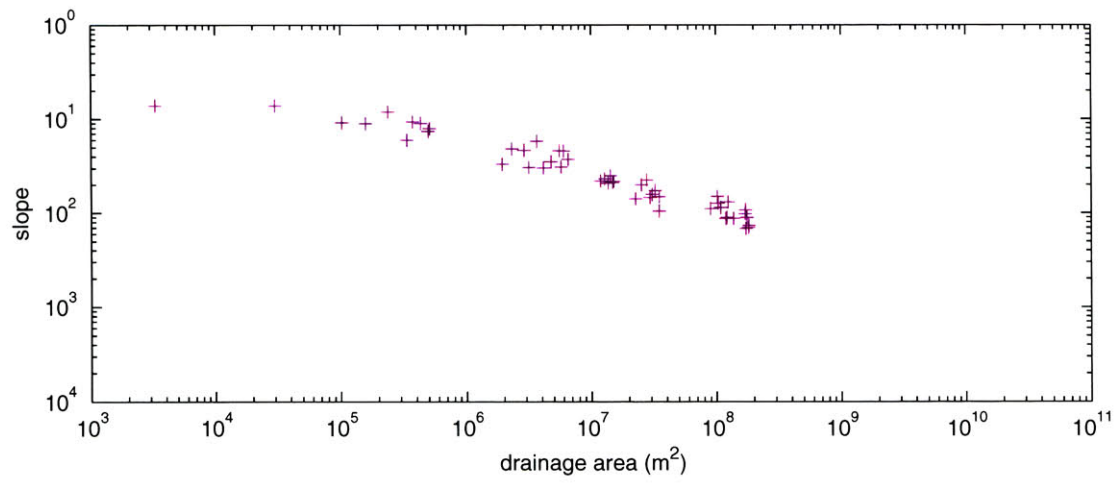
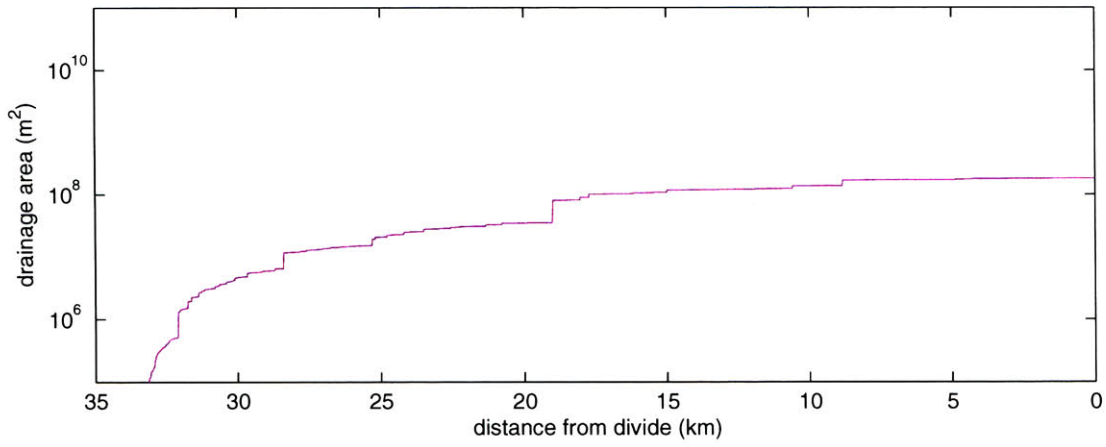
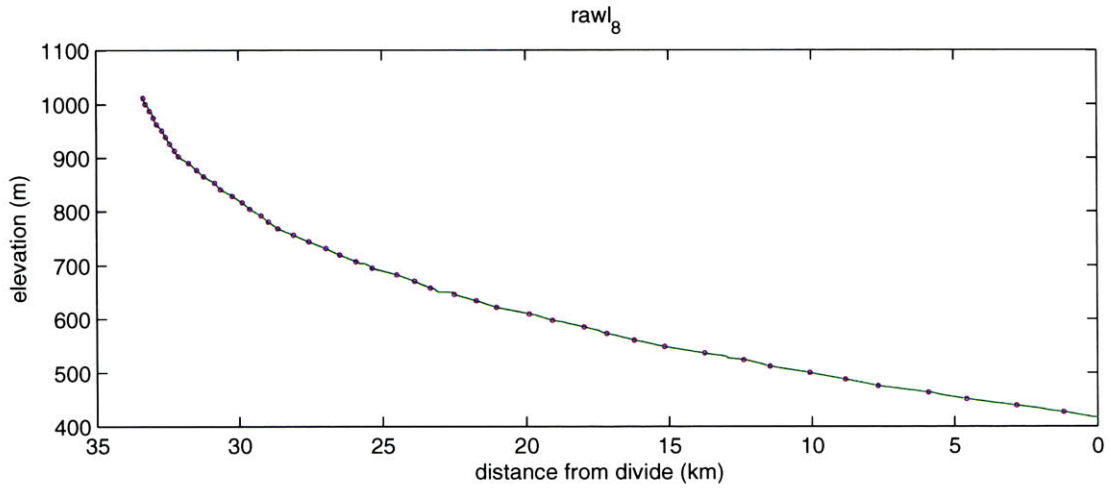


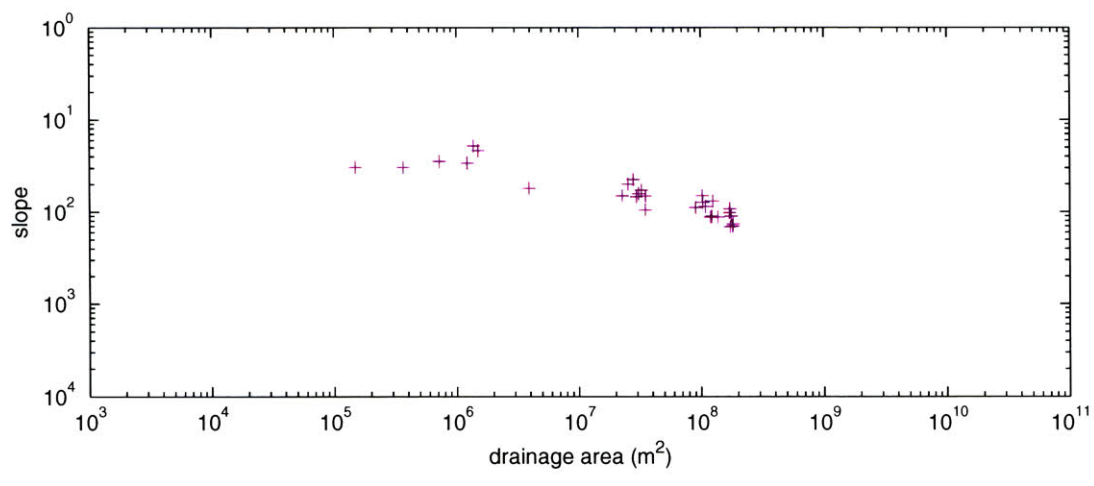
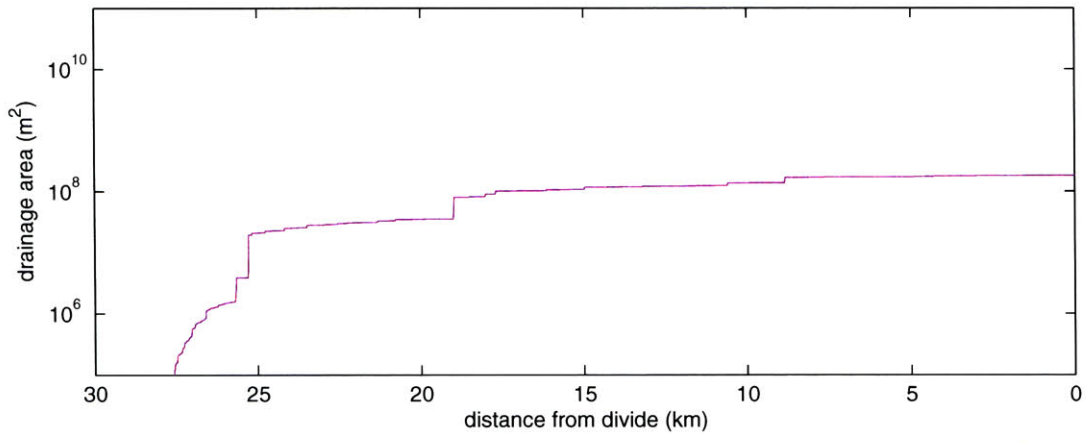
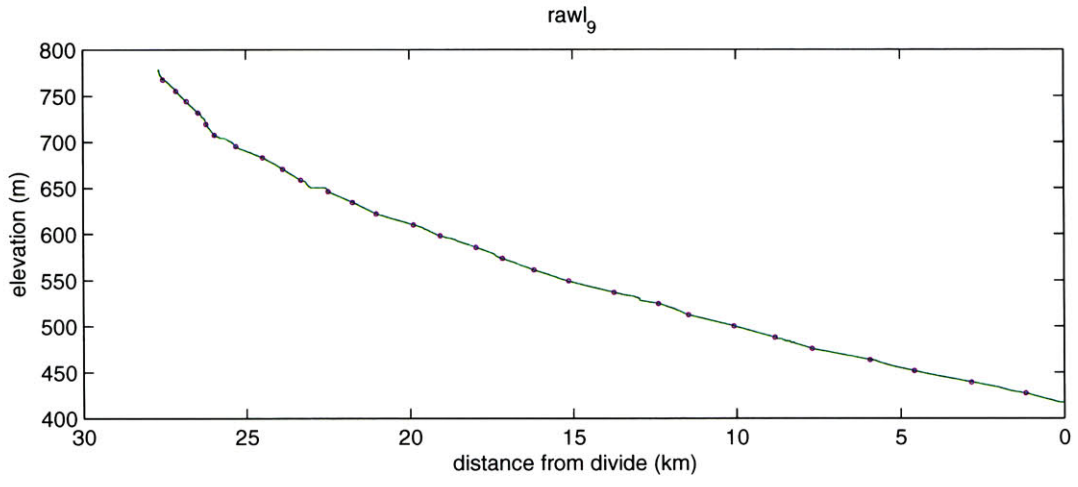




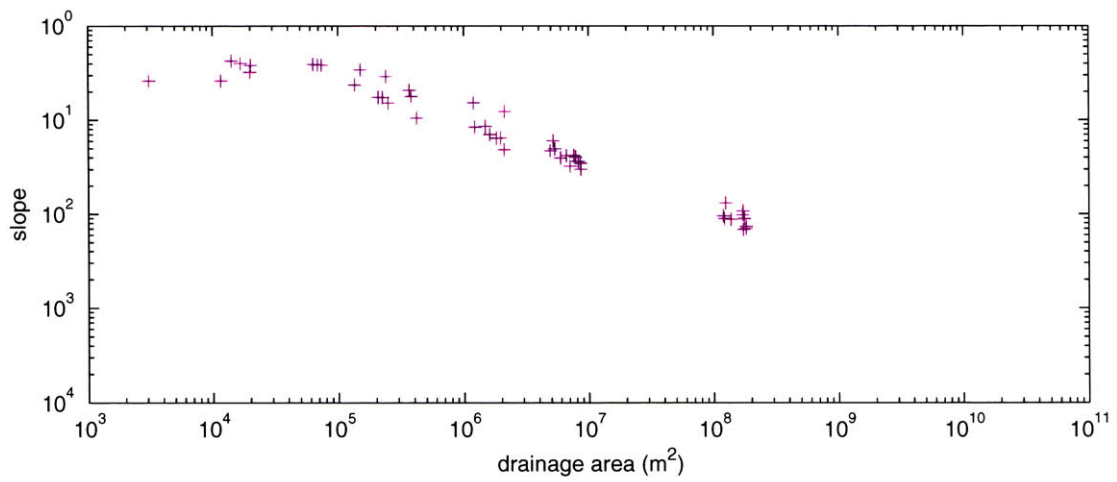
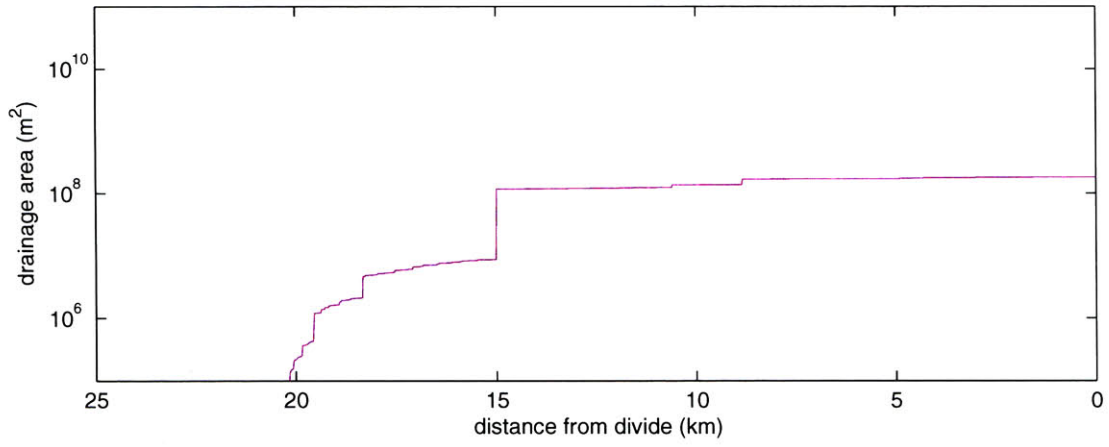
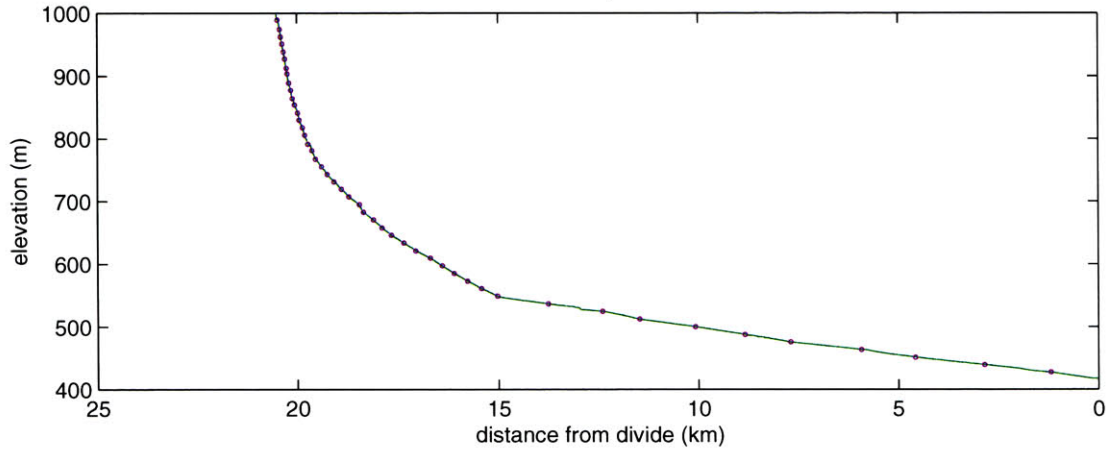


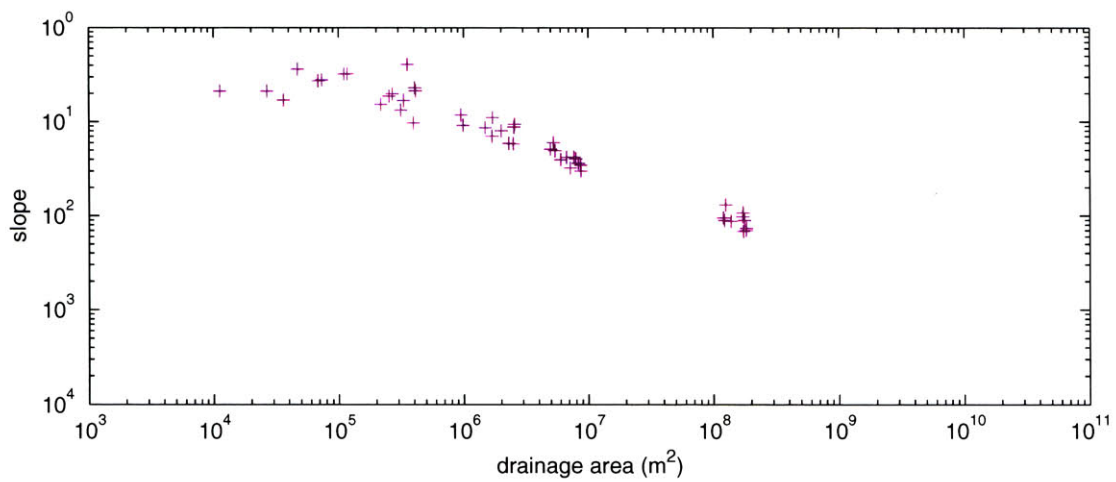
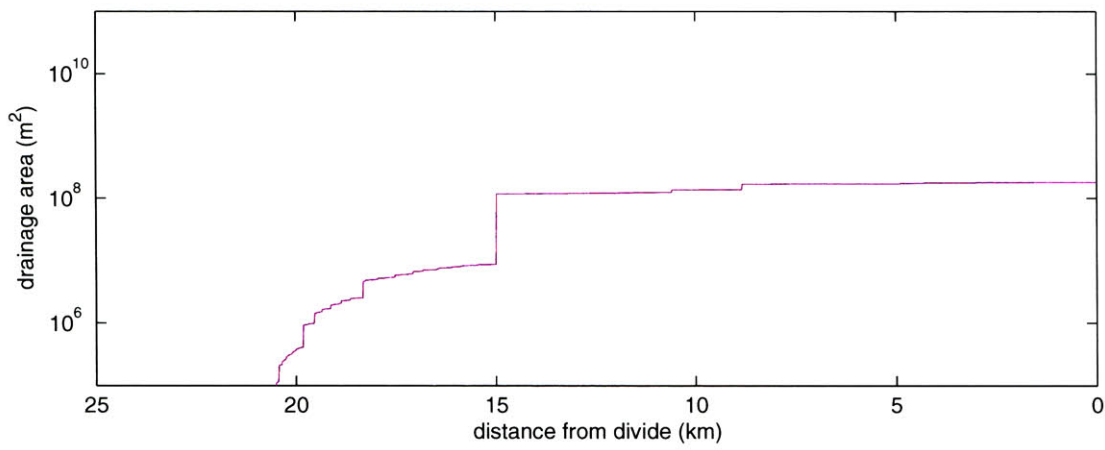
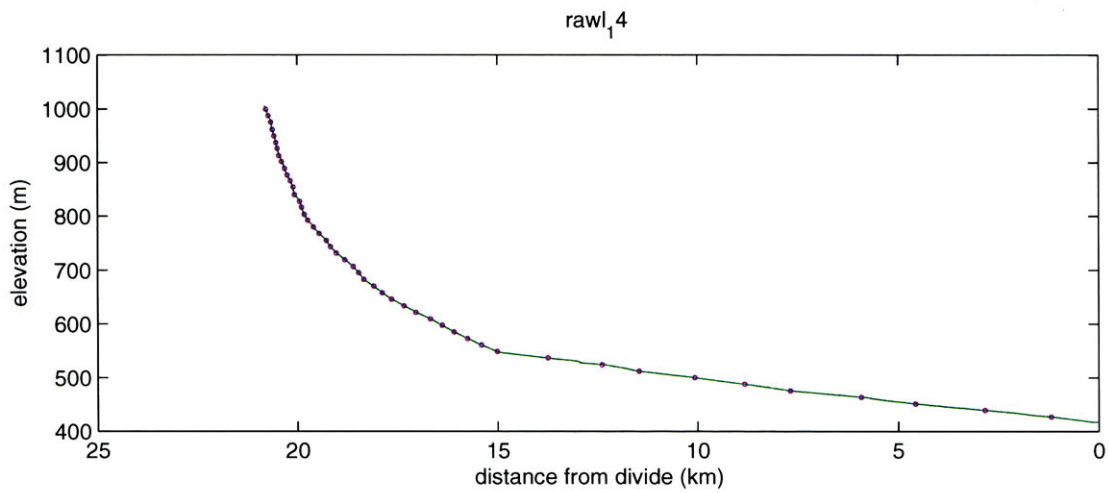




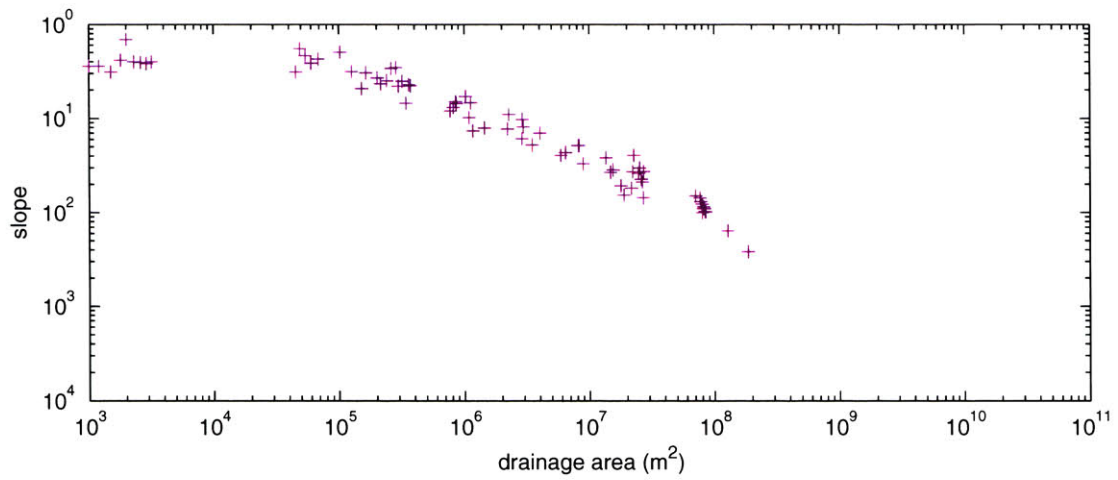
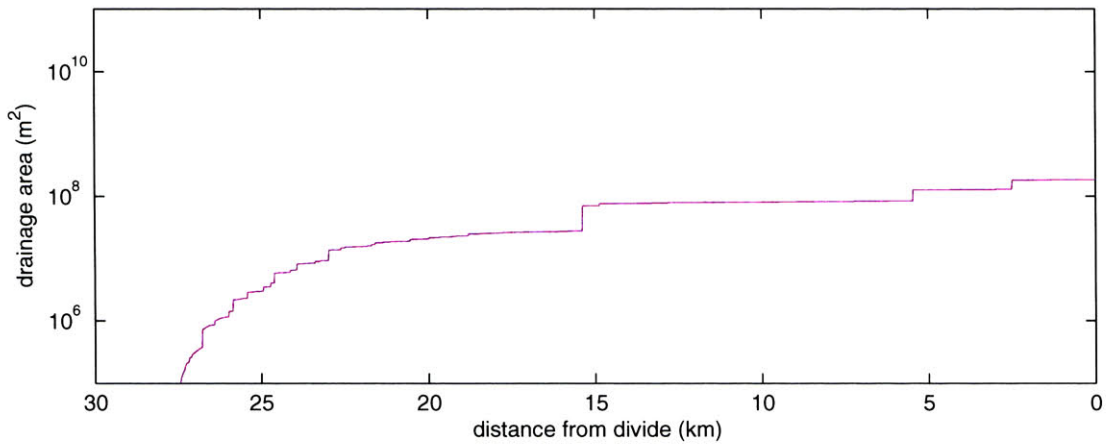
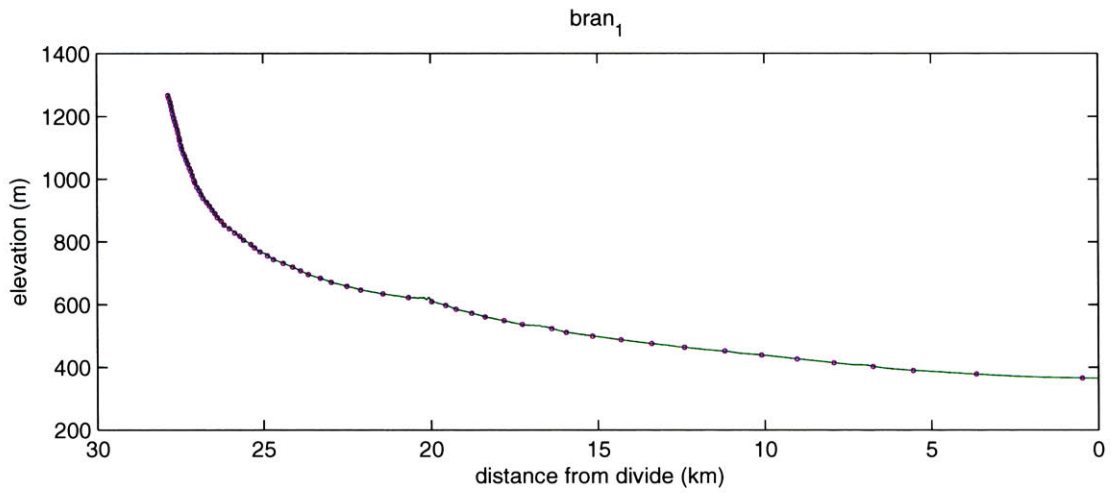


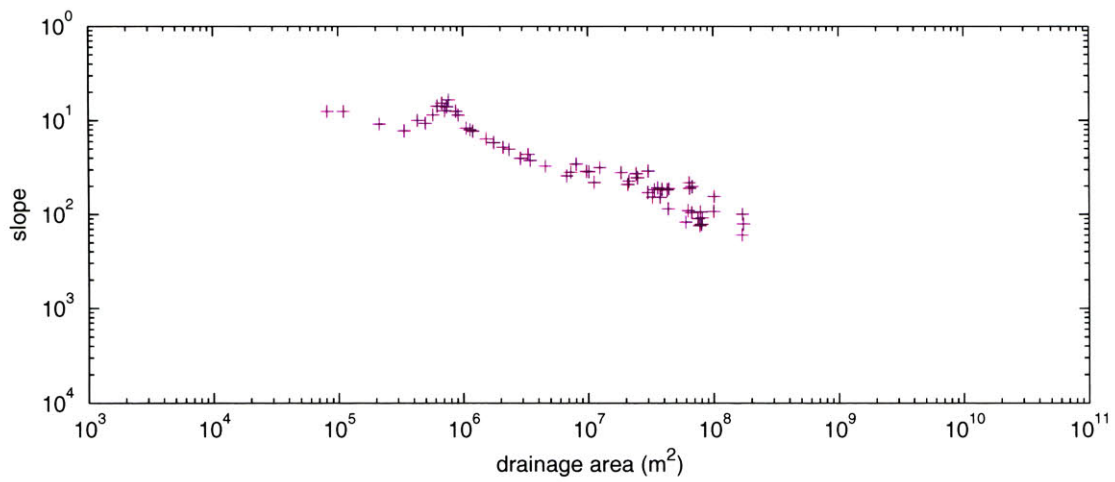
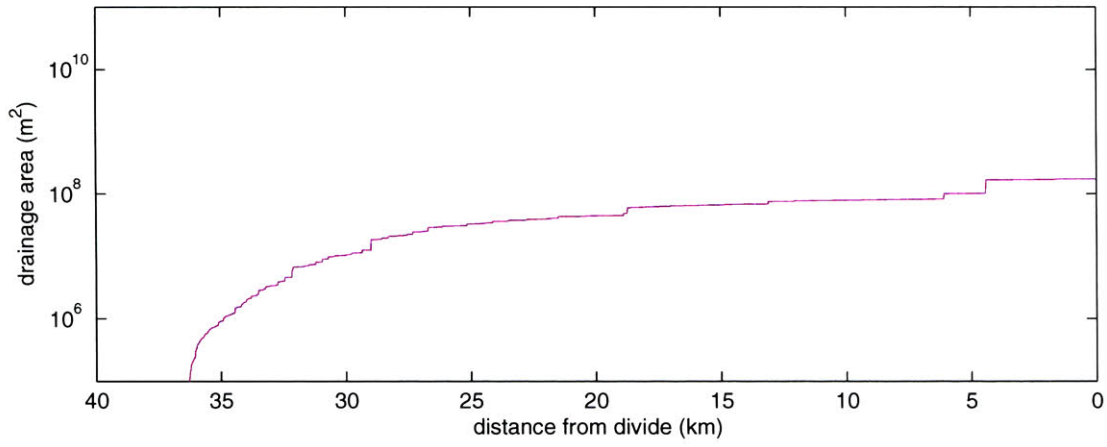
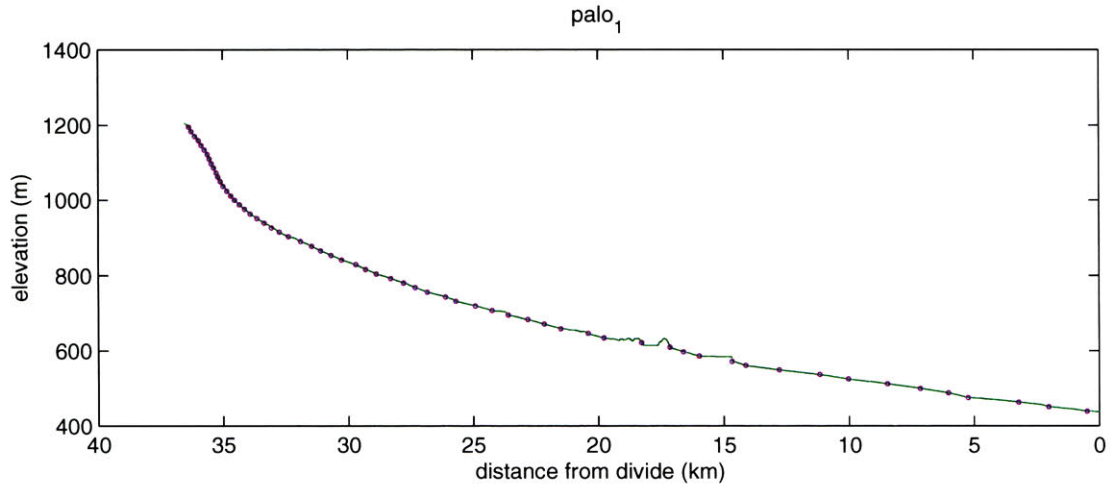
raw1_3

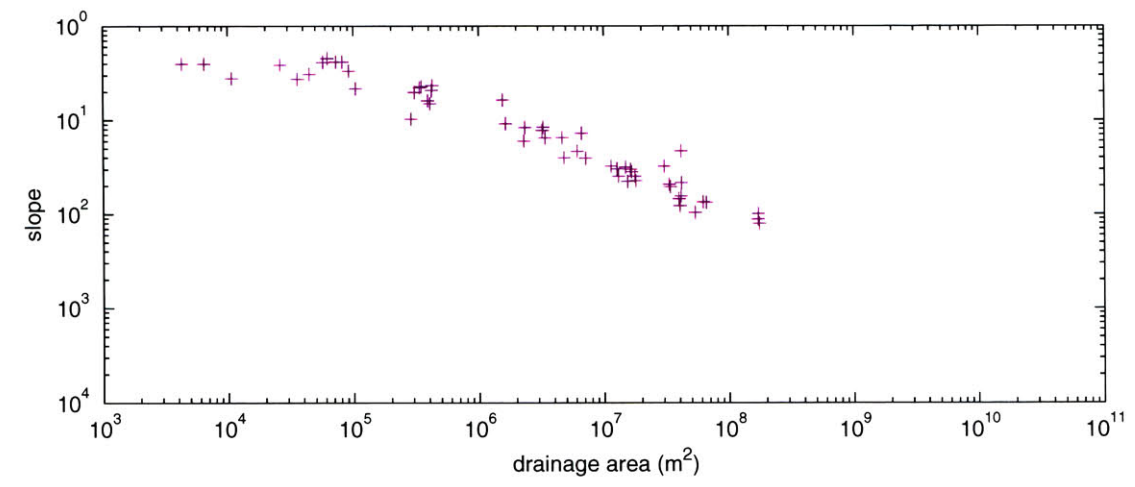
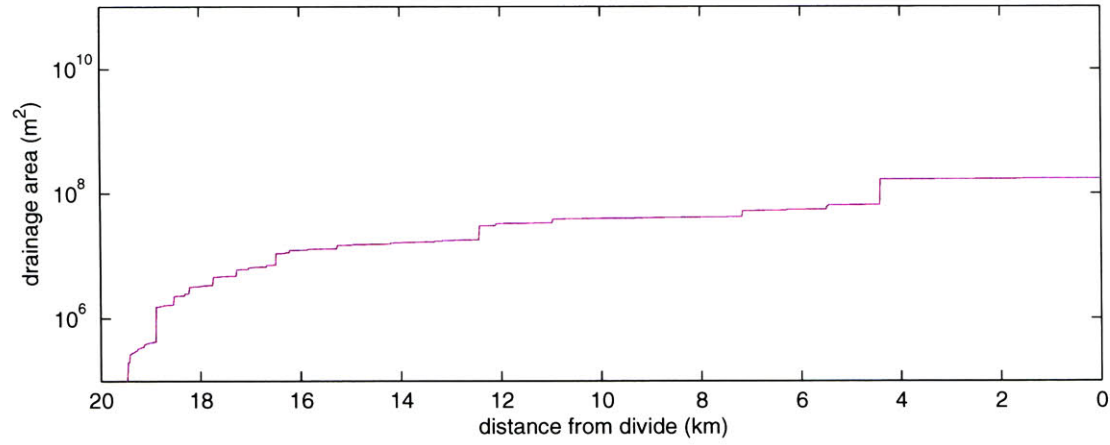
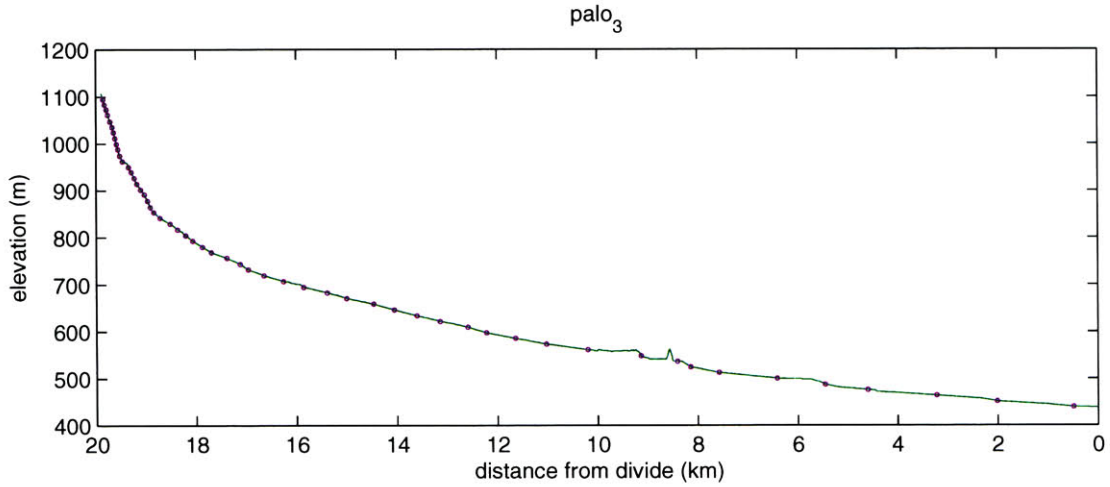


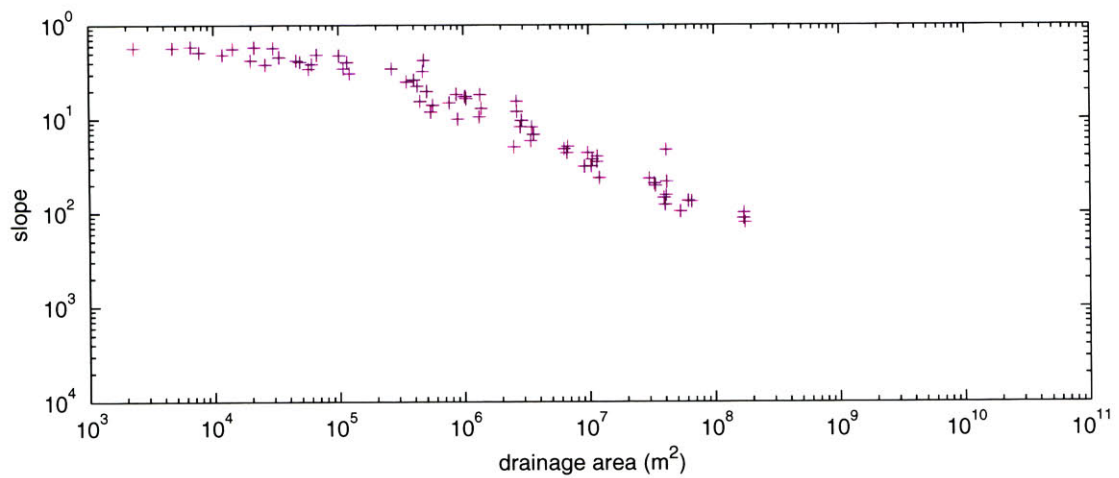
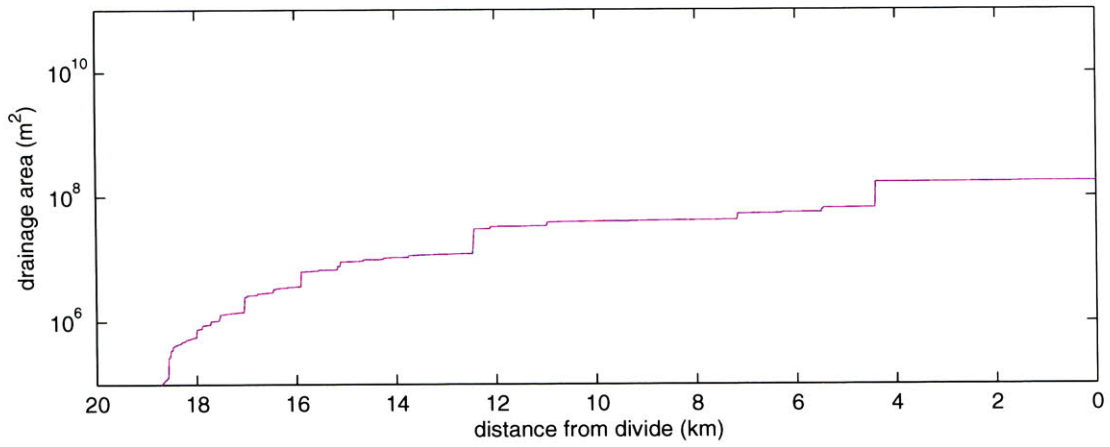
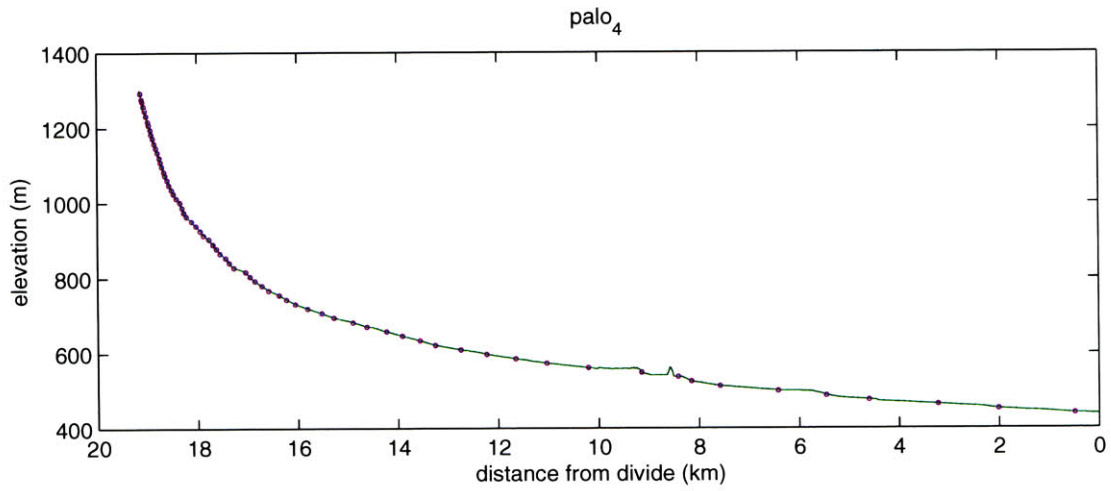


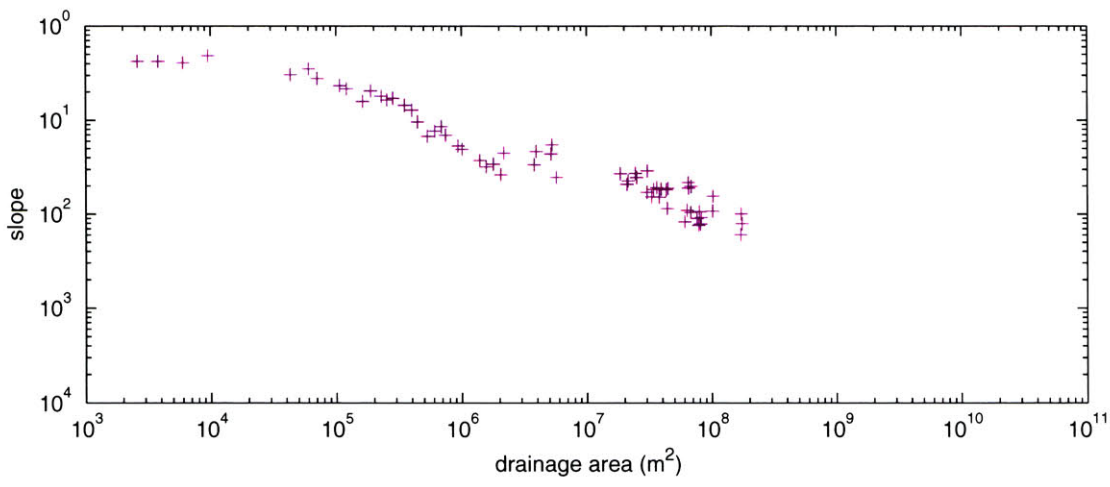
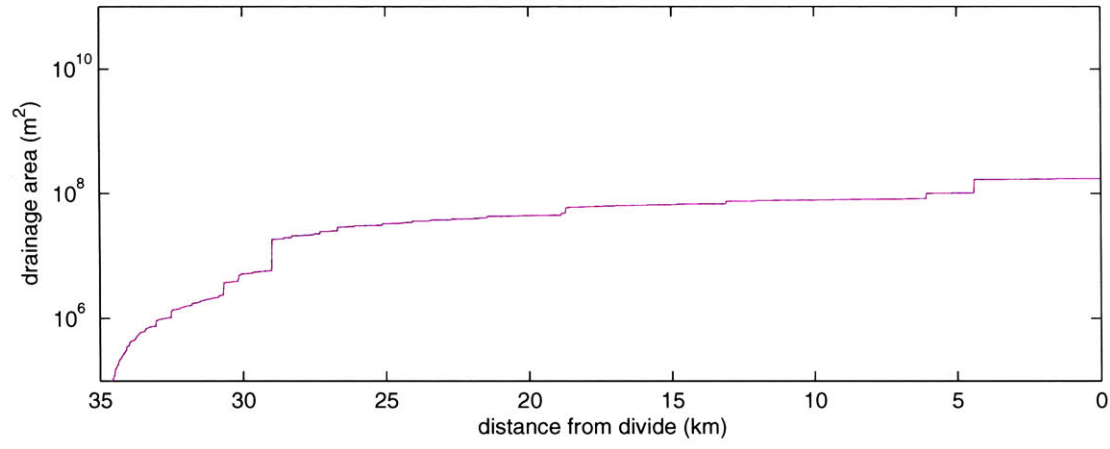
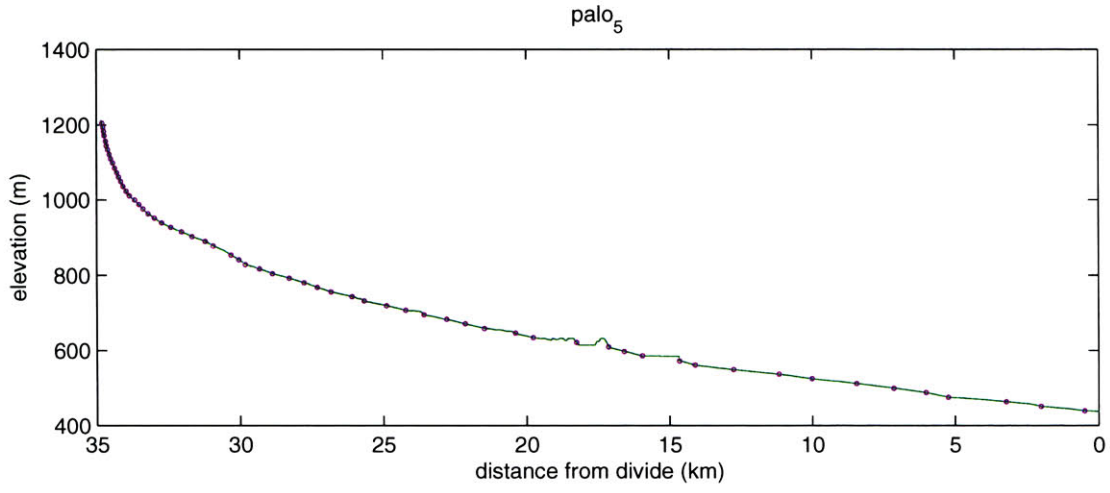
9.2.3 North River Basin

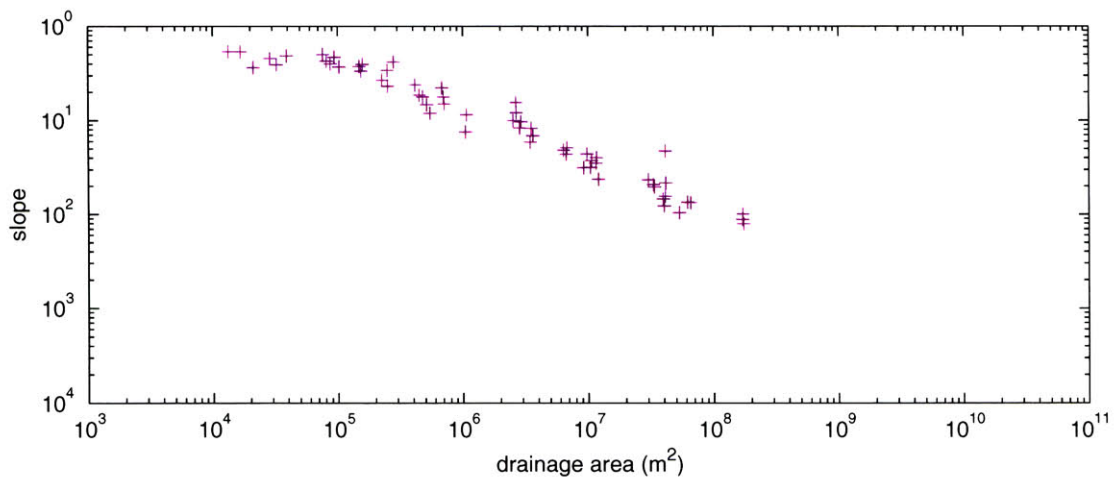
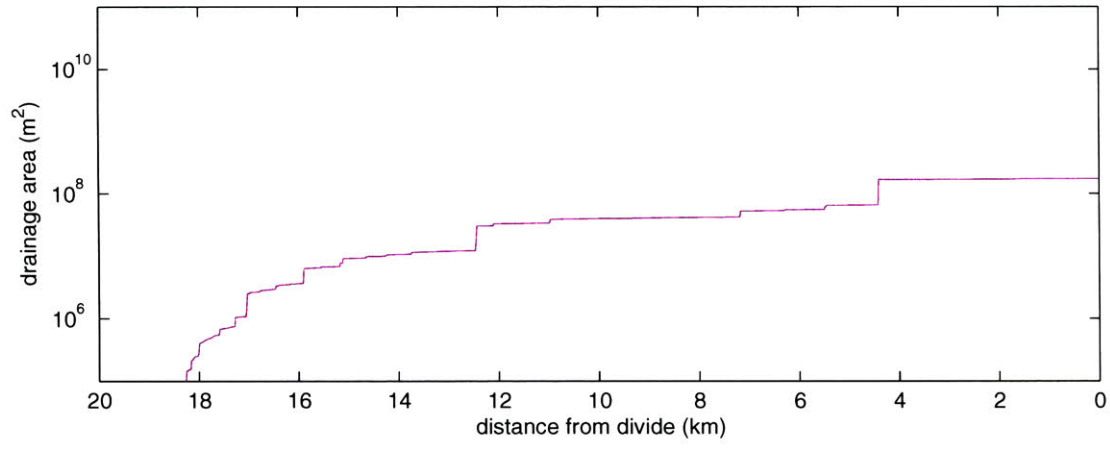
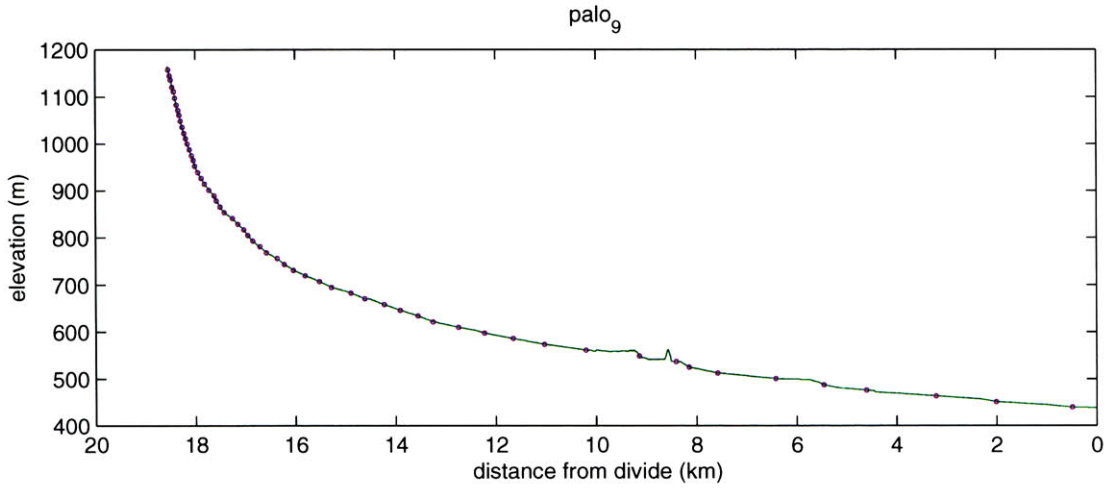


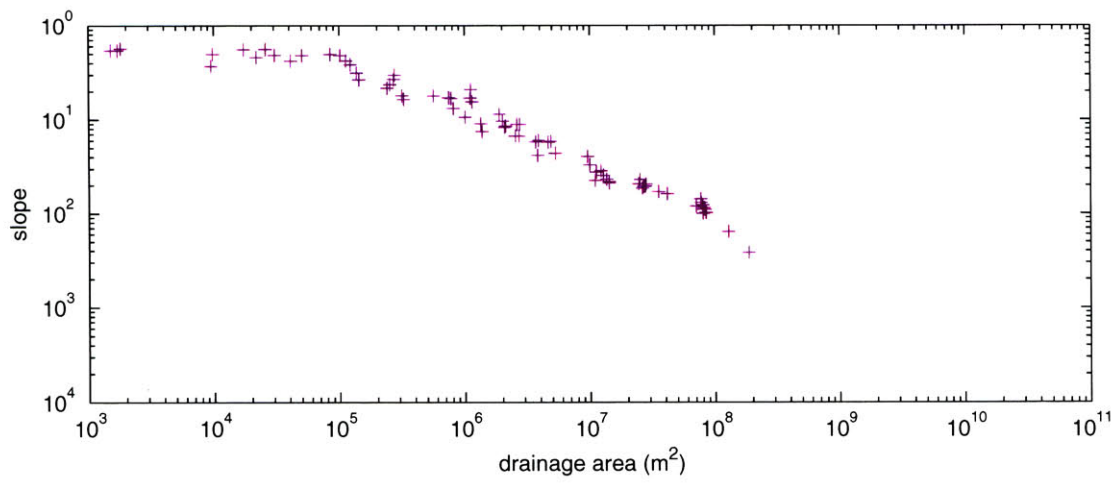
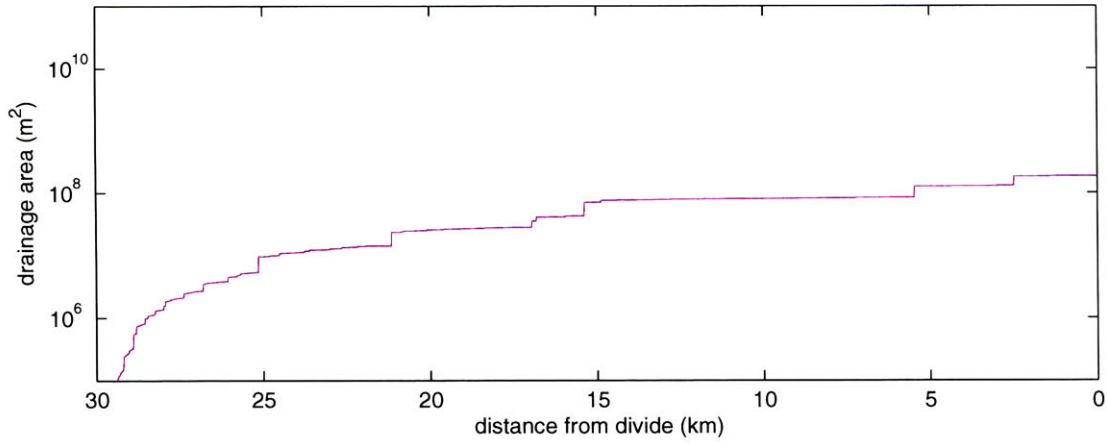
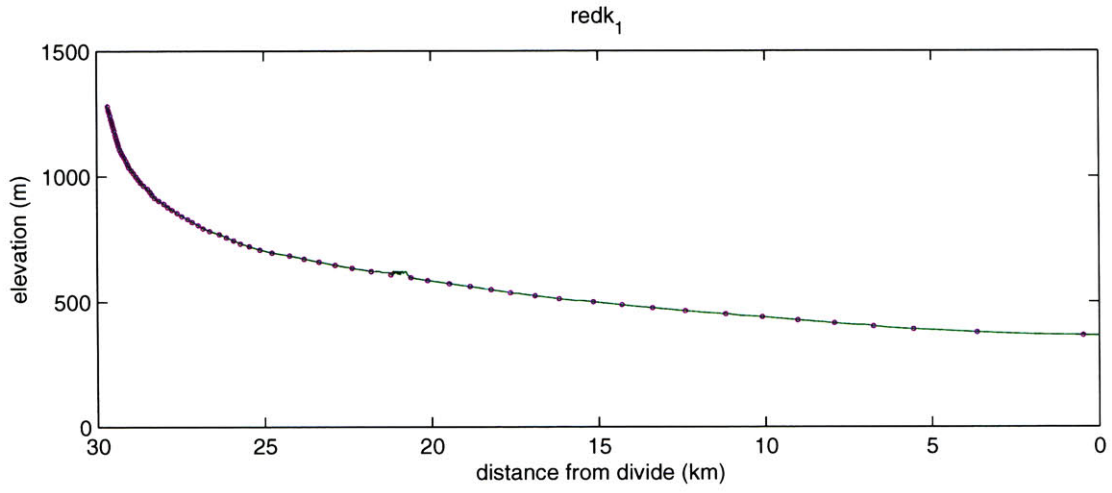


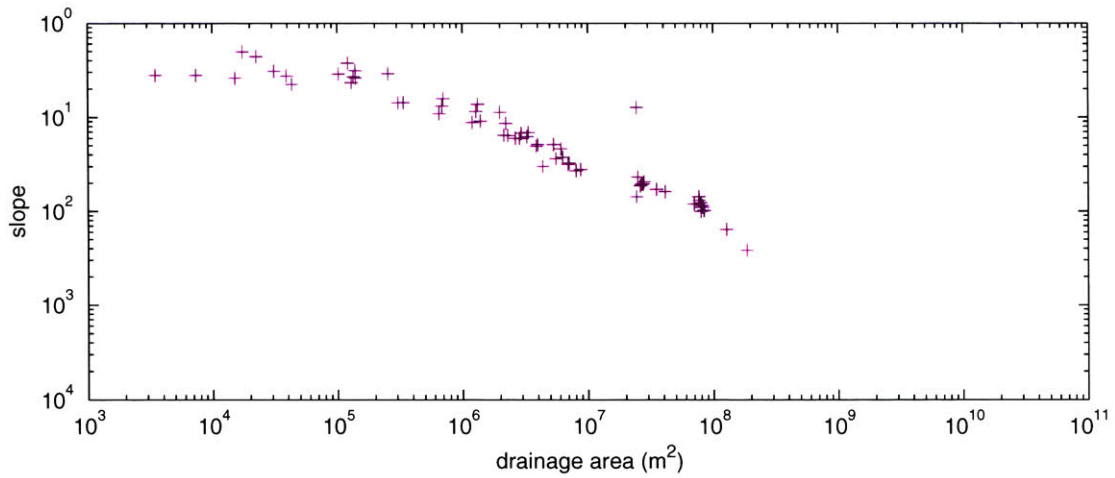
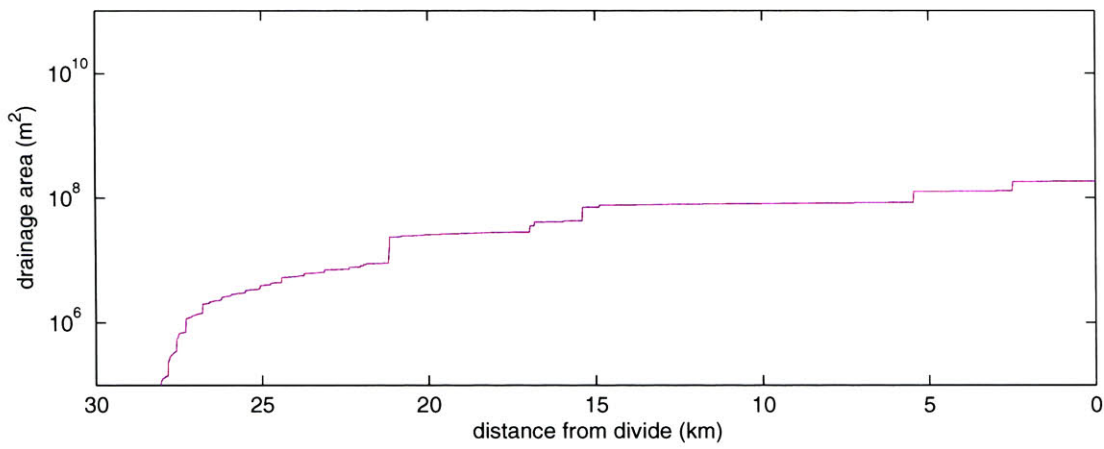
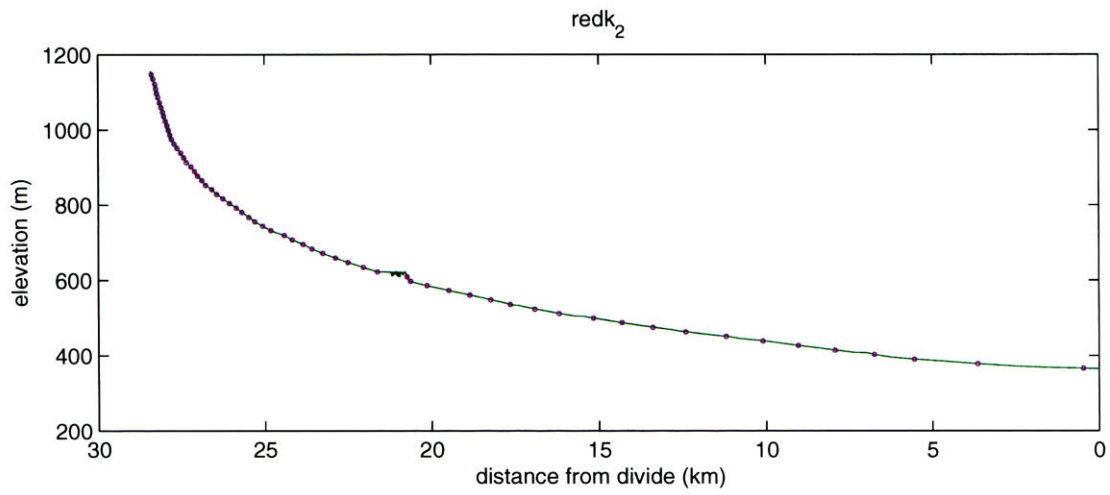


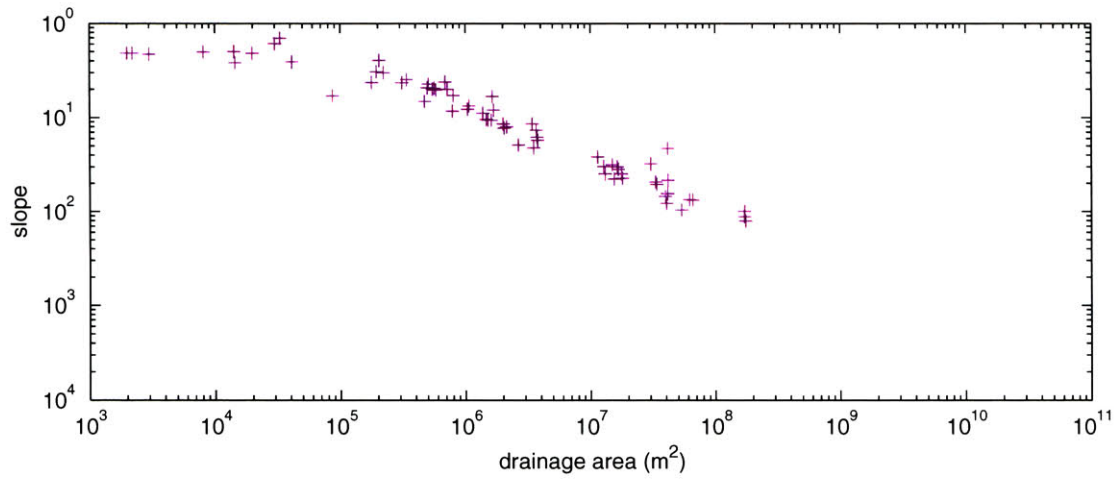
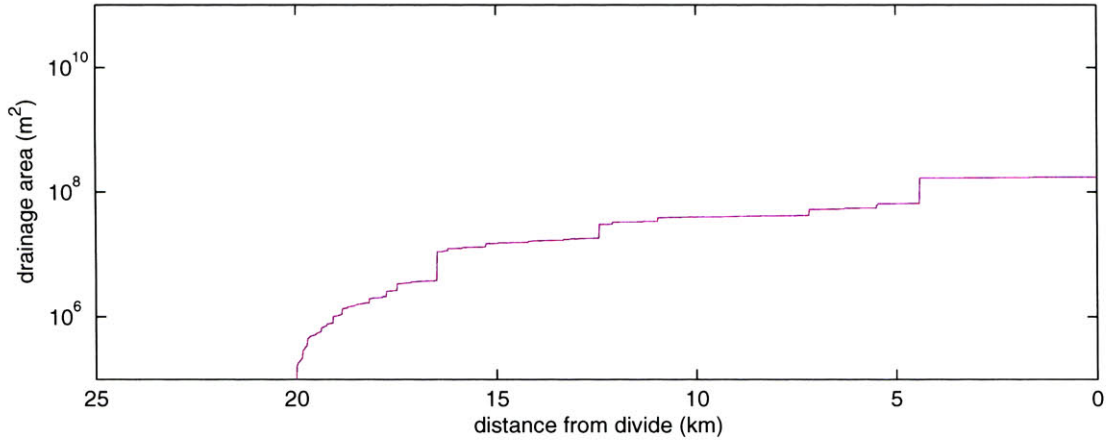
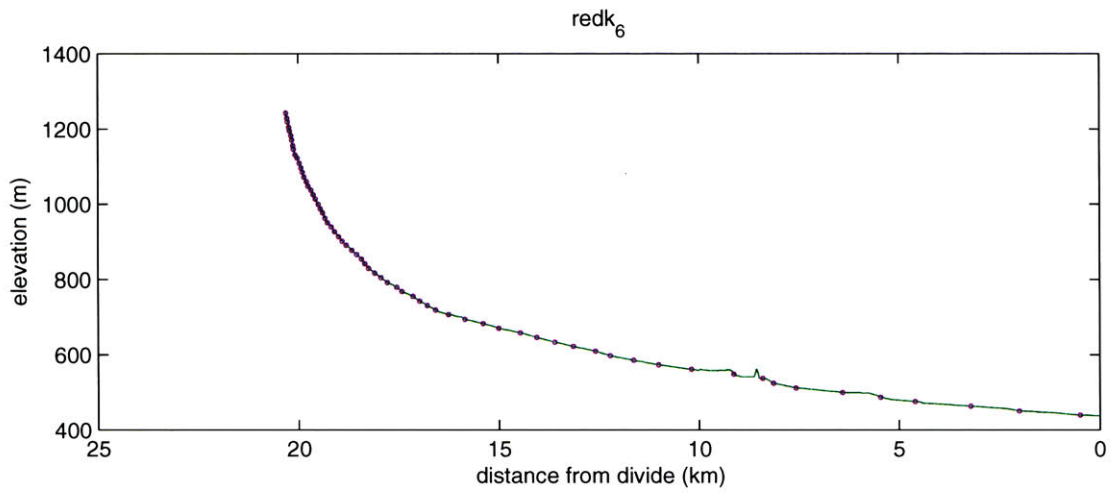


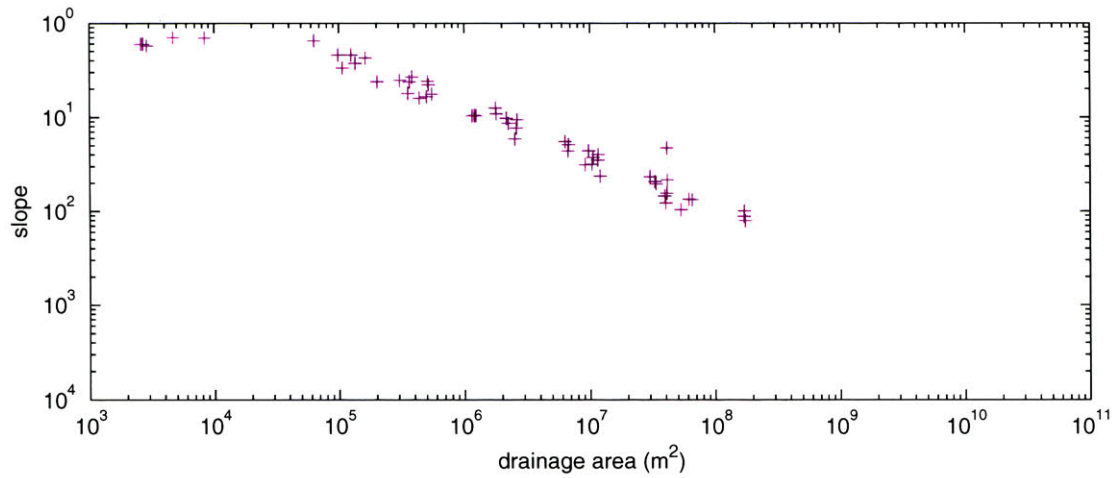
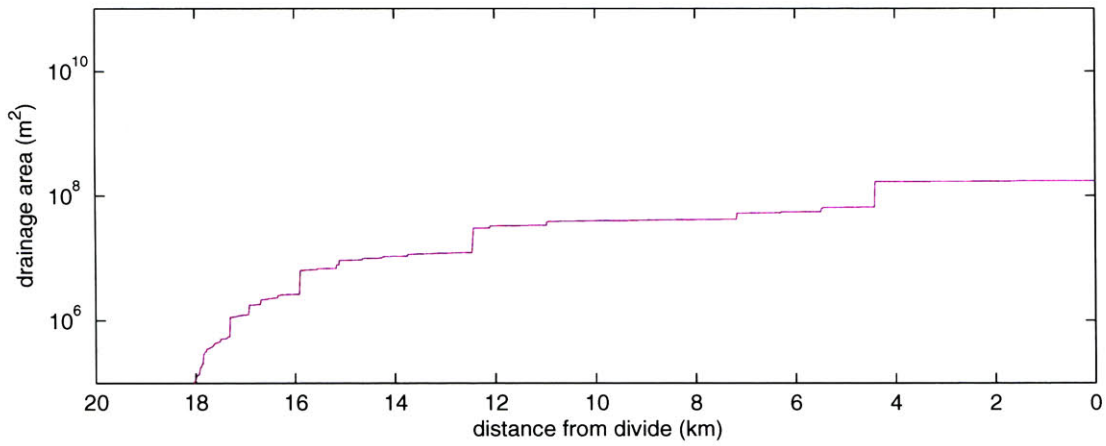
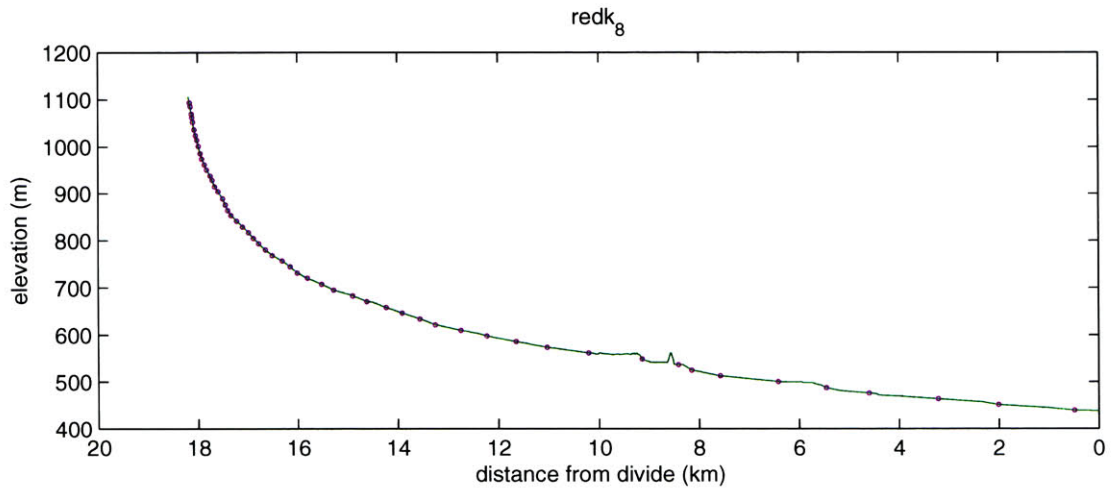




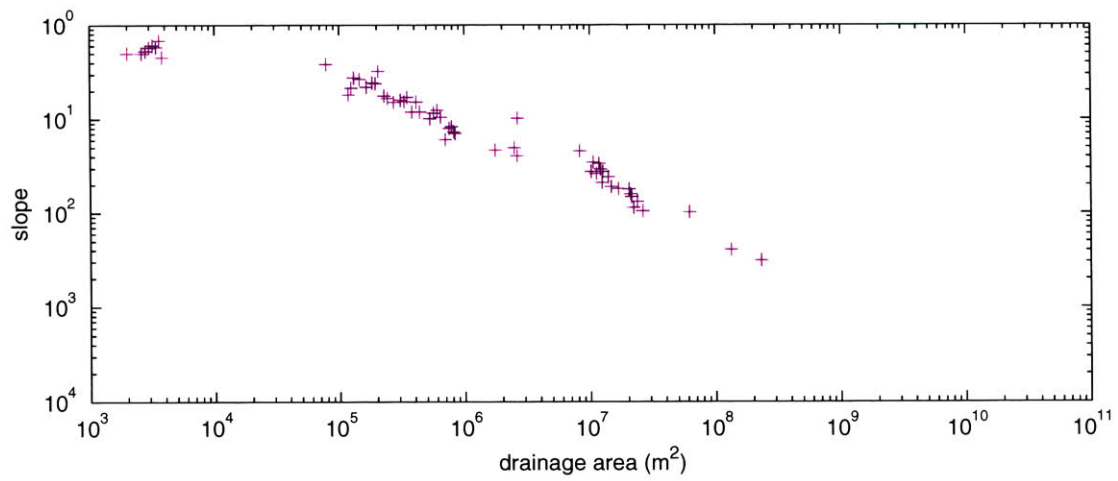
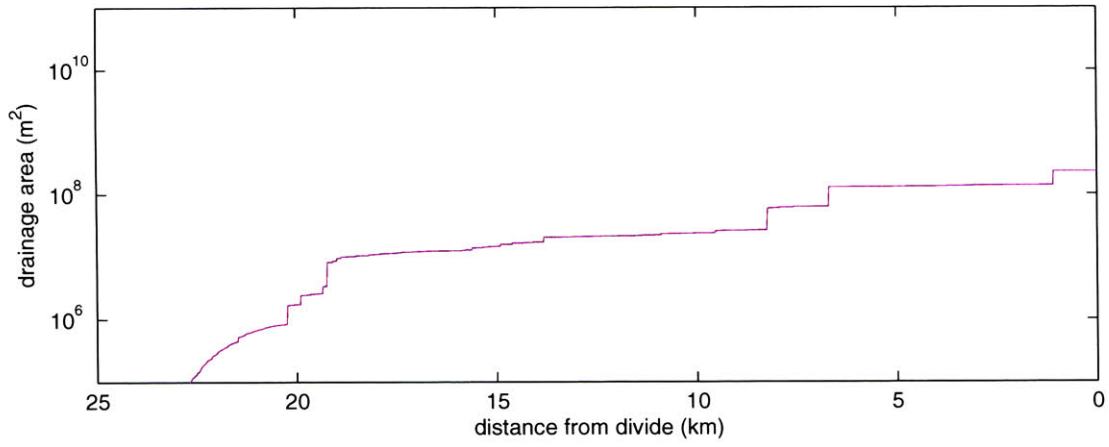
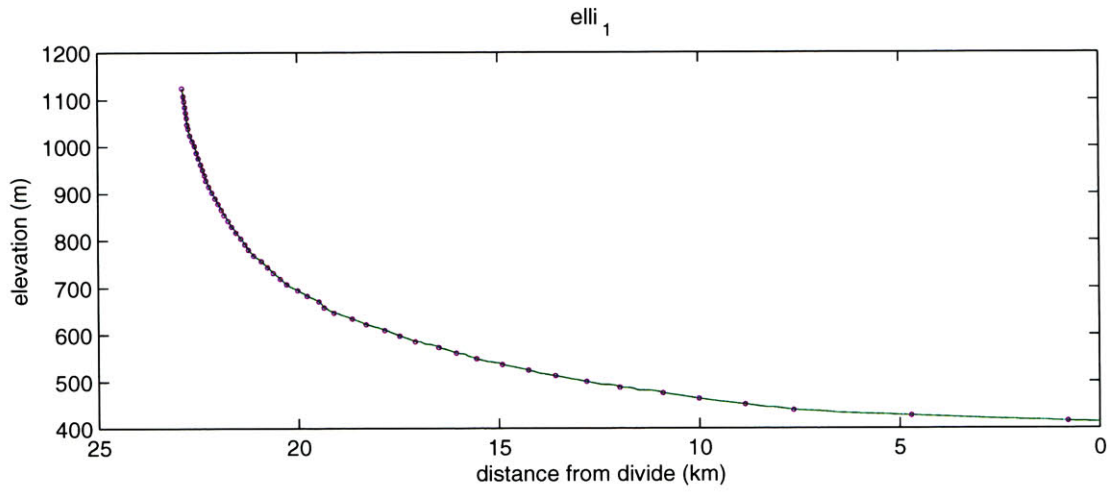


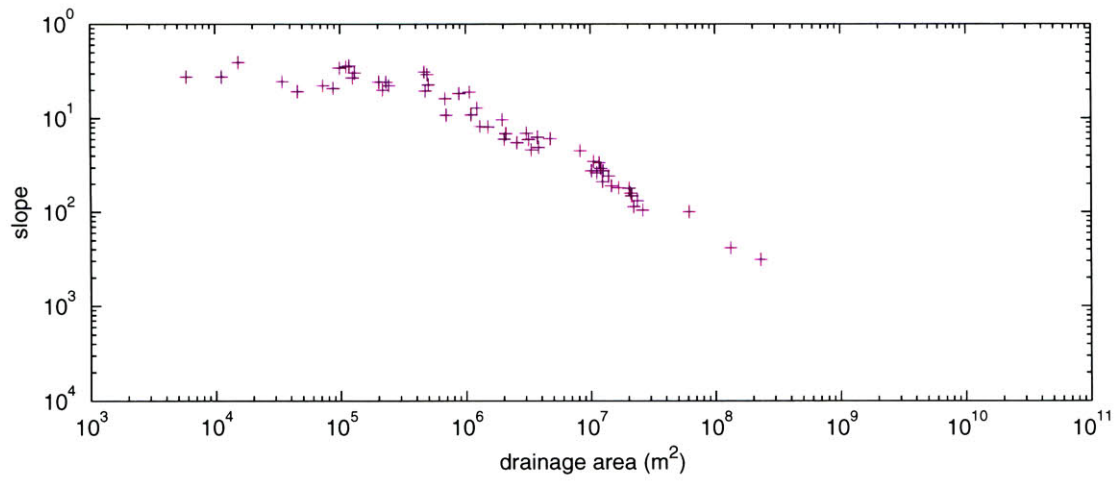
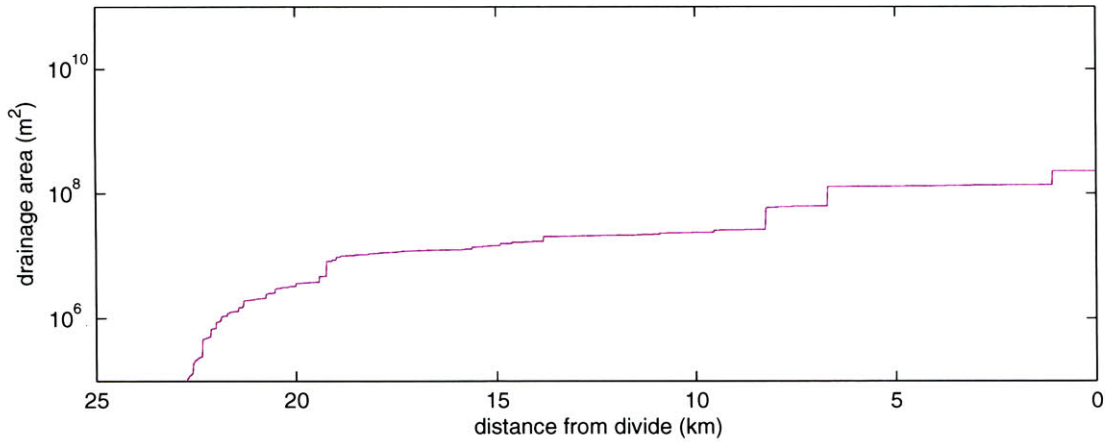
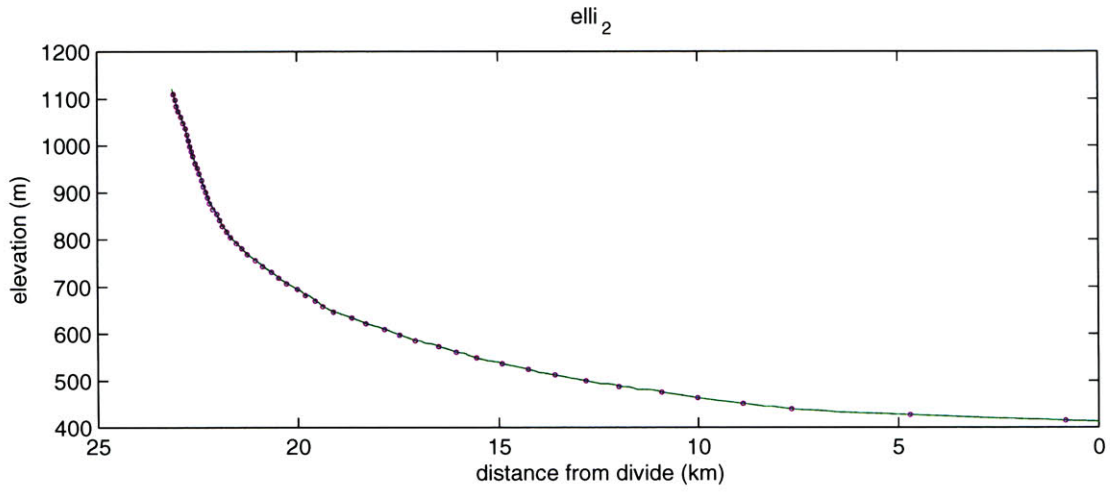




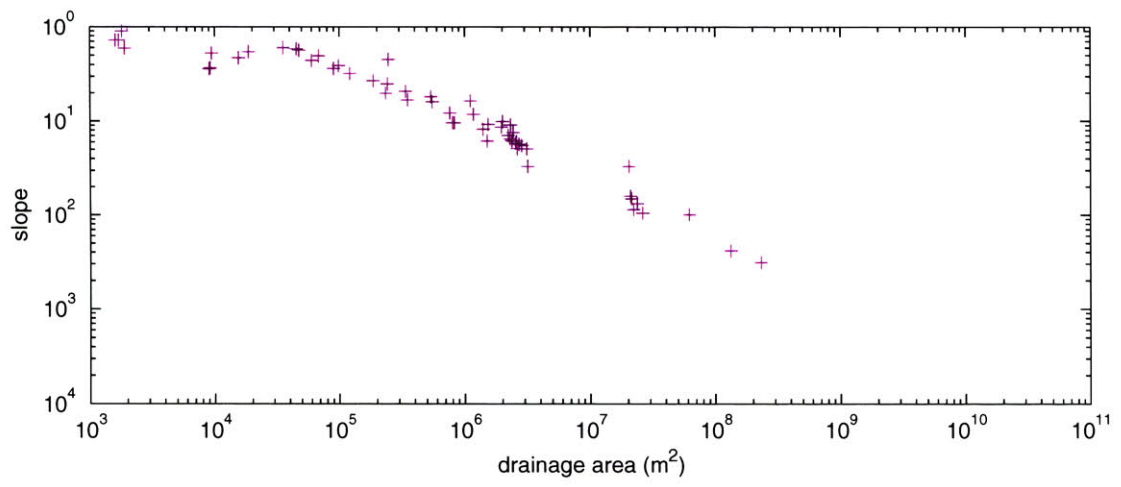
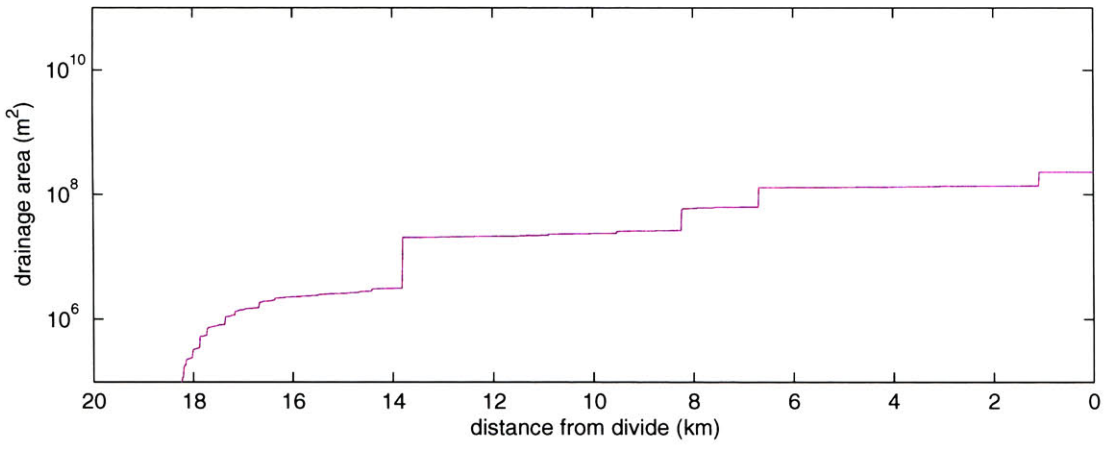
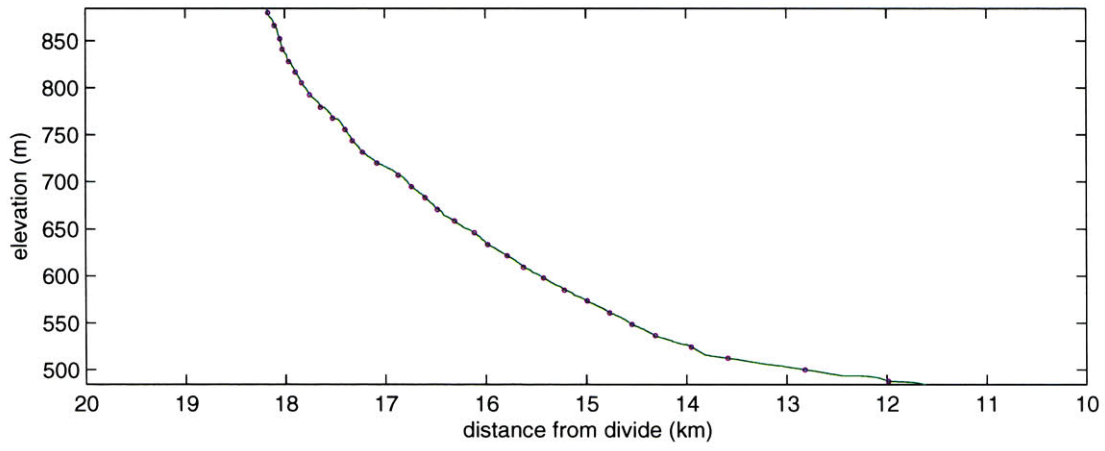


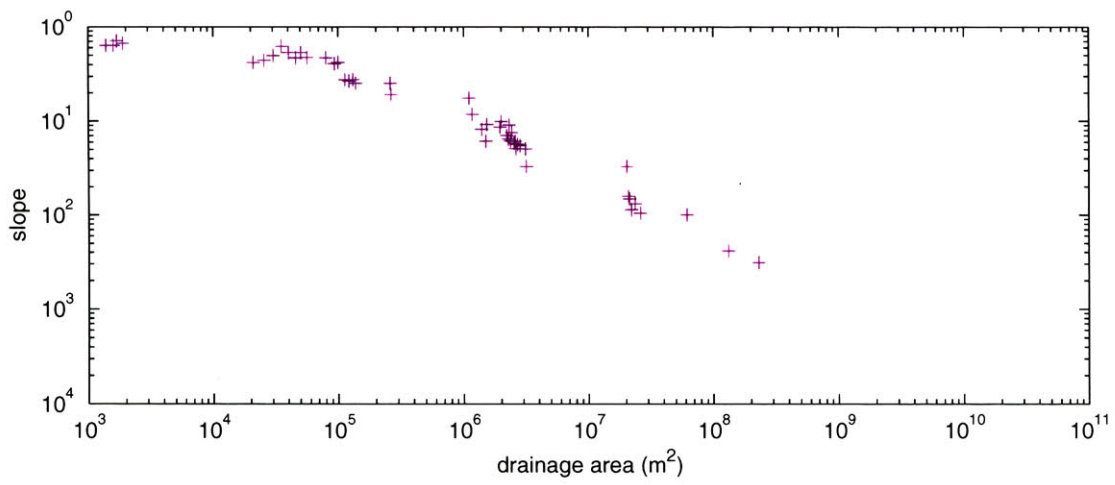
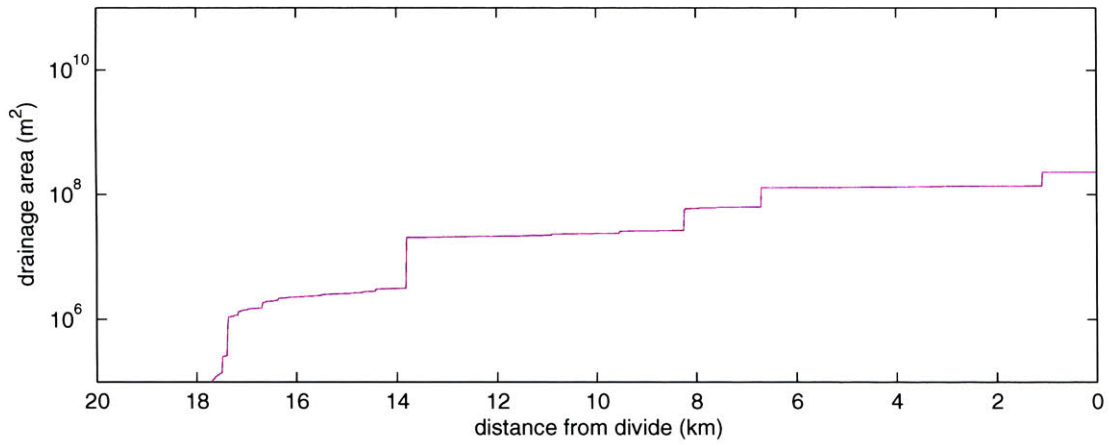
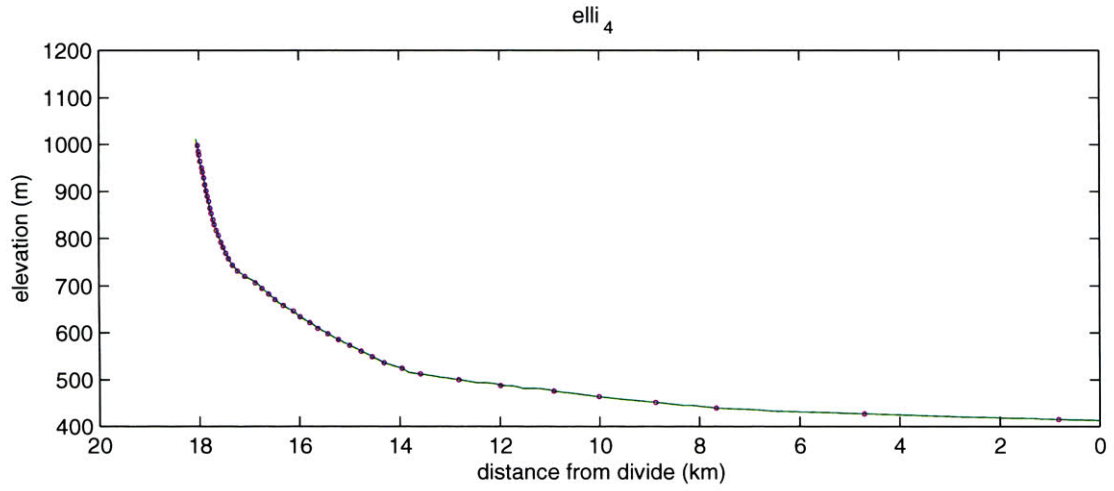
9.2.4 Middle River Basin

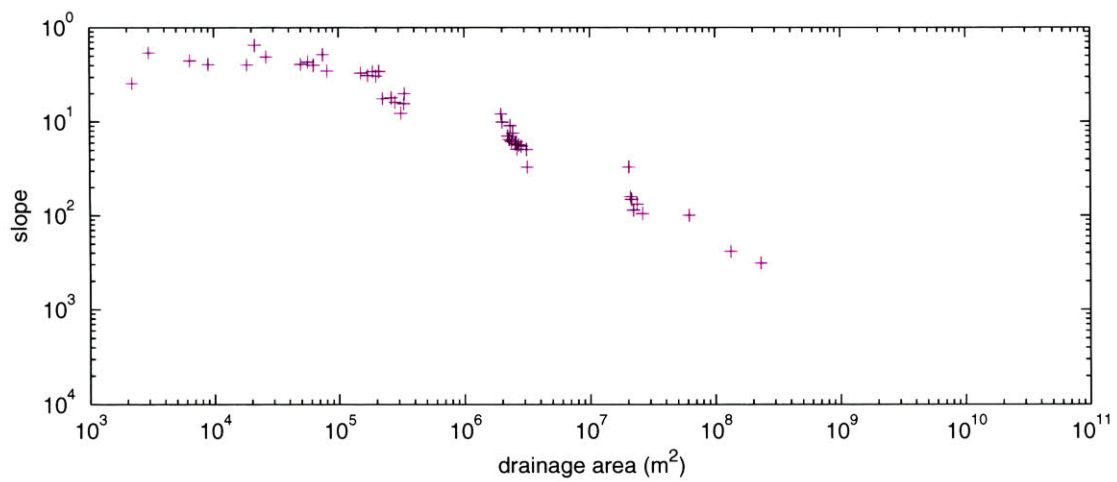
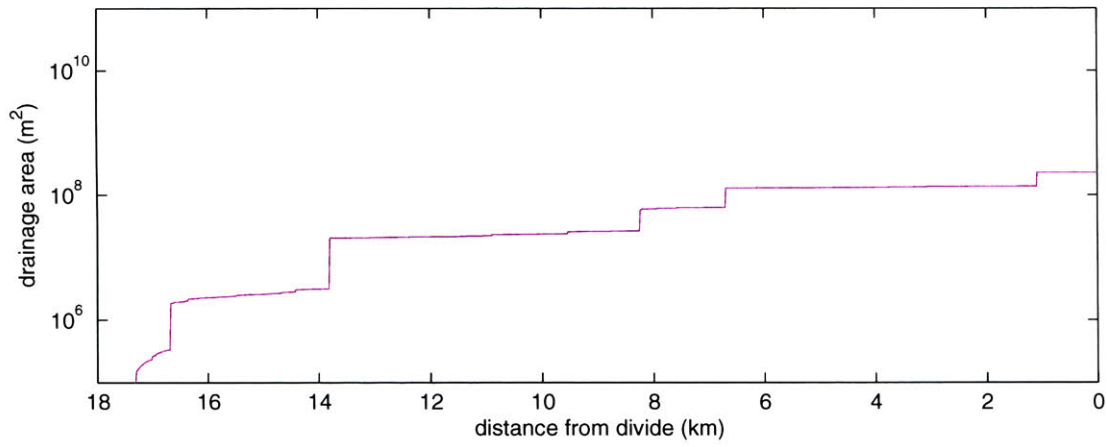
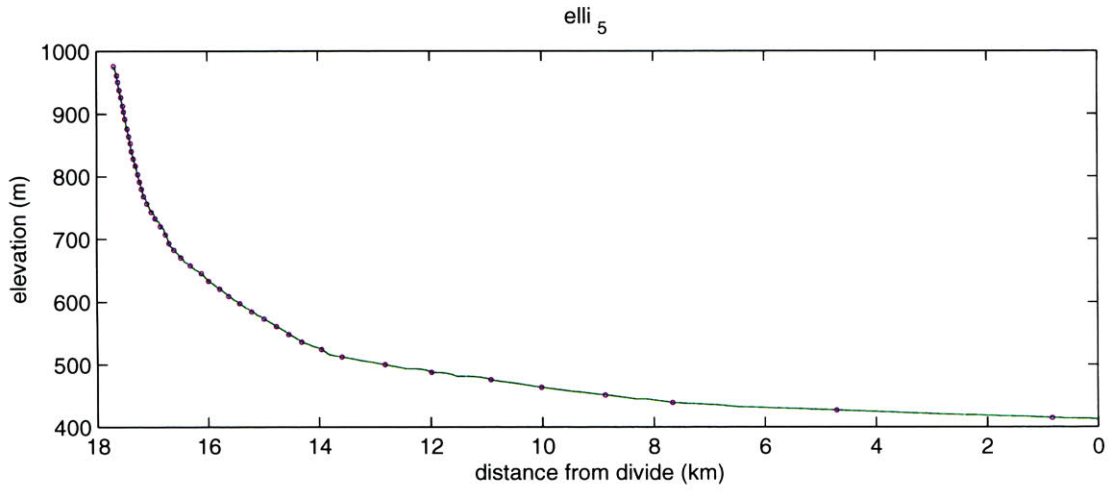


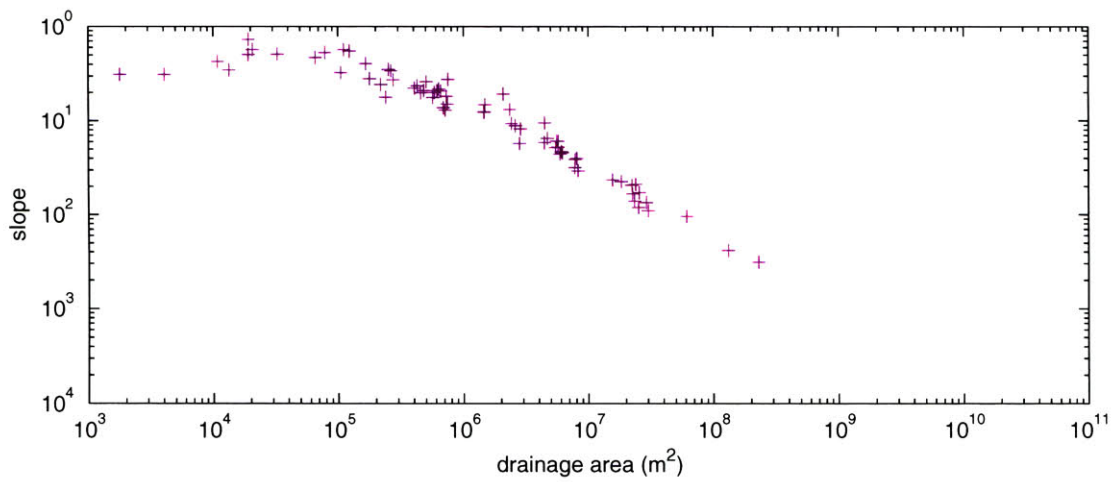
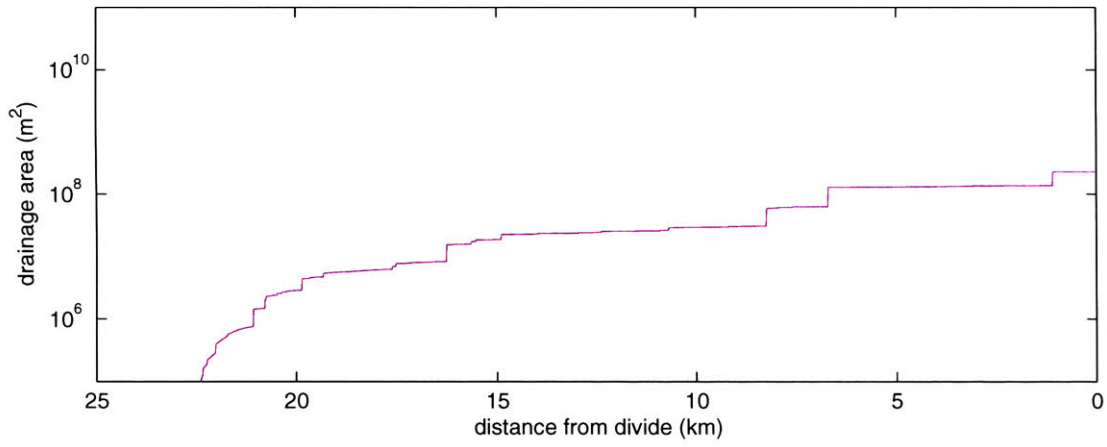
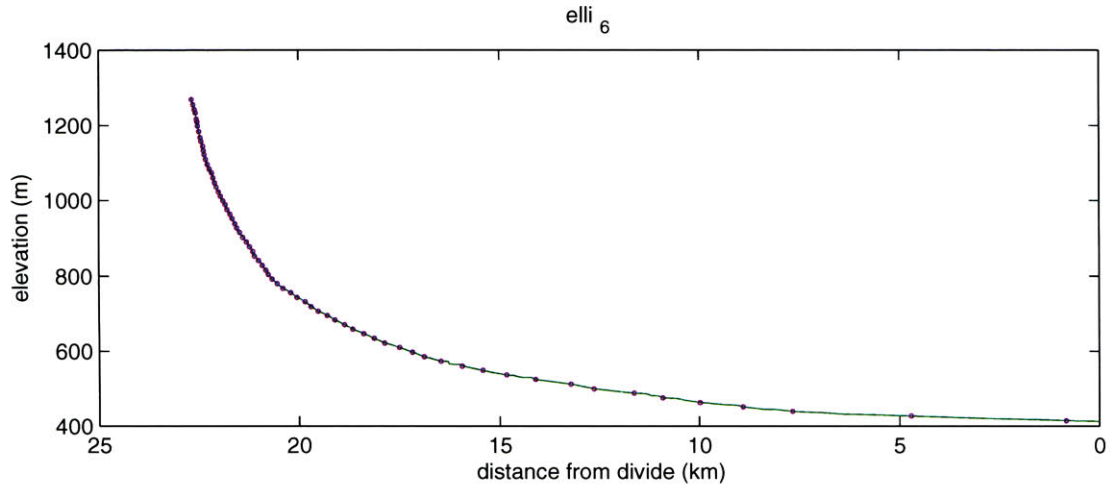


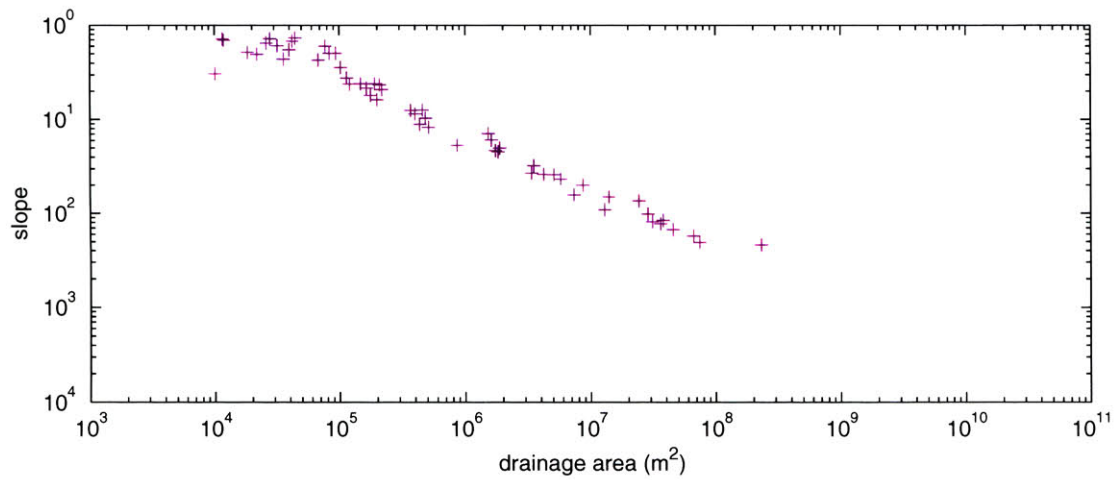
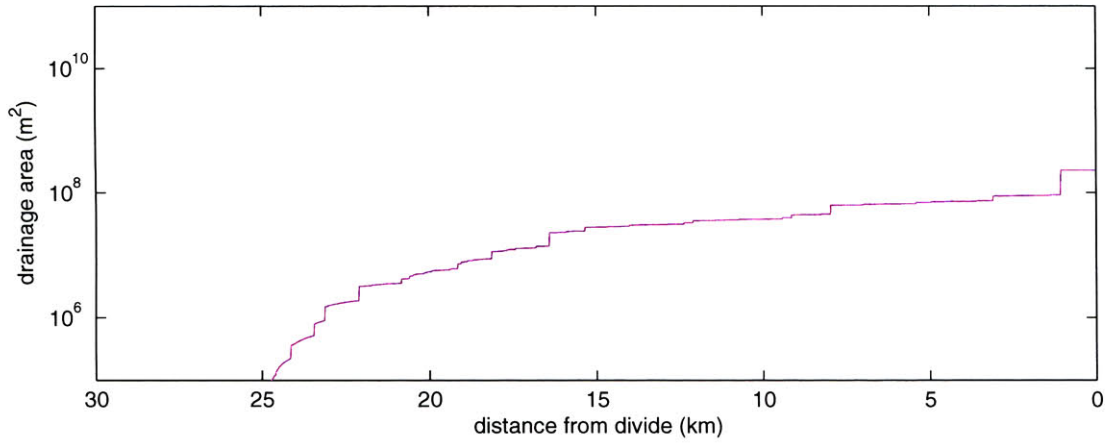
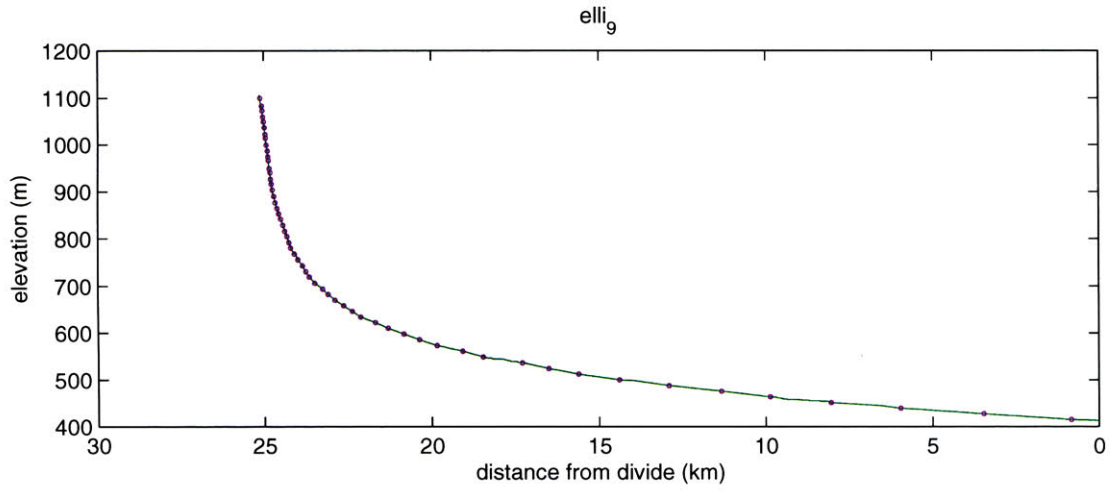
elli₃



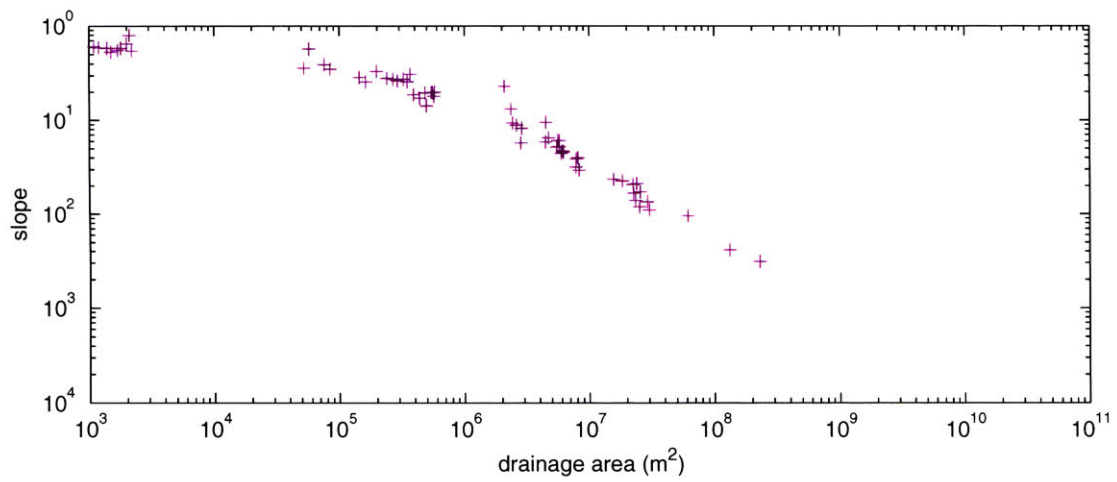
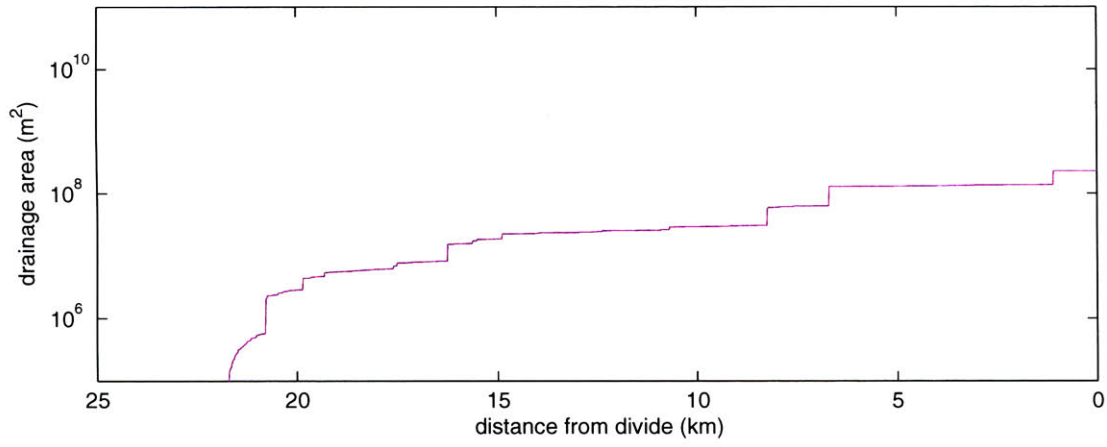
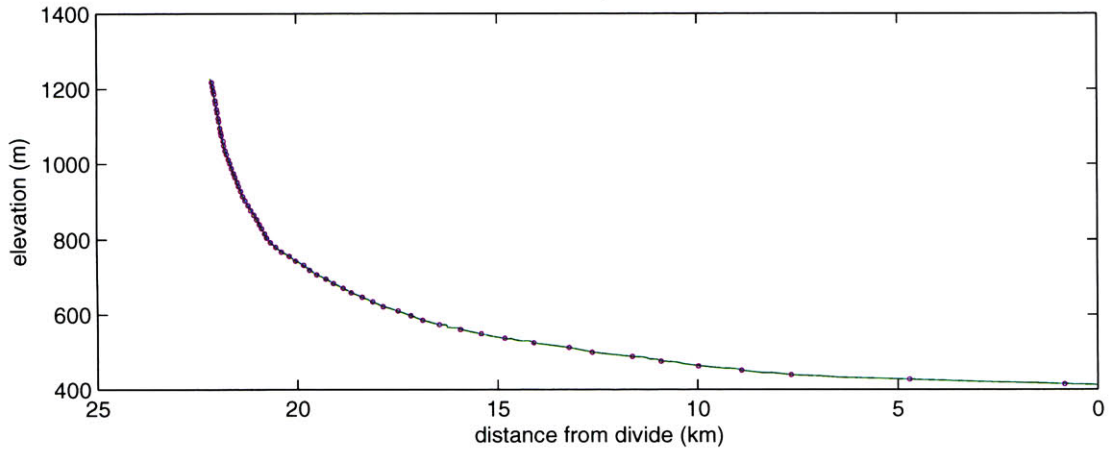








elli_{1,2}



elli₁,4

